

Susan Dorothy Lyimo

# Experimentation on Surge waves in Three phase pipe flows

August 2020

---

# Acknowledgements

First and foremost, I would like to give praise to God. He has shown his gracious mercy and blessing upon me to allow me to work on this thesis.

I would like to thank my supervisor, Ole Jørgen Nydal, for his guidance and advice on the work that is presented in this document. I'd like to also well thank my colleague Godwin Nsemwa for his shared effort in the many hours of collective work on time-consuming experiments and data processing.

Lastly, I would like to send my heartfelt gratitude to my family, my partner and my friends for their unending prayer and support during this time.

---

---

---

---

# Abstract

Surge waves are a common flow assurance phenomenon during multiphase transport in subsea systems. The challenge with these waves is that they are not easily predictable. The science behind the formation of these waves is not well understood. The formation and propagation of these waves in three-phase systems of air, oil and water is even more complex. This is the motivation behind this master thesis.

Experiments were performed in the NTNU multiphase laboratory to make a study on surge waves in three-phase flow. The technique used for the formation of three-phase surge waves in the laboratory was by manipulation of the air flow. Air flow rate was ramped down, accumulations occurred at the lower points of the pipe, and then subsequently ramped up. Similar experiments to this were done previously during project work at NTNU multiphase laboratory. Modification of the test matrix was done by lowering air velocities and lowering liquid volume. This ensured maintenance of the stratified flow regime and absence of roll waves.

Seven cases were selected and are highlighted in this work. The cases were arranged in descending order of liquid mass flow rate. Most cases would form a set of two waves - an initial smaller wave with a smooth front and a larger wave that followed with a somewhat sharper front. There was difficulty in distinctly predicting the end of the waves since visual perception was used for determination. The waves would last between 10 to 25 seconds, with the period increasing as the wave propagated towards the end. In real cases, surge waves are known to last even for over an hour. The waves gradually decreased in amplitude as they flowed along the pipe. Cases with higher amounts of water in the liquid mixture distinctly showed water towards the end of the wave.

Water cut is a ratio of water produced out of total liquid. Varying water cuts were observed for a single case of  $U_{SG} = 8.95$  m/s and  $U_{SL} = 0.0144$  m/s. The water cuts were 0%, 50% and 100%. It was found that with increasing water cut, the waves would increase in amplitude, meaning the oil wave amplitude is smaller than the water wave.

OLGA 2019.1 was applied for evaluation of some cases. Two-phase simulations performed in previous work by different versions of OLGA were replicated using the latest version. A fluid file was provided by SINTEF. The wave hold up results from OLGA2019.1 corresponded most with those from OLGA 7.1 and OLGA 7.3.5. The results from OLGA 2016.2.1 did not correlate well. For wave velocity results, there was very little correlation with older versions of OLGA. The closest correspondence was with OLGA 2016.2.1 HD result.

OLGA 2019.1 was applied to evaluate three-phase surge waves for the same case with  $U_{SG} = 8.95$  m/s and  $U_{SL} = 0.0144$  m/s. This case that was selected had a water cut of 37%. One stand-out characteristic of the resulting plots was a large accumulation towards the end of the pipe during ramp down which was discharged soon after ramp up. This corresponded to laboratory data for that particular case. Two peaks were visible on wave fronts, with the first one smaller than the next. The two peaks blended in with each other

---

as they moved along the pipe. Simulated waves lasted longer than the experiment waves, ranging from 60 seconds to 85 seconds. This could mean that the waves observed in the lab lasted much longer than what was perceived. This case was also simulated for different water cuts of 0%, 50% and 100%. The behavior of the waves was indicative of them being able to last for longer lengths of pipeline.

Wave velocities for both experimental and simulated results were compared. Lower water cuts showed better correlation in wave velocity than higher water cuts. Generally, the simulated data highlighted similar trends to the experimental data. For further experimental work, it would be very useful with instrumentation for rapid three phase fraction measurements.

---

# Sammendrag

Det er utført forsøk i flerfaselaboratoriet ved NTNU med enkeltbølger (“surge waves”) i olje-vann-luft strøm i rør. Studien er en oppfølging av et tidligere prosjektarbeid. Forsøkene ble utført ved så lave luftrater som mulig, for å muliggjøre stratifisering av olje-vann strømmingen. Flere forsøk ble utført ved varierende vannkutt. Bølgene ble dannet ved at luft raten ble redusert en kort periode. Væske ble da akkumulert i et lavpunkt nær innløpet og en bølge ble dannet når luftraten ble økt igjen. Bølgen gikk deretter gjennom et horisontalt rør som var om lag 50 m langt.

Syv forsøk er rapportert i dette arbeidet. Forsøkene er gjort med reduserende væskerate. De fleste forsøkene viste et sett av to bølger. Den første bølgen vavr liten, med med lav amplitude og slak front. Den andre var større med skarpere front. Det kunne være vanskelig å avgjøre enden av bølgen, ettersom studien er visuelt basert. En bølge varte typisk mellom 10 to 25 sekunder gjennom røret. En bølge gjennom en rørledning kan vare over en time. Amplitudene til bølgene kunne gradvis bli redusert gjennom røret. Forsøk med høye vannkutt viste høye vannfraksjoner mot enden av bølgen. Det kan også tolkes som høyere oljefraksjoner i fronten. Høyere vannkutt gav også større bølger.

OLGA 2019.1 ble benyttet for evaluering av forsøkene. To-fase simuleringer fra et tidligere arbeid ble gjentatt med siste versjonen av OLGA. Fluid filer var tilgjengelig fra SINTEF. Bølgeformen fra siste OLGA versjon samsvarte bra med resultatene fra OLGA 7.1 and OLGA 7.3.5, men mindre bra med resultatene fra OLGA 2016.2.1. For bølgehastighetene var det mindre samsvar mellom alle OLGA versjonene. Beste samsvar med siste versjon var med OLGA 2016.2.1 HD.

Et forsøk med  $USG = 8.95$  m/s,  $USL = 0.0144$  m/s og vannkutt 37% ble sammenlignet med OLGA 2019.1. Væskeakkumulering ble observert ved enden av røret under reduksjonen av luftraten. Denne ble blåst ut raskt etter økningen av luftraten igjen, i samsvar med laboratorieresultatene for dette tilfellet. To topper ble observert i bølgefronten, med den første mindre enn den andre. Toppene ble gradvis slått sammen ettersom bølgen propagerte gjennom røret. Den simulerte bølgen varte lenger enn den eksperimentelle, fra 60 til 85 sekunder. Dette kan også bety at bølgene i laboratoriet varte lenger enn det som ble anslått visuelt. Dette forsøket ble også simulert for vannkuttene 0%, 50% og 100%. Bølgene ved disse strømningsratene gir inntrykk av å kunne vare for lengre rør.

Simulerte og målte bølgehastigheter ble sammenlignet. De målte bølgehastighetene var større enn de simulerte. Lave vannkutt viste bedre overenstemmelse for bølgehastigheter enn høyere vannkutt.

Det generelle inntrykket er at simuleringene viste samme trender som forsøksdata. Videre forsøk med trefasestrøm ville være nyttig om instrumentering for hurtig måling av trefase fraksjoner var tilgjengelig.

---

# Table of Contents

<b>Abstract</b>	<b>i</b>
<b>Sammendrag</b>	<b>iii</b>
<b>Table of Contents</b>	<b>vi</b>
<b>List of Tables</b>	<b>viii</b>
<b>List of Figures</b>	<b>xiii</b>
<b>1 Introduction</b>	<b>1</b>
1.1 Objectives . . . . .	2
1.2 Thesis Structure . . . . .	2
<b>2 Theoretical and Conceptual Framework</b>	<b>3</b>
2.1 Introduction to Multiphase Flow . . . . .	3
2.1.1 Definitions . . . . .	3
2.1.2 Key Parameters . . . . .	3
2.1.3 Flow Regime Classification . . . . .	5
2.2 Introduction to Multiphase Numerical Modeling . . . . .	9
2.2.1 Two Fluid Model for Separated flows . . . . .	10
2.2.2 Drift flux or Mixture Model . . . . .	11
2.3 Surge Waves Phenomenon . . . . .	12
2.3.1 Definition . . . . .	12
2.3.2 Mechanism . . . . .	12
2.4 Numerical Modeling Contribution . . . . .	14
2.5 Surge Waves in Gas Condensate Fields . . . . .	15
2.5.1 Åsgard Field - Mikkell and Midgard . . . . .	15
2.5.2 Ormen Lange Field . . . . .	17
2.5.3 Snøhvit Field . . . . .	19
2.5.4 Tanzania Field - Block 2 Offshore . . . . .	21
2.6 Previous Work on Surge Waves . . . . .	23
2.6.1 IFE experiments . . . . .	23
2.6.2 Master Thesis two-phase Surge Wave Experiments . . . . .	27
2.6.3 Master Thesis Numerical Simulation of Surge Waves . . . . .	32



---

2.6.4	Project Work two-phase Surge Wave Experiments . . . . .	33
<b>3</b>	<b>Experimental Work and Analysis</b>	<b>37</b>
3.1	Laboratory facilities and methodology . . . . .	37
3.1.1	The multiphase flow laboratory at NTNU . . . . .	37
3.2	Experimental Setup . . . . .	41
3.2.1	Calibration and measurement . . . . .	42
3.2.2	Data handling and presentation . . . . .	42
3.2.3	Camera Recording . . . . .	43
3.3	Performed Experiments . . . . .	43
3.3.1	Test procedures . . . . .	44
3.3.2	Selected Three Phase Cases . . . . .	44
3.3.3	Varying Water cuts . . . . .	45
3.4	Observations . . . . .	47
3.4.1	Case Study: Varying water cut experiments . . . . .	50
3.5	Limitations . . . . .	53
<b>4</b>	<b>Computational Simulation and Analysis</b>	<b>55</b>
4.1	OLGA Multiphase Dynamic Simulator . . . . .	55
4.1.1	Basic Equations . . . . .	56
4.2	Simulation setup . . . . .	58
4.2.1	Geometric setup and Input conditions . . . . .	58
4.3	Analysis and Discussion . . . . .	60
4.3.1	Repeated Two Phase Surge Wave Simulations . . . . .	60
4.3.2	Three Phase Simulations . . . . .	66
4.3.3	Limitations . . . . .	76
<b>5</b>	<b>Conclusion</b>	<b>77</b>
5.1	Concluding Remarks . . . . .	77
5.2	Suggestions for further work . . . . .	79
	<b>Bibliography</b>	<b>81</b>
	<b>Appendix</b>	<b>85</b>
A	Camera Images: Initial Cases . . . . .	86
B	Camera Images: Varying Water Cuts . . . . .	107
C	Simulation: Repetition of Two Phase Flow Surge Wave Simulations	116
D	Simulation: Three-Phase Surge Wave Simulation . . . . .	124
E	Risk Assessment Report . . . . .	130

# List of Tables

3.1	Table showing the test matrix values for air,water and oil experiments employed for this work . . . . .	44
3.2	Table showing the test matrix values for air,water and oil experiments employed for this work . . . . .	44
3.3	Table showing the test matrix used for Case 1 experiments with varying water cut . . . . .	45
3.4	Table showing the test matrix used for Case 2 experiments with varying water cut . . . . .	45
3.5	Table showing the test matrix used for Case 3 experiments with varying water cut . . . . .	45
3.6	Table showing the test matrix used for Case 4 experiments with varying water cut . . . . .	46
3.7	Table showing the test matrix used for Case 5 experiments with varying water cut . . . . .	46
3.8	Table showing the test matrix used for Case 6 experiments with varying water cut . . . . .	46
3.9	Table showing the test matrix used for Case 7 experiments with varying water cut . . . . .	46
4.1	Setup geometry applied for simulations . . . . .	58
4.2	Flow rate input used to initiate waves for Case 2 [ $U_{SG} = 10.9$ m/s $U_{SL} = 0.0113$ m/s] . . . . .	60
4.3	Flow rate input used to initiate waves for Case 1 [ $U_{SG} = 8.95$ m/s $U_{SL} = 0.0144$ m/s] . . . . .	66
5.1	Flow rate input used to initiate waves for Case 1 . . . . .	116
5.2	Additional Input Case 1 . . . . .	116
5.3	Flow rate input used to initiate waves for Case 2 . . . . .	117
5.4	Additional Input Case 2 . . . . .	117
5.5	Flow rate input used to initiate waves for Case 3 . . . . .	118
5.6	Additional Input Case 3 . . . . .	118
5.7	Flow rate input used to initiate waves for Case 4 . . . . .	119
5.8	Additional Input Case 4 . . . . .	119
5.9	Flow rate input used to initiate waves for Case 5 . . . . .	120

---

5.10	Additional Input Case 5 . . . . .	120
5.11	Flow rate input used to initiate waves for Case 6 . . . . .	121
5.12	Additional Input Case 6 . . . . .	121
5.13	Flow rate input used to initiate waves for Case 7 . . . . .	122
5.14	Additional Input Case 7 . . . . .	122
5.15	Flow rate input used to initiate waves for Case 8 . . . . .	123
5.16	Additional Input Case 8 . . . . .	123
5.17	Flow rate input used to initiate waves for Case 1 [ $U_{SG} = 8.95$ m/s $U_{SL} =$ 0.0144 m/s] . . . . .	124

# List of Figures

2.1	A cross sectional view of a typical two-phase gas liquid flow in a horizontal or near horizontal circular pipe. . . . .	4
2.2	An image showing flow regimes in horizontal channel orientation. a.bubble flow b.plug flow c.stratified flow d.wavy flow e.slug flow f.annular flow g.spray or drop flow . . . . .	5
2.3	An image showing flow regimes in vertical channel orientation. a.bubble flow b.plug flow c.churn flow d.wispy annular flow e.annular flow f.spray or drop flow . . . . .	6
2.4	Images showing flow regimes in three-phase horizontal channel orientation described in (i) and (ii) recalled from [6, p. 332] . . . . .	6
2.5	Images showing flow regimes in three-phase horizontal channel orientation described in (iii) and (iv) recalled from [6, p. 333] . . . . .	7
2.6	Images showing flow regimes in three-phase horizontal channel orientation described in (v) and (vi) recalled from [6, p. 333] . . . . .	8
2.7	Images showing flow regimes in three-phase horizontal channel orientation described in (vii) and (viii) recalled from [6, p. 334] . . . . .	8
2.8	Images showing flow regimes in three-phase horizontal channel orientation described in (ix) and (x) recalled from [6, p. 334] . . . . .	9
2.9	Illustration of a wave flowing through a pipe from previous experiments. .	12
2.10	Relationship between Liquid accumulation and Production rates of condensate and glycol. . . . .	13
2.11	Roll wave observed in laboratory from previous experiments for air/water systems. . . . .	14
2.12	Pressure drop and liquid level simulation from PMS module in Ormen Lange field [25, p. 12] . . . . .	15
2.13	Field layout for Mikkell and Midgard fields tied to Åsgard B facility. . . .	16
2.14	A figure showing rates of gas, condensate and MEG during low rate test - though there are oscillations, it can be seen that condensate precedes MEG surge [36, p. 4] . . . . .	16
2.15	A figure showing effect of choke on rates of gas, condensate and MEG [36, p. 9] . . . . .	17
2.16	Field layout for Ormen Lange Field. . . . .	18

---

2.17	Liquid holdup profiles in Ormen Lange at start time and after 4 hours[25, p. 10] . . . . .	18
2.18	Liquid holdup profiles in Ormen Lange at 18 hours after start time [25, p. 10]	19
2.19	Field layout for Snøhvit field [13, p. 8] . . . . .	19
2.20	Snøhvit field location and installation [23, p. 1][14, p. 18] . . . . .	20
2.21	Comparisons of simulated and measured start-up rates after shutdown [23]	20
2.22	Geographic description of location of Block 2 Offshore Tanzania Field. . .	21
2.23	Subsea Layout of Tanzania Field . . . . .	22
2.24	Phase envelopes for the fields . . . . .	22
2.25	Liquid Fractions at Typical Operating conditions for different fields . . .	23
2.26	An image showing the experimental setup used for experimentation on surge waves at IFE. Gamma densitometers and pressure transducers arrangement is visible . . . . .	24
2.27	Schematic layout of the front and tail of the liquid surges. . . . .	25
2.28	Layout showing phenomenon of surge wave end shock. . . . .	25
2.29	Schematic layout of the dip configured into the test setup shown in <b>Fig. ??</b> .	26
2.30	Layout showing characteristic phenomenon of surge wave formed by dip geometry. . . . .	26
2.31	Schematic layout showing geometry of the test rig at NTNU multiphase laboratory used for the master thesis. . . . .	28
2.32	The test matrix employed in the master thesis work. . . . .	28
2.33	Screenshots of Case 2 [ $U_{SG} = 10.9$ m/s $U_{SL} = 0.0113$ m/s] showing surge wave passing through test section at first camera at position 6,44m [18, p. 43]	29
2.34	A plot showing the wave shape changes and hold up behavior for a case in the previous master thesis work . . . . .	29
2.35	Excerpts of plots from previous master thesis [18, p. 45-46] . . . . .	30
2.36	Excerpts of plots from previous master thesis [18, p. 68,71] . . . . .	31
2.37	Excerpts of plots showing comparisons of simulator performance to experimental data from previous master thesis [14, p. 45-46] . . . . .	32
2.38	Schematic layout of rig used in project work . . . . .	33
2.39	The air-water test matrix employed in the project work . . . . .	33
2.40	Laboratory data showing hold up vs time for case 1 $U_G = 13.4$ m/s $U_L = 0.0113$ m/s at Probe 1,2 and 3 . . . . .	34
2.41	The air-water-oil test matrix employed in the project work . . . . .	34
3.1	A schematic illustration of the air loop at the multiphase flow lab at NTNU. [Provided by NTNU] . . . . .	38
3.2	A schematic illustration of the water loop at the multiphase flow lab at NTNU. [Provided by NTNU] . . . . .	39
3.3	A schematic illustration of the oil loop at the multiphase flow lab at NTNU. [Provided by NTNU] . . . . .	40
3.4	Schematic layout of the test rig at the NTNU multiphase laboratory employed for the experimentation of this project work. This shows the distances and positioning of equipment and specific geometry manipulations to achieve initiation of surge waves . . . . .	41
3.5	Plots showing the effect of curve smoothing with different filters 0.01,0.05 and 0.1 . . . . .	43

---

---

3.6	Images showing Case 1 [ $U_{SG} = 8.95$ m/s, $U_{SL} = 0.0144$ m/s] at Camera 1 position at the 6.4m . . . . .	48
3.7	Images showing Case 1 [ $U_{SG} = 8.95$ m/s, $U_{SL} = 0.0144$ m/s] at Camera 2 position at 26.7m . . . . .	49
3.8	Images showing Case 1 at 0% water cut at Camera 1 position (6.4m) . . .	50
3.9	Images showing Case 1 at 0% water cut at Camera 2 position (26.7m) . .	51
3.10	Images showing Case 1 at 0% water cut at Camera 3 position (52.3m) . .	52
3.11	Images showing comparison of main waves for Case 1 at 50% water cut at all camera positions . . . . .	52
3.12	Images showing comparison of main waves for Case 1 at 0%, 50% and 100% water cut at camera 2 position (26.7m) Orientation: right to left . .	53
4.1	Geometry setup in OLGA . . . . .	59
4.2	OLGA 2019.1 hold up plot for Case 2 [ $U_{SG} = 10.9$ m/s $U_{SL} = 0.0113$ m/s]	61
4.3	Experimental Results hold up plot for Case 2 [ $U_{SG} = 10.9$ m/s $U_{SL} = 0.0113$ m/s] [18, p. 85] . . . . .	61
4.4	OLGA 7.1 hold up plot for Case 2 [ $U_{SG} = 10.9$ m/s $U_{SL} = 0.0113$ m/s][18, p. 85] . . . . .	62
4.5	OLGA 7.3.5 hold up plot for Case 2 [ $U_{SG} = 10.9$ m/s $U_{SL} = 0.0113$ m/s] [14, p. 44] . . . . .	62
4.6	OLGA 2016.2.1 hold up plot for Case 2 [ $U_{SG} = 10.9$ m/s $U_{SL} = 0.0113$ m/s] [14, p. 44] . . . . .	63
4.7	OLGA 2019.1 wave peak hold up comparison for Cases 1 through 8 . . .	64
4.8	OLGA 2019.1 wave velocity comparison for Cases 1 through 8 . . . . .	64
4.9	OLGA 2019.1 Flow Regime Identification for Case 4 [ $U_{SG} = 7.6$ m/s $U_{SL} = 0.0113$ m/s] . . . . .	65
4.10	OLGA 2019.1 Flow Regime Identification for Case 8 [ $U_{SG} = 7.6$ m/s $U_{SL} = 0.0264$ m/s] . . . . .	65
4.11	Images showing influence of different mesh on the resulting wave, $\Delta x=1D$ and $\Delta x=2D$ . . . . .	67
4.12	Images showing influence of different meshes on the resulting wave, $\Delta x=5D$ and $\Delta x=10D$ . . . . .	68
4.13	Case 1 simulation with 2nd Order scheme at $\Delta x = 1D$ . . . . .	69
4.14	Flow regime identity for the flow path. A point at the very beginning of the pipe is included to show no formation of slugs . . . . .	70
4.15	Case 1 simulated result showing flow behavior as a result of air flow manipulation . . . . .	71
4.16	Case 1 experimental data - Conductance probe readings . . . . .	71
4.17	OLGA 2019.1 plot of Case 1 at 0% water cut . . . . .	72
4.18	OLGA 2019.1 plot of Case 1 at 50% water cut . . . . .	73
4.19	OLGA 2019.1 plot of Case 1 at 100% water cut . . . . .	74
4.20	Conductance probe readings for 0% case . . . . .	75
4.21	Plot showing comparisons of experiment and simulated results for wave velocity at 37%, 50% and 100% . . . . .	75
5.1	Images showing Case 1 [ $U_{SG} = 8.95$ m/s, $U_{SL} = 0.0144$ m/s] at Camera 1 position at 6.4m . . . . .	86

---

---

5.2	Images showing Case 1 [ $U_{SG} = 8.95$ m/s, $U_{SL} = 0.0144$ m/s] at Camera 2 position at 26.7m . . . . .	87
5.3	Images showing Case 1 [ $U_{SG} = 8.95$ m/s, $U_{SL} = 0.0144$ m/s] at Camera 3 position at 52.3m . . . . .	88
5.4	Images showing Case 2 [ $U_{SG} = 8.37$ m/s, $U_{SL} = 0.0127$ m/s] at Camera 1 position at 6.4m . . . . .	89
5.5	Images showing Case 2 [ $U_{SG} = 8.37$ m/s, $U_{SL} = 0.0127$ m/s] at Camera 2 position at 26.7m . . . . .	89
5.6	Images showing Case 2 [ $U_{SG} = 8.37$ m/s, $U_{SL} = 0.0127$ m/s] at Camera 3 position at 52.3m . . . . .	90
5.7	Images showing Case 3 [ $U_{SG} = 8.52$ m/s, $U_{SL} = 0.0124$ m/s] at Camera 1 position at 6.4m . . . . .	91
5.8	Images showing Case 3 [ $U_{SG} = 8.95$ m/s, $U_{SL} = 0.0144$ m/s] at Camera 2 position at 26.7m . . . . .	92
5.9	Images showing Case 3 [ $U_{SG} = 8.95$ m/s, $U_{SL} = 0.0144$ m/s] at Camera 3 position at 52.3m . . . . .	93
5.10	Images showing Case 4 [ $U_{SG} = 8.52$ m/s, $U_{SL} = 0.0106$ m/s] at Camera 1 position at 6.4m . . . . .	94
5.11	Images showing Case 4 [ $U_{SG} = 8.52$ m/s, $U_{SL} = 0.0106$ m/s] at Camera 2 position at 26.7m . . . . .	95
5.12	Images showing Case 4 [ $U_{SG} = 8.52$ m/s, $U_{SL} = 0.0106$ m/s] at Camera 3 position at 52.3m . . . . .	96
5.13	Images showing Case 5 [ $U_{SG} = 8.52$ m/s, $U_{SL} = 0.0060$ m/s] at Camera 1 position at 6.4m . . . . .	97
5.14	Images showing Case 5 [ $U_{SG} = 8.52$ m/s, $U_{SL} = 0.0060$ m/s] at Camera 2 position at 26.7m . . . . .	98
5.15	Images showing Case 5 [ $U_{SG} = 8.52$ m/s, $U_{SL} = 0.0060$ m/s] at Camera 3 position at 52.3m . . . . .	99
5.16	Images showing Case 6 [ $U_{SG} = 7.65$ m/s, $U_{SL} = 0.0043$ m/s] at Camera 1 position at 6.4m . . . . .	100
5.17	Images showing Case 6 [ $U_{SG} = 7.65$ m/s, $U_{SL} = 0.0043$ m/s] at Camera 2 position at 26.7m . . . . .	101
5.18	Images showing Case 6 [ $U_{SG} = 7.65$ m/s, $U_{SL} = 0.0043$ m/s] at Camera 3 position at 52.3m . . . . .	102
5.19	Images showing Case 7 [ $U_{SG} = 8.52$ m/s, $U_{SL} = 0.0025$ m/s] at Camera 1 position at 6.4m . . . . .	103
5.20	Images showing Case 7 [ $U_{SG} = 8.52$ m/s, $U_{SL} = 0.0025$ m/s] at Camera 2 position at 26.7m . . . . .	105
5.21	Images showing Case 7 [ $U_{SG} = 8.52$ m/s, $U_{SL} = 0.0025$ m/s] at Camera 3 position at 52.3m . . . . .	106
5.22	Images showing Case 1 at 0% water cut at Camera 1 position (6.4m) . . .	107
5.23	Images showing Case 1 at 0% water cut at Camera 2 position (26.7m) . .	108
5.24	Images showing Case 1 at 0% water cut at Camera 3 position (52.3m) . .	109
5.25	Images showing Case 1 at 50% water cut at Camera 1 position (6.4m) . .	110
5.26	Images showing Case 1 at 50% water cut at Camera 2 position (26.7m) . .	111
5.27	Images showing Case 1 at 50% water cut at Camera 3 position (52.3m) . .	112
5.28	Images showing Case 1 at 100% water cut at Camera 1 position (6.4m) . .	113

---

---

5.29	Images showing Case 1 at 100% water cut at Camera 2 position (26.7m)	114
5.30	Images showing Case 1 at 100% water cut at Camera 3 position (52.3m)	115
5.31	OLGA 2019.1 hold up plot for Case 1	116
5.32	OLGA 2019.1 hold up plot for Case 2	117
5.33	OLGA 2019.1 hold up plot for Case 3	118
5.34	OLGA 2019.1 hold up plot for Case 4	119
5.35	OLGA 2019.1 hold up plot for Case 5	120
5.36	OLGA 2019.1 hold up plot for Case 6	121
5.37	OLGA 2019.1 hold up plot for Case 7	122
5.38	OLGA 2019.1 hold up plot for Case 8	123
5.39	OLGA 2019.1 hold up plot for Case 1 - 37% Water Cut	124
5.40	Plot showing experimental data for Case 1 with 37% water cut	125
5.41	OLGA 2019.1 hold up plot for Case 1 - 0% Water Cut	125
5.42	Plot showing experimental data for Case 1 with 0% water cut	126
5.43	OLGA 2019.1 hold up plot for Case 1 - 50% Water Cut	126
5.44	Plot showing experimental data for Case 1 with 50% water cut	127
5.45	OLGA 2019.1 hold up plot for Case 1 - 100% Water Cut	127
5.46	Plot showing experimental data for Case 1 with 100% water cut	128



# Introduction

The value chain of subsea oil and gas production incorporates the transportation of gas-condensate through gas-condensate pipelines from offshore to onshore. The flow at this stage of the value chain is defined as multiphase flow, where oil, gas and water flow together under different conditions of pressure and temperature. In the oil and gas industry, the handling of multiphase flow is called flow assurance. This subgroup of multiphase flow denotes the safe and uninterrupted transport of well stream mixtures in pipelines [30]. Long subsea pipelines are designed to operate with sufficiently high flow rates in order to avoid liquid accumulations in the pipes. In periods of low production rates or changes in operation, these accumulations may occur and propel out as surge waves. They are quite spontaneously occurring.

Three-phase flows are known to be complex due to uncertainty in predicting the form of interaction between oil-water and gas-liquid interfaces during the flow, as well as how they are coupled. Because of the abundance of three-phase flow applications in the petroleum and chemical industries, a better understanding of this complex flow phenomena is needed. The study of such flows is of great importance due to the immense lack of literary work currently present today. Surge waves can occur in gas-condensate pipeline flows and are of concern with regard to the capacity of the receiving slug catcher. The effect of three-phase flow is in particular questioned.

Experimentation in small scale is helpful in better understanding two-liquid flows and different phenomena occurring as a result. The science explaining the formation and propagation of surge waves in flowlines is not very well understood and research within this field is highly sought after.

Some two-phase ramp up experiments have previously been done in the multiphase flow laboratory at NTNU, where a temporal dip in the gas flow rate has initiated the propagation of a wave. A similar approach has been established for three-phase flows during a student project, and will be the basis for an experimental campaign in this master study.

As there is very little experimental base work on this area of study, dynamic flow simulators have not been well qualified to predict the surge wave initiation and propagation.

---

## 1.1 Objectives

The **main objective** of this master thesis were generally to perform an experimental study on **the formation and behavior** of three-phase surge waves. The **specific goals in this work are outlined as follows**

- Determine the conditions for three-phase surge wave formation in the NTNU laboratory
- Analyse the flow behavior of liquids in surge waves in two-liquid flow
- Examine the effect of varying water cuts on the flow behavior of surge waves in two-liquid flow
- Perform simulations for a select case and compare result with experimental data

## 1.2 Thesis Structure

This thesis is divided into five chapters.

The first chapter includes an introduction to surge waves and a layout of the objectives of this work.

The second chapter discusses different related back ground pertaining to multiphase flows. It includes an introduction to basic knowledge about multiphase flows and numerical modelling of multiphase flows. It discusses different real cases of three phase flow instabilities in the industry. It continues to highlight different previous works that have already been done on this specific topic.

The third chapter describes the experimental basis of this work including a concise description of the experiments performed and their respective results.

The fourth chapter describes the modelling basis of this work, with inclusion of basic theory of the simulator applied. The modelling procedures as well as the results are discussed.

The fifth chapter is the conclusion. It gives a summary of the findings in chapters 3 and 4. It also includes some suggestions for further work.

The bibliography and appendix follow after these chapters and are useful as a reference.

# Theoretical and Conceptual Framework

## 2.1 Introduction to Multiphase Flow

### 2.1.1 Definitions

A multiphase flow is the flow of a mixture of phases such as gases (bubbles) in a liquid, or liquid (droplets) in gases, and so on.[29]. In fluid mechanics, it can also be defined as the simultaneous flow of materials with two or more thermodynamic phases [4]. Numerous industrial and energy conversion processes rely on the flow of multiphase mixtures.

A phase refers to the solid, liquid, or vapor state of matter. A phase is classified as continuous when it occupies a connected region of space. A phase is classified as dispersed when it occupies a disconnected region of space. The continuous phase could be gaseous or liquid. The dispersed phase could be either solid, liquid or gaseous. As an example, water flow with air bubbles has water as the continuous phase and air as the dispersed phase [37].

The most common form of multiphase flows are two-phase flows, which may consist of gas-liquid flows, gas-solid flows, liquid-liquid flows or solid-liquid flows. Gas-liquid flows are a strong basis for the work presented in this paper. three-phase flows consist of gas-solid-liquid flows, gas-liquid-liquid flows and solid-liquid-liquid flows. Gas-liquid-liquid flows are the primary type of three-phase flow highlighted in this paper. Multiphase flows are not restricted to three-phase flows alone, there are also four phase flow systems on some occasions. [3]

### 2.1.2 Key Parameters

In fluid dynamics, single phase flows can be described using velocity, pressure and density. When multiple phases are involved additional parameters need to be considered to fully describe the flow. Velocity, pressure and density distributions are completed by phase configuration. Phase configuration in a conduit is not easily determined in situations with several phases.[22, p. 3]

---

Taking a look at **Fig. 2.1** liquid is seen as the continuous phase at the bottom layer with entrained gas bubbles and gas as the continuous phase at the top with entrained liquid droplets.

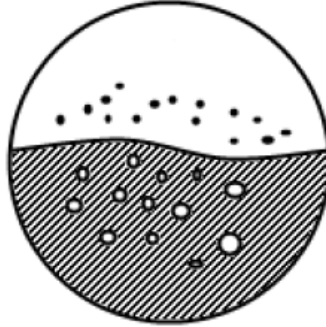


**Figure 2.1:** A cross sectional view of a typical two-phase gas liquid flow in a horizontal or near horizontal circular pipe.

Average flow rates and phase velocities can be defined from known simple relations. The areas for each phase include both the continuous and entrained components. Total flowrate and total area are equal to the sum of the flowrates as seen in eq.(2.1) and areas eq.(2.2) for each phase respectively. The number of phases are denoted by the subscript 'z'. The flowing phase is identified by the subscript 'k'.

$$Q = \sum_{z=1}^n Q_z \quad (2.1)$$

$$A = \sum_{z=1}^n A_z \quad (2.2)$$

$$U_k = \frac{Q_k}{A_k} \quad (2.3)$$

Phase velocity is defined as the average cross sectional velocity where  $A_k$  is the area occupied by that particular phase, eq.(2.3). Superficial velocity is defined as the velocity of a fluid as if it is solely flowing in a pipe. This is usually used because it is readily known and unambiguous unlike real velocity which varies from place to place. This is shown in (2.4).

$$U_{sk} = \frac{Q_k}{A} \quad (2.4)$$

The relationship between liquid amounts relative to gas are important to consider when discussing two-phase flows[22, p. 3]. A measure of this relationship is what portion of the cross sectional area is covered by liquid. This is called the holdup and is denoted by the

letter H. The portion covered by gas is known as the void fraction and is usually denoted by  $\alpha$ . To avoid confusion  $\alpha_k$  will be used to reference respective phase fractions.

$$H = \alpha_L = \frac{A_L}{A} \quad \alpha = \alpha_G = \frac{A_G}{A} \quad (2.5)$$

$$\sum_{k=1}^n \alpha_k = 1 \quad (2.6)$$

$$U_k = \frac{U_{sk}}{\alpha_k} \quad (2.7)$$

The sum of all phase fractions always equal to 1. It is necessary to note other forms of expression for the same equations such as the phase velocities in terms of phase fractions by joining equations (2.3) and (2.4) to get the expression in equation (2.7).

### 2.1.3 Flow Regime Classification

Multiphase flows can appear in different morphological configurations which are called flow regimes or flow patterns. These regimes give a description of the geometrical distribution of a multiphase fluid moving through a pipe. Flow regimes are significant in this topic because the physical transfer process in the phase-interface interaction is highly dependant on the flow regime. Thus, in selection of suitable models used for interfacial transport in multiphase flows, the flow regime must be identified. In general, the flow regime depends on the physical properties of the fluid as well as the channel geometry [37].

The flow regimes below are generally classified for two-phase flow regimes and have been adapted by many researchers experimenting on two-phase flows. The configurations in **Fig. 2.2** and **Fig. 2.3** are classified for horizontally and vertically oriented non-heated pipes [7].

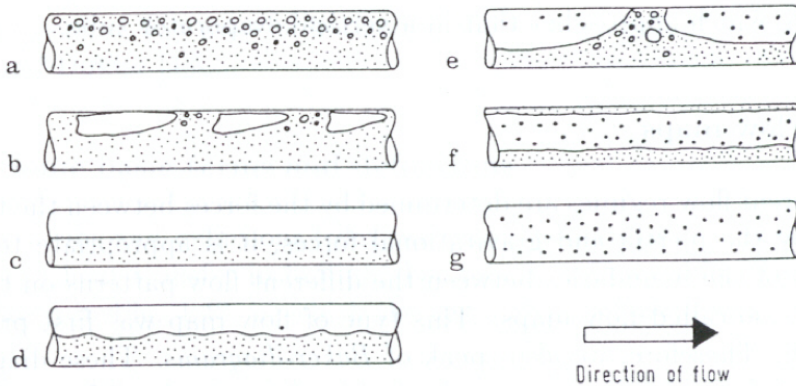


**Figure 2.2:** An image showing flow regimes in horizontal channel orientation. a.bubble flow b.plug flow c.stratified flow d.wavy flow e.slug flow f.annular flow g.spray or drop flow

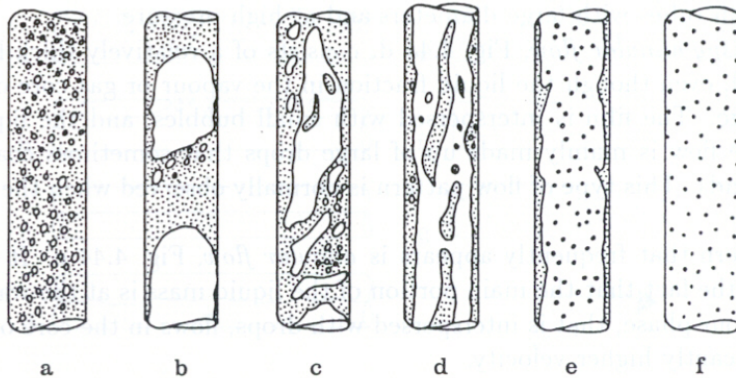


**Figure 2.3:** An image showing flow regimes in vertical channel orientation. a.bubble flow b.plug flow c.churn flow d.wispy annular flow e.annular flow f.spray or drop flow

There have been numerous investigations of two-phase flow regimes where maps have been created, whereas, three-phase flow regimes have not been studied thoroughly. From previous research publishing, some new flow regimes not present in two-phase flows are known to be present in three-phase flow. Since the work presented for this thesis is focused on a phenomenon observed in the stratified flow regime and is performed in horizontal pipes, it is useful to understand flow regimes in the same setup. These regimes are presented well by Açıkoğlu et.al [6]. They are classified based on the dominant liquid flowing through the pipe.

- (i) Oil-based dispersed plug flow Used to describe flows with relatively low water and air superficial velocities. At these flow rates, water mixes with oil causing a liquid mixture which was foamy in appearance. See 2.4a

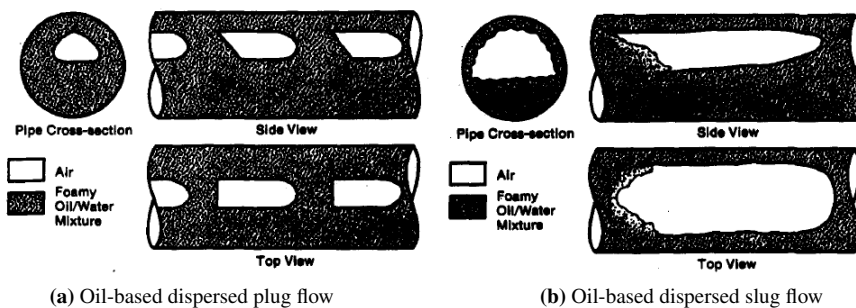


**Figure 2.4:** Images showing flow regimes in three-phase horizontal channel orientation described in (i) and (ii) recalled from [6, p. 332]

- (ii) Oil-based dispersed slug flow Increased air superficial velocity transformed flow into slug flow where air phase drove the liquid phases. The oil based flow was foamy. See 2.4b

- (iii) Oil-based dispersed stratified/wavy flow Stratification and gravitational phase separation was observed in this regime. On top of a continuous layer of water, there was an oil-based mixture having relatively large water droplets. Small-amplitude surface waves were observed on the oil/water layer. See 2.5a
  
- (iv) Oil-based separated stratified/wavy flow For this flow regime the oil and water phases were completely separated by gravitational stratification. A complicated wave structure was observed on the top of the pipe. Ripple waves were as well seen on the interface between the oil and water phase. See 2.5b

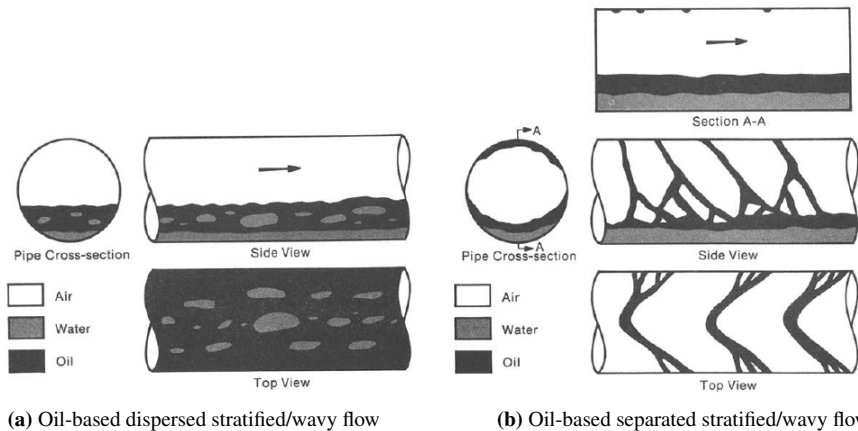
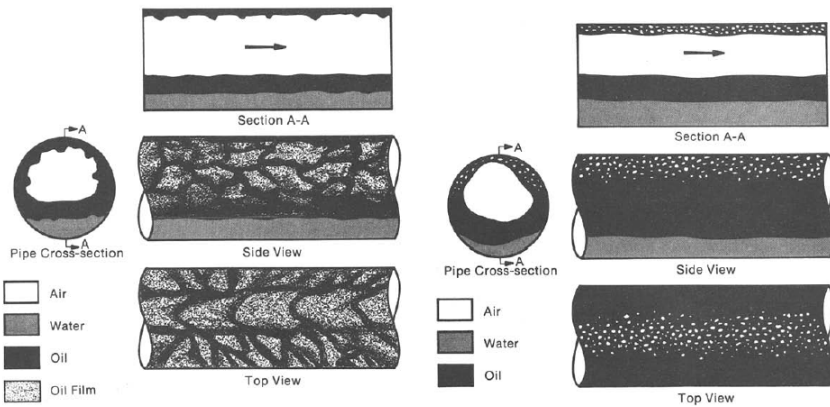


**Figure 2.5:** Images showing flow regimes in three-phase horizontal channel orientation described in (iii) and (iv) recalled from [6, p. 333]

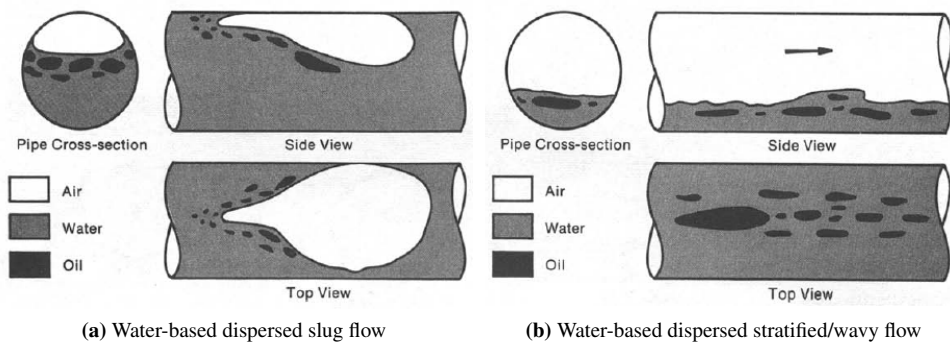
- (v) Oil-based separated wavy stratifying-annular flow Though stratification played an important role in this regime, the upper oil structures observed in (iv) became more dense in this flow regime and were connected with a thinner oil film causing wetting of the upper pipe wall. See 2.6a
  
- (vi) Oil-based separated/dispersed stratifying-annular flow As the air flow rate increases variations in the oil film thickness on the upper pipe wall disappeared. This characterized the previous flow regime in (v). Small air bubbles in the oil film were observed towards the top of pipe, see 2.6b. There is still stratification seen in the flow.



(a) Oil-based separated wavy stratifying-annular flow (b) Oil-based separated/dispersed stratifying-annular flow

**Figure 2.6:** Images showing flow regimes in three-phase horizontal channel orientation described in (v) and (vi) recalled from [6, p. 333]

- (vii) Water-based dispersed slug flow The air phase is the driving phase for this regime. Air bubbles with distinct tails were observed for relatively low air and high water flow rates. A high concentration of oil droplets were observed in the areas following the air bubbles. See 2.7a
- (viii) Water-based dispersed stratified/wavy flow This flow regime looked similar to two-phase stratified/wavy flow without the dispersed oil droplets.

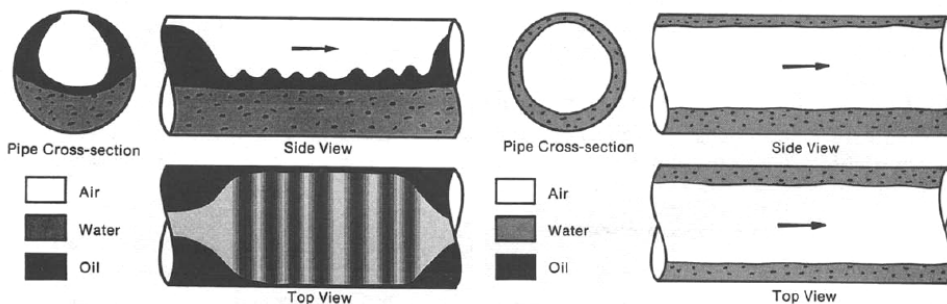


(a) Water-based dispersed slug flow (b) Water-based dispersed stratified/wavy flow

**Figure 2.7:** Images showing flow regimes in three-phase horizontal channel orientation described in (vii) and (viii) recalled from [6, p. 334]

- (ix) Water-based separated/dispersed incipient stratifying-annular flow A complicated flow is visible and said to be a transition to stratifying-annular flow. As the air flow is increased waves transform into roll waves. Liquid "phase" separation occurs, presumably due to gravitational and shear effects. See 2.8a





(a) Water-based separated/dispersed incipient stratifying-annular flow (b) Water-based dispersed stratifying-annular flow

**Figure 2.8:** Images showing flow regimes in three-phase horizontal channel orientation described in (ix) and (x) recalled from [6, p. 334]

- (x) Water-based dispersed stratifying-annular flow A water-based film continuously wetted the pipe. It contained small oil droplets dispersed in it. The water film thickness differed between the top and the bottom of the channel and was more evident at low superficial air velocities. Visibility of this diminished as air flow rate increased. Apart from the dispersed oil droplets, this flow regime was similar to two-phase stratifying-annular flow. See 2.8b

These flow regimes were made with varying oil velocities ranging from 0.043 m/s to 0.24 m/s. Regimes (iii) and (iv) diminished as superficial oil velocity increased. Air superficial velocities ranged from 0.14 m/s to 17.27 m/s. Water superficial velocities ranged from 0.004 m/s to 0.6m/s. Liquid velocities were higher than those visualized in this work. Despite this, the above list may be helpful in understanding the flows visualized in this work.

## 2.2 Introduction to Multiphase Numerical Modeling

In order for multiphase simulations to be correct and accurate, models have to be selected. These models must take into account both flow physics and fluid relative phenomenon. Theoretically, using the Navier-Stokes set of equations along with with appropriate source terms to solve for all flow parameters in a direct numerical simulation approach. This approach will not account for the flow complexity as it will be computationally demanding. In this case, it is necessary to apply other approaches [22, p. 11].

Historically, empirical models were put to use in acquiring estimates on multiphase flows. Experimental data has been used to correlate structures of important parameters such as pressure drop and velocities. They are easier to obtain and understand but are very dependant on data availability. Thus empirical models are better used to give accurate trends in flow behavior [22, p. 12] [21]. Some examples include Lockhart-Martinelli [24] for horizontal flows and Beggs and Brill [8] for inclined flows, to mention a few. These empirical models proved useful then with lack of effective mechanistic models. With the introduction of phenomenistic or mechanistic modeling, fundamental knowledge of flow

---

physics was used to define structuring between core parameters. A typical approach is using equations of continuity to get mathematical systems that can be solved numerically and are known to provide general models suited to give realistic predictions. Even with these mechanistic models, empirical models are still used at some level for closure of equation sets. This is due to limitations in the fundamental knowledge on certain effects in multiphase flow such as mass transfer and shear stress. The average models are solved with resolution that is not high enough to resolve for the smaller dynamics. Having knowledge of when and where transitions occur is important since these models differ for different flow regimes [22, p. 12] [11].

Some common mechanistic models which are the basis for the software applied in this study are described further in the following. Typical models are based on transport equations for mass, momentum and energy resulting in coupled partial differential equations. These PDEs are then integrated over control volumes. Empirical models for friction, chemical effects, mass transfer, heat transfer and other possible occurrences are used to resolve fluid relative and inter-phase interaction.

## 2.2.1 Two Fluid Model for Separated flows

For the description of stratified and annular two-phase flow, the most accurate hold up and pressure loss predictions are obtained with a two fluid approach. In the most general form, which are time-dependant and non-isothermal, there are six equations for the conservation of mass, momentum and energy of the two-phases. The two momentum equations will bring two equations of two unknowns: phase hold up and two-phase pressure gradient [29, p. 2.10]. To solve these, a number of empirical correlations are specified. The mass equations can be written as follows;

$$\delta_t(\alpha_G \rho_G) + \delta_x(\alpha_G \rho_G U_G) = \Gamma_{GL} + \Gamma_{WG} \quad (2.8)$$

$$\delta_t(\alpha_L \rho_L) + \delta_x(\alpha_L \rho_L U_L) = \Gamma_{WL} \quad (2.9)$$

Making an assumption that there is no mass transfer between the phases and through the walls,  $\Gamma_{GL} = \Gamma_{WG} = \Gamma_{WL} = 0$  leading to a simplified expression for mass conservation;

$$\delta_t(\alpha_k \rho_k) + \delta_x(\alpha_k \rho_k U_k) = 0 \quad (2.10)$$

where relation similar to (2.7) is used as a closure. The momentum equations are written as follows;

$$-\alpha_G \frac{dp}{dx} - \tau_{WG} \frac{P_G}{A} - \tau_i \frac{P_i}{A} - \alpha_G \rho_G g \sin\theta + \alpha_G \rho_G g \cos\theta \frac{dh_G}{dx} - \frac{d}{dx} G_G u_G = 0 \quad (2.11)$$

$$-\alpha_L \frac{dp}{dx} - \tau_{WL} \frac{P_L}{A} - \tau_i \frac{P_i}{A} - \alpha_L \rho_L g \sin\theta + \alpha_L \rho_L g \cos\theta \frac{dh_L}{dx} - \frac{d}{dx} G_L u_L = 0 \quad (2.12)$$

along with the relation similar to eq.2.7. The expressions  $h_G$  and  $h_L$  represent the heights of the gas layer and the liquid layer respectively.

$P_G$ ,  $P_L$  and  $P_i$  represent the perimeters for gas, liquid and the interface on the pipe wall respectively. For separated flow the shear stresses  $\tau_{Wk}$  and  $\tau_i$  are calculated by the known expression for  $\tau$

$$\tau = f \frac{\rho u^2}{2} \quad \tau_{Wk} = f_k \frac{\rho_k u_k^2}{2} \quad \tau_i = f_i \frac{\rho_G (u_G - u_i)^2}{2} \quad (2.13)$$

with  $f$  as the Fanning friction factor. For each respective phase the actual average velocities can be calculated with the expression in eq.(2.7). Difficulty arises in determination of interfacial velocity,  $u_i$ , and interfacial roughness,  $k_i$ . Hydraulic diameters are a practical way to solve the two fluid model with regard to the two fluid model as they account for pressure loss in conduits. This function uses the perimeter and area of the conduit to provide the diameter of a pipe which has proportions where the conservation of momentum is maintained. It is expressed by equation (2.14). Friction relations from single phase are employed by altering their length scale to adapt to the multiphase model [31][29, p. 2-8].

$$D_h = \frac{4A}{P} \quad (2.14)$$

For stratified flows, gas feels its flow friction as if flowing in a closed cross-sectional area  $A_G$  with the wetted perimeter covering the pipe wall perimeter,  $P_G$  and the liquid-gas interface perimeter,  $P_i$ . Liquid is treated as an open channel flow like gas is not present with a cross-sectional area  $A_L$  and wetted perimeter  $P_L$ . All variables mentioned depend on the liquid height  $h_L$  and thus on liquid holdup  $\alpha_L$  [31].

The hold up equation for stratified flow can then be formulated combining equations (2.11) and (2.12), ignoring acceleration terms and solving for liquid height,  $h_L$ :

$$F = \tau_{WG} \frac{P_G}{A_G} - \tau_{WL} \frac{P_L}{A_L} + \tau_i P_i \left[ \frac{1}{A_L} + \frac{1}{A_G} \right] - (\rho_L - \rho_G) g \sin \theta - \Delta \rho g D \cos \theta \frac{\partial h_L}{\partial \alpha_L} \frac{\partial \alpha_L}{\partial x} \quad (2.15)$$

## 2.2.2 Drift flux or Mixture Model

The basic concept of the drift flux model is the consideration of two separate phases as a mixture. Though both models are widely used and similar, this model is simpler to deal with numerically. All properties are represented as those of mixtures making it simpler than the two fluid model approach. The assumptions used to build the model eliminate some two-phase flow characteristics which attests to its simplicity and usefulness in several engineering applications[28].

Considering a simple one dimensional model with two-phases, mass conservation equations for each phase and a mixture momentum are applied. The mass equations for each phase can be defined from the expression (2.10) under the same assumption of no mass transfer between phases. The drift flux model combines the two dynamic momentum equations by summarizing the two equations defined in eq.(2.11) and eq.(2.12), [12, p. 58]. An expression for the mixture momentum is given below;

$$\delta_t (\alpha_G \rho_G U_G + \alpha_L \rho_L U_L) + \delta_x (\alpha_G \rho_G U_G^2 + \alpha_L \rho_L U_L^2 + p) = -q \quad (2.16)$$

$\alpha$ ,  $\rho$  and  $U$  represent the phase fractions, densities and phase velocities as defined in 2.1.2. The term  $p$  is the common pressure for liquid and gas and the term  $q$  is the source

term [16]. The source term is defined as the sum of the friction force contribution,  $F_w$  and the gravitational contribution,  $F_g$ . The friction force term takes into account viscous forces and forces between the wall and fluids[28].

$$F_g = g(\alpha_G \rho_G + \alpha_L \rho_L) \sin \theta \quad (2.17)$$

Closure laws are applied in terms of density models for each phase, wall friction models and a slip relation since there is relative motion of one phase with respect to the other. The term 'slip' denotes velocity differences between phases. Simple models can be used for numerical demonstration however they are known to be quite complex and given in tables based on experimental data [17][28]. The volume fractions are related using eq.(2.7).

## 2.3 Surge Waves Phenomenon

### 2.3.1 Definition

Liquid surges can be defined as separated segments of liquid film that propagate through a conduit [18]. They are identified as oscillations in liquid flow through a pipeline outlet. These oscillations can be quite slow, with typical periods ranging from 1 hour to a day or two for a 100-200km pipeline before stabilization [10]. They often have long wavelengths, making the liquid volume transported through it of significant importance. Gas is often transported along with the liquid. The pipe cross-section is not filled with liquid when these waves propagate along the flowline. This means that the dominant flow regime is stratified flow regime. Surge wave phenomenon can be termed as a special stratified flow regime.

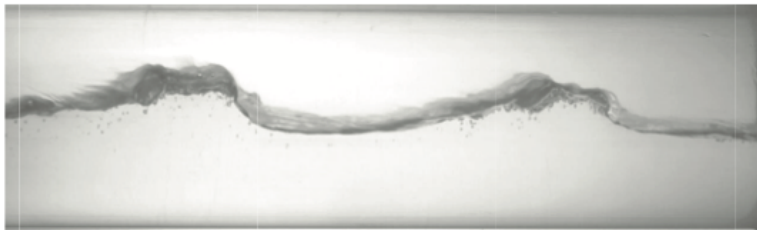


**Figure 2.9:** Illustration of a wave flowing through a pipe from previous experiments.

### 2.3.2 Mechanism

In steady stratified flows, waves may exist due to interfacial drag forces. Surge waves are experienced during transient flows. In transient flows, changes in velocity and pressure with time cause instabilities in the flow. Surge waves are a transient phenomenon formed by continuous change from one steady state to another. Surge waves in gas-condensate systems are initiated through fluctuations in local production rates. These fluctuations in flow rates can be due to operations such as shutdowns, well testing and other common operations of a production well. The fluctuations in rates form oscillations in liquid flow.

---

These oscillations are due to liquid mass waves propagating along the pipeline with a velocity close to the transport velocity of liquid [10].

During wet gas transmission through long distance pipelines, liquid accumulation occurs in lower regions of the pipe when rates are ramped down. Sudden ramp up in production flow rate propagates these accumulations as liquid surges or liquid flow oscillations through the pipeline to the receiving facilities. In flowlines with higher liquid content, unstable surge waves can be formed at lowered production rates. Production decline will cause the production rate to decline naturally, leaving the liquid to accumulate at low regions of the pipe. At the receiving facility outlet, these accumulations arrive as surges. Thus, at both low flow rates and high flow rates, surge waves can be formed. The driving force of this phenomenon is liquid accumulation.

Liquid accumulation is highly affected by the production rates through a flowline. At lower production rates, there is more liquid accumulation. Thus, small changes to the system flow rates can expel large surge waves to the outlet. Rapid increase in production rate can possibly change the state of the flow drastically, causing large surges to be expelled at the outlet. From the figure **Fig.2.10**, it can be seen that a minimum flow rate can be set in order to avoid surge waves initiation and propagation.

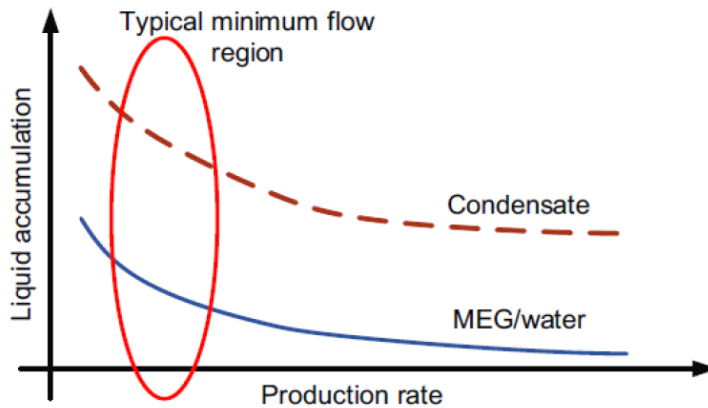


**Figure 2.10:** Relationship between Liquid accumulation and Production rates of condensate and glycol.

Surge waves can easily be confused with roll waves and slug flow. Distinguishing characteristics of surge waves are that, firstly, they bring about sudden pressure drop when the interfacial waves are above a certain size. Secondly, they usually have breaking wave fronts. Waves tend to become steep at the front and more gently sloping towards the back. Breaking of waves occurs when the particle velocities at the crest exceed the velocity of the phase travelling through a vessel. It is common to not have breaking wave fronts in small scale laboratory experiments where only small surges can be formed. In large surges however, this characteristic is visible.

---

Flows with roll waves in two-phase flows are often due to flows with higher gas densities. They are often treated as averaged stratified flow in flow models [15]. Roll waves are waves with large amplitudes that tend to roll over and create breaking waves. The fronts of roll waves are steep. The speeds and oscillations are faster than those in surge waves. Roll waves can be considered a transitional scheme to slug flow.



**Figure 2.11:** Roll wave observed in laboratory from previous experiments for air/water systems.

Slug flows are also formed when there is accumulation of liquid in the pipeline. Slug Flow is a typical two-phase flow where a wave is picked up periodically by the rapidly moving gas to form a frothy slug, which passes along the pipe at a greater velocity than the average liquid velocity. In slug flow, the pipe cross-section is blocked by liquid slugs with long lengths. The slug fronts propagate over a liquid layer, which is absorbed and accelerated to the liquid velocity in the slug front [15]. Slugging is usually a problem when the flow is liquid dominated. Surge waves are a characteristic of gas dominated flows.[14] Formation of roll waves and slugging should be carefully avoided during experimentation.

Surge waves are easily studied in the laboratory with two-phase flows. With three-phase flows the study of surge waves becomes more complicated because of the two liquids present. Similar surge wave instabilities as in three-phase flow are not reported for two-phase field flowlines, and it might therefore not be possible to reproduce this exact phenomena in two-phase in the lab.[32]

## 2.4 Numerical Modeling Contribution

Commercial multiphase fluid software have been previously applied in understanding surge waves. OLGA software is common in use. It did not seem to make a good prediction of the emerging surge waves under field conditions [10, p. 13]. Comparison made with field measurements showed that OLGA largely provides a low prediction of the onset gas rate for liquid accumulation in general. This in turn leads to an underestimation of the liquid content at low rates [23]. OLGA is not known for predicting surge waves in three-phase flow very well. It has performed well in the simulation of surge waves in two-phase flow at low-rate test, according to preceding studies.

Another alternative model simulator is called PMS which stands for pipeline management system. This is a module of a Flow Assurance System. In the Ormen Lange production system, it is documented that the PMS can compute and exhibit the condensate, water and MEG transportation [25]. Accurate predictions of the liquid surge waves in the pipelines and the liquid level in the slug catchers are noted by an upgraded PMS. **Fig.**

---

2.12 shows a series of pressure drops and liquid holdup profiles in pipeline, including the corresponding calculated and measured liquid level trends in the slug catcher [25, p. 9].

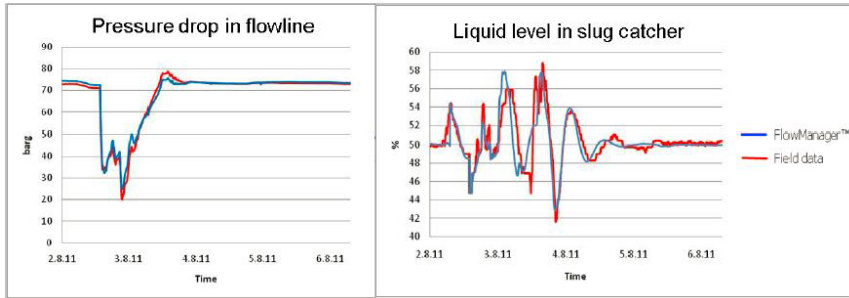


**Figure 2.12:** Pressure drop and liquid level simulation from PMS module in Ormen Lange field [25, p. 12]

## 2.5 Surge Waves in Gas Condensate Fields

Surge waves experienced at a lab scale are different from those experienced in real life cases. Surge waves are a flow assurance problem in oil and gas fields. The occurrence of surge waves is somewhat spontaneous and difficult to predict in oil and gas fields. Short reviews on some fields are made for this section.

### 2.5.1 Åsgard Field - Mikkel and Midgard

The Åsgard field is located 200 km west of Mid-Norway in 300m water depth and is one of the more complex subsea field developments on the Norwegian continental shelf. Many fields are tied back to the processing facilities which comprise of Åsgard A, Åsgard B and Åsgard C, each with a different processing facility. The Mikkel and Midgard gas condensate fields are tied back to Åsgard B which is a semi-submersible platform for gas processing[35].

For the Midgard and Mikkel condensate fields long liquid surge waves were experienced at the topside facility. This occurred at lowered rates, when liquid started to accumulate in the flowlines. The behavior of the surges depended on the gas-oil-ratio of the condensate. From data provided, the surges from these fields were of condensate and MEG, with the condensate surge arriving firstly and the MEG surge arriving after. The volumes of the surges would increase in size with decreasing rates and the handling capacity of the water/MEG at the topside defined the minimum flow rate for the flowlines. [35, p. 1].

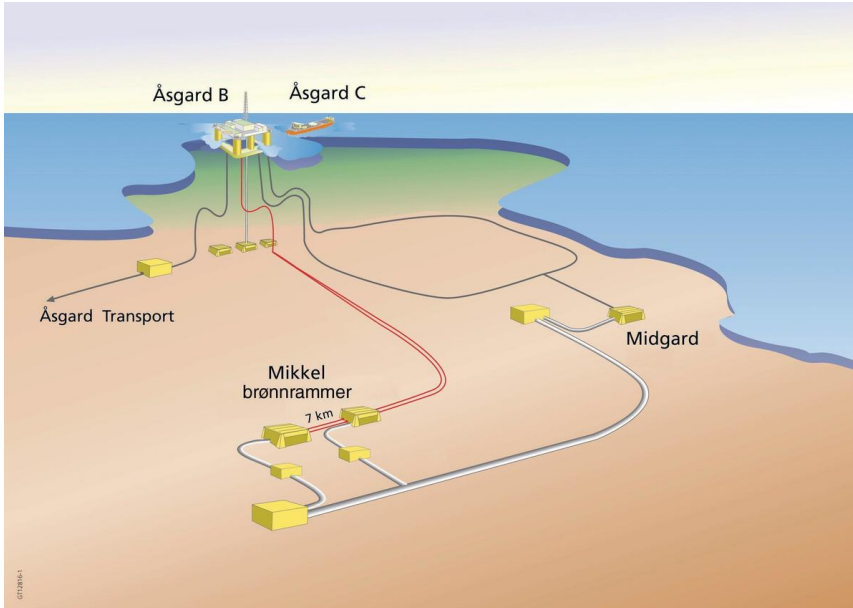


**Figure 2.13:** Field layout for Mikkel and Midgard fields tied to Åsgard B facility.

For visual representation, the figure below shows oscillations after 4 days of steady gas rate. A surge of condensate appeared first. A surge consisting of the MEG followed behind the condensate surge. After the MEG surge, the gas flow rate returns to normal, see **Fig.2.14** [36, p. 4]. At low production rates, even with unchanged gas rates, there would be oscillatory behavior of the MEG and condensate when the liquid content in the pipeline was observed.

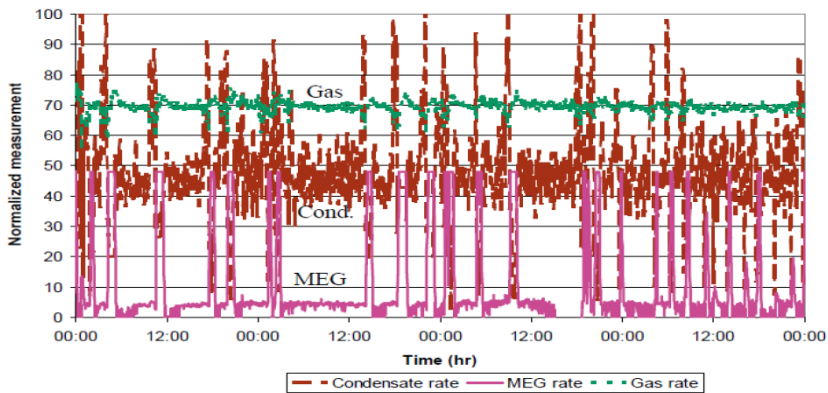


**Figure 2.14:** A figure showing rates of gas, condensate and MEG during low rate test - though there are oscillations, it can be seen that condensate precedes MEG surge [36, p. 4]

A proposed method of control was reduction in pressure in the flowlines to allow gas flow rate increase. This would allow the liquids to move through the pipeline efficiently



and avoid accumulations. Production chokes were used to implement this as they affected liquid rates more than air rates, see **Fig. 2.15**. This is a cheaper method applied in the fields [36, p. 9].

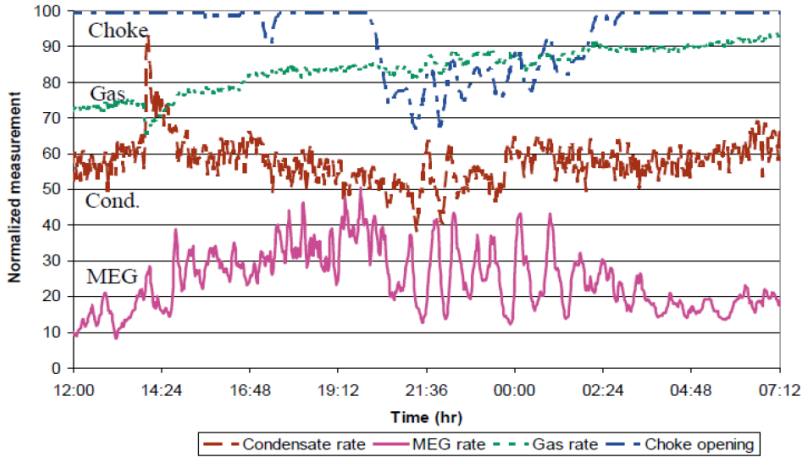


**Figure 2.15:** A figure showing effect of choke on rates of gas, condensate and MEG [36, p. 9]

## 2.5.2 Ormen Lange Field

Ormen Lange is located in the southern part of the Norwegian Sea. It was approved for development in 2004. Ormen Lange is a gas and condensate field, with sea depths between 800 to more than 1 100 meters. It has been developed with up to 32 wells and contains up to four subsea templates [20]. The flow assurance challenges experienced at the Ormen Lange field are extremely significant. The main challenge faced at this field is the liquid surges. Fluids that are not treated and are transported over long distances in the hilly terrains cause surge waves in the pipelines.[25]

A pipeline management system module (PMS) is used to calculate pipeline flowing conditions and the values of receiving devices [20, p. 1]. It was indicated that long transportation of untreated fluids in a hilly seabed terrain induces liquid surges in the pipelines due to liquid accumulation at low rates. The result can bring about flooding of topside receiving facilities such as the slug catchers.

Some evidence of surge waves at the field can be seen from the liquid holdup profiles in **fig. 2.17** and **fig. 2.18**. These profiles were generated during a shut-in procedure of all wells. In 4 hours, the accumulated liquid travelled through the pipeline as a considerably large surge wave [25, p. 9]. After 18 hours the liquid accumulation was not as visible in the holdup profile, similar with the fluctuations. This possibly indicates the surge wave arrived in the slug catcher.

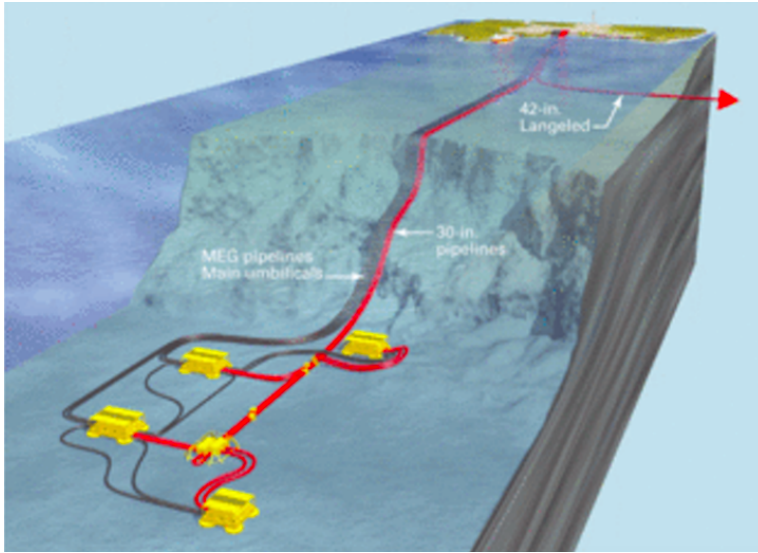


**Figure 2.16:** Field layout for Ormen Lange Field.

PMS plays a good role in predicting the surge waves and monitoring the changes of liquid holdup. Because of the established module, the ramp-up speed is optimized so that the flooding at the receiving facilities is avoided [20, p. 13].

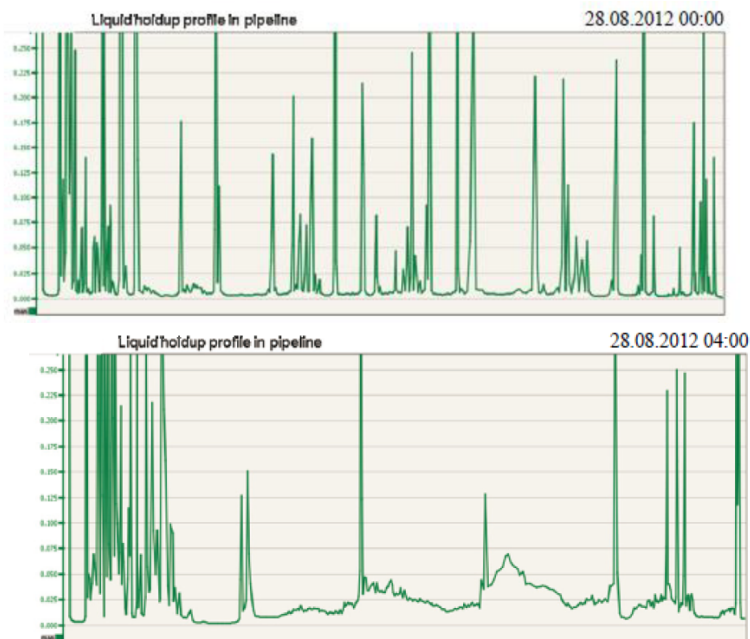


**Figure 2.17:** Liquid holdup profiles in Ormen Lange at start time and after 4 hours [25, p. 10]

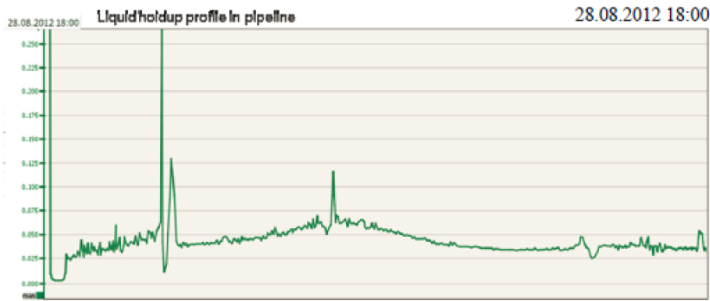


**Figure 2.18:** Liquid holdup profiles in Ormen Lange at 18 hours after start time [25, p. 10]

### 2.5.3 Snøhvit Field

Snøhvit field is in the central part of the Hammerfest basin in the south part of Barents Sea on the North Continental Shelf. It was the first developed in the Barents Sea with a water depth of 310-340 metres. The field includes Snøhvit, Albatross and Askeladd structures which has been developed in multiple phases overtime. Several subsea templates are employed in the development of the field. The well stream is transported in a 160 km pipeline to the LNG processing facilities at Melkøya. CO<sub>2</sub> separation is performed for re-injection to the underground aquifer. Produced fluids are natural gas and condensate.[1]

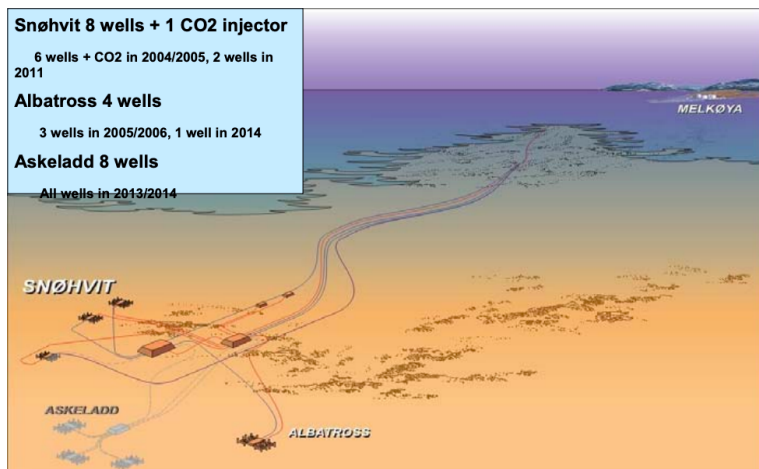


**Figure 2.19:** Field layout for Snøhvit field [13, p. 8]

One among the challenges in operation at Snøhvit is the long distance multiphase flow. The two relevant flow patterns for this field are stratified flow and slug flow [13]. At the onset stage of operation of the LNG facility, production was shut down often. Liquid accumulation is a common phenomenon during shutdown operations. In order to avoid surges of accumulations during start-up operations, production should be gradually increased to the preexisting state before shut-down. In this way the liquid accumulations of condensate and MEG travelling along the pipe can be monitored [23, p. 8][14, p. 18].

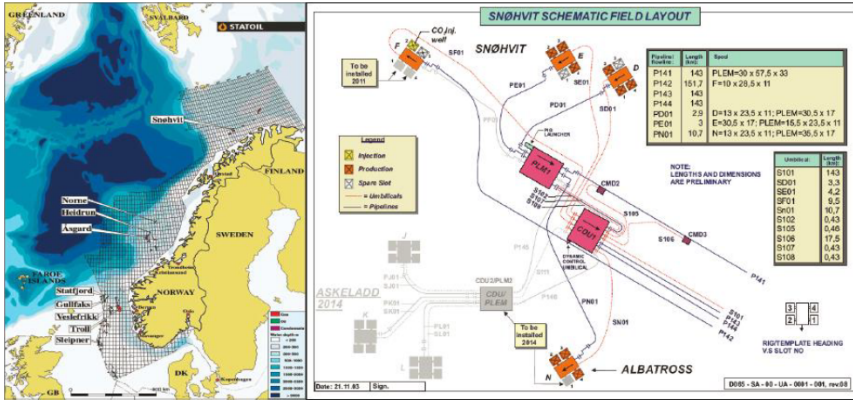
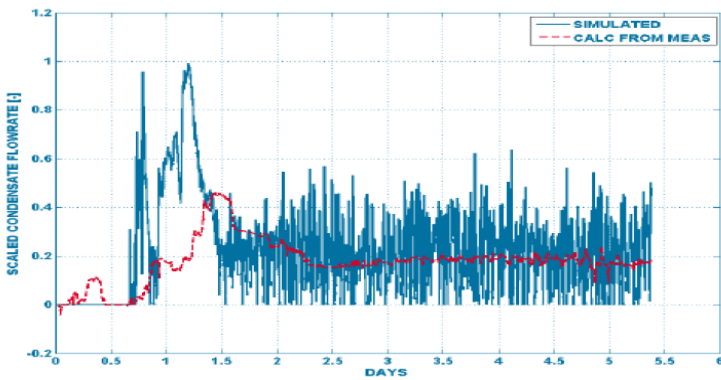
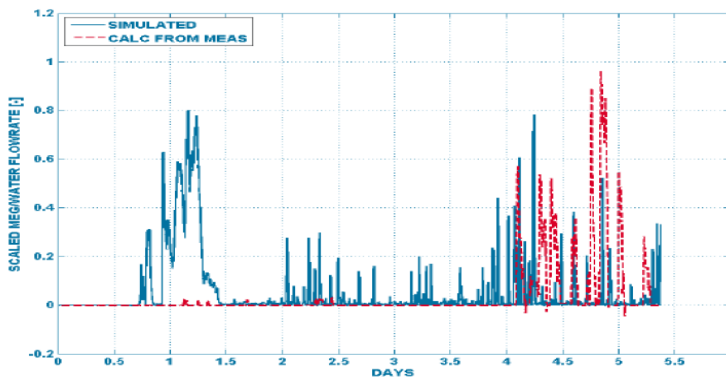


Figure 2.20: Snøhvit field location and installation [23, p. 1][14, p. 18]



(a) Predicted and measured condensate start-up rates after long shutdown



(b) Predicted and measured MEG/H<sub>2</sub>O start-up rates after long shutdown

Figure 2.21: Comparisons of simulated and measured start-up rates after shutdown [23]

The simulated plots were created from a tuned model using OLGA software. **Fig.2.21a** shows that the prediction made by simulation appears to have a higher condensate peak

---

value and appears earlier than the measured value on field. For MEG/H<sub>2</sub>O in **Fig.2.21b**, there is a large delay in appearance of surge peak between the simulated prediction and the actual measurement on field. The accumulation also lasts for a longer period in reality than the simulated estimate[23, p. 9-10].

Conclusively, in this case, OLGAs were not the best tool to be used for prediction of accumulation. In both situations the accumulations were found to be predicted earlier than actual time. This is to be expected from simulated prediction models.

## 2.5.4 Tanzania Field - Block 2 Offshore

The subsea gas development of Block 2 offshore Tanzania is characterized with water depths up to 2600 meters and a 100 km distance from shore. The fluid flow is three-phase. Though multiphase models have been made for the field, there is a lack in experimental data for conditions of low liquid loading at high gas velocities.[19, p. 409]

It is noted that local differences in water depth at the field introduce significant static head in flow lines caused by liquid accumulation in low flow parts of the flow line. In reality these accumulations contain hydrate inhibitors like MEG which adds hydrate risk. [19, p. 412]

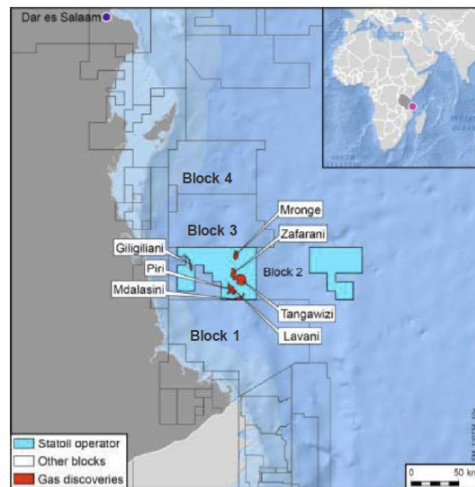


**Figure 2.22:** Geographic description of location of Block 2 Offshore Tanzania Field.

These experiments were carried out at a large scale at the SINTEF large scale multiphase flow laboratory in Trondheim, Norway. The pipelines used were near-horizontal with diameters of 8 inch and 12 inches. Experiments were performed based on low liquid loading at higher water cuts. The combined effect of very low content of condensate combined with relatively high reservoir temperature and high water saturation of the gas is known to result in high water cuts at typical pipeline operating conditions [19, p. 413]. MEG injection adds to the increase of water cut along the pipeline. This can be observed by looking at the typical phase envelopes for the fields.



**Figure 2.23:** Subsea Layout of Tanzania Field

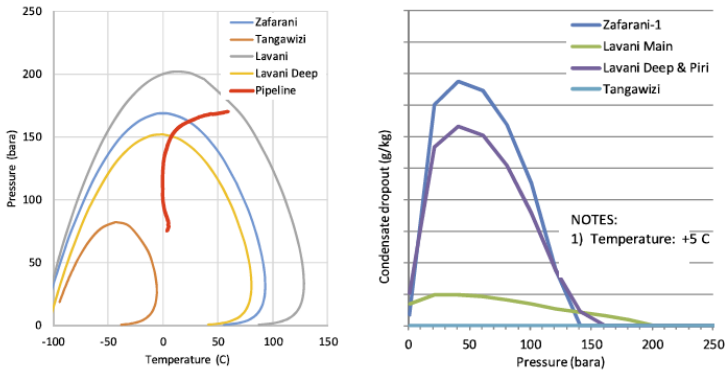


**Figure 2.24:** Phase envelopes for the fields

The Tanzania fields were characterized by higher water cuts in comparison with other fields such as Ormen Lange and Snøhvit in Norway. This is a characteristic of the reservoir fluids present. In combination with MEG injections and reservoir temperatures being high, at higher gas superficial velocities there is a higher possibility of low liquid loading. As well, from the experiments performed in 2017 and 2018, the frictional pressure drop increased when there were three-phases flowing with higher water cut. This could not be easily projected on dynamic simulators OLGA and Leda Flow [19, p. 418]. As a result of this low liquid loading phenomenon, surge waves are a risk.

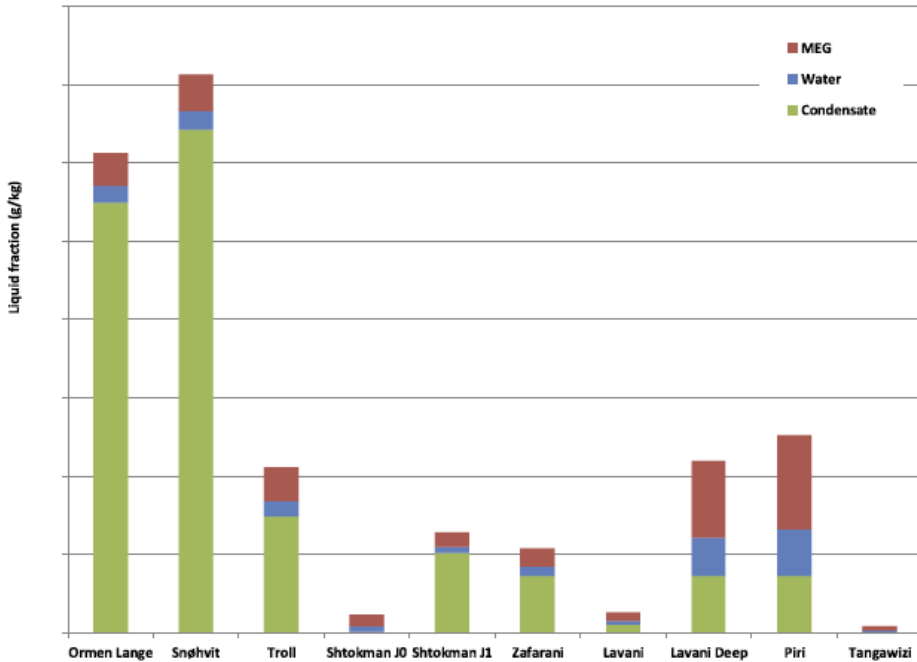


Figure 2.25: Liquid Fractions at Typical Operating conditions for different fields

## 2.6 Previous Work on Surge Waves

### 2.6.1 IFE experiments

IFE conducted studies on two-phase surge waves. The evaluation included analysis of both experimentation and numerical simulation. The experiments were performed using a closed multiphase loop with a 25 meter long test section at the IFE facility. PVC pipes were employed with an inner diameter of 10 cm. Gamma densitometers and differential pressure transducers were used to measure holdup and pressure gradients respectively along the pipeline test section [14].

SF6-water, SF6-ExxsolD80 and SF6-Marcos were the gas-liquid combinations used for the experiments. SF6 is used as a gas phase because it possesses a molecular mass five times that of air. It makes the phenomena through the transparent pipes similar to those in gas condensate pipes due to its high gas density at moderate pressures. The liquid phase (water) is ordinary tap water. The ExxsolD80 is a transparent, light, solvent oil. SF6-ExxsolD80 has a density higher than ExxsolD80 at standard atmospheric conditions. The Marcos oil is a mixture of the two oils Marcos 82 and Marcos 52. Marcos is a medical white oil, without color and odor. A mixture ratio of 3:2 between the 82 and 52 oils should give a mixture lower viscosity. [27, p. 14]. The gas and liquid are separated before entering into the test section, mixed when entering the pipe, and flows as layered fluid along the pipe. [27, p. 12].

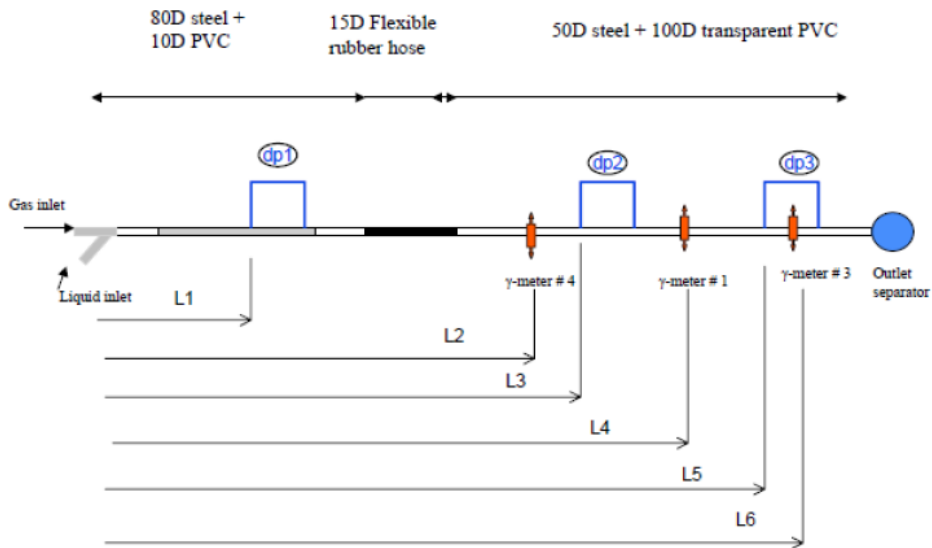


**Figure 2.26:** An image showing the experimental setup used for experimentation on surge waves at IFE. Gamma densitometers and pressure transducers arrangement is visible

### 2.6.1.1 Propagation of long liquid surge waves

Long surge waves were studied. This was done in order to gain an understanding of the velocities of the front and tail of long surge waves for a range of gas flow rates and initially dry pipe wall ahead of the surge wave. Experiments were carried out with variations in pressure, surface tension, gas density and pipeline inclination for all three combinations. The pipeline was set up with straight geometry and had an inclination of  $-1^\circ$  to  $4^\circ$  [27, p. 12].

The mechanism used to initiate the long surge waves was as follows:

- Dry pipe and single phase gas flow was created using the gas compressor in the pipeline.
- The gas flow rate was adjusted to a predefined value and a long surge wave was initiated by a sudden start of the liquid pump.
- Liquid entered upstream of the pipeline, and propagated as a positive surge wave
- After some time, the holdup increase stopped creating a steady state two-phase flow along the pipeline.
- The liquid pump was switched off, holdup decreased and a negative surge was initiated. The entire surge wave was eventually expelled out of the pipeline.

The observations for the long liquid surges were as follows [27, p. 14]:



- The positive surge front moved faster for water than the oil. The positive surge front velocity also increased with rise in superficial liquid velocity ( $U_{sl}$ ) and decreasing inclination.
- The negative surge tail velocity moved slower than the front.
- The velocity increased with increasing gas velocity.
- The tail velocity does not depend on pipeline inclination and is less for liquid with highest viscosity.

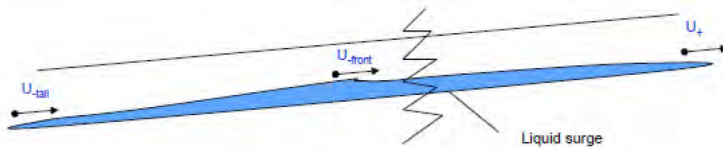


**Figure 2.27:** Schematic layout of the front and tail of the liquid surges.

At certain ranges of gas flow rates, the surge wave end would have an end shock. This would occur as a result of the gas flow rates being lower than the minimum gas flow rate needed to expel liquid out of the pipe. This phenomenon is illustrated below in **Fig. 2.28**

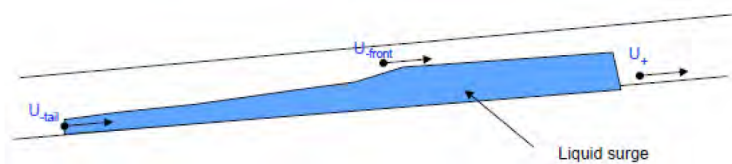


**Figure 2.28:** Layout showing phenomenon of surge wave end shock.

### 2.6.1.2 Finite length surges generated by dip

Dips in pipe geometry are often referred to as 'low regions' in the flowline. It is at these locations where liquid accumulation in flows with liquid phase present occur. In gas-condensate pipeline flows, accumulation in lower regions is common at low rates such as during ramp up after a shut down. Thus, this is a method used to induce surges in experimental setting. The driving force for this accumulated liquid is the interfacial drag force between the gas and the liquid. [27, p. 23]

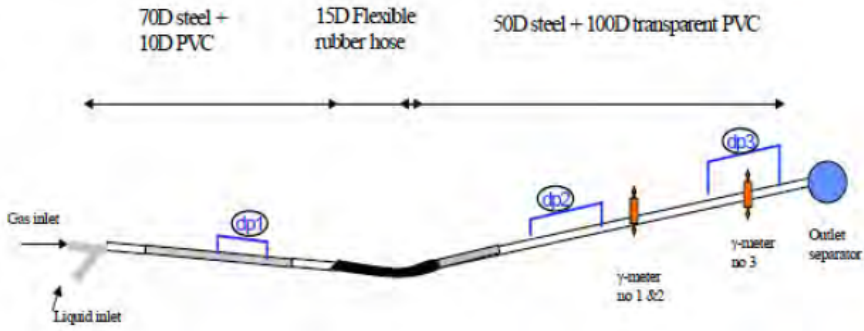


**Figure 2.29:** Schematic layout of the dip configured into the test setup shown in Fig. ?? .



**Figure 2.30:** Layout showing characteristic phenomenon of surge wave formed by dip geometry.

The test section in the lab was modified to incorporate a dip in the geometry with 10 m downward inclination from the start to the dip and a 15 m upward inclination from the dip onward. The upward inclination was varied between  $0.5^\circ$  and  $2^\circ$ . Surge wave experiments were then carried out after the test section was dried. The waves were initiated after pumping liquid through the section causing a blow-out to occur. The waves generated using this method are characterized by a distinct front, a hold up peak value and a long tail to follow, as seen in **Fig. 2.30**. [27, p. 23-24].

The shape of the waves created did not reach a steady state condition. It is probable that these waves do reach a steady state with time or remain unstable for long periods as thin liquid films in long conduits. [27, p. 25]

Observations made for waves generated by dip geometry can be noted as follows [27, p. 25]:

- The front and peak velocities are quite close; with the tail velocity significantly lower.
- Amount of liquid accumulated in the low point of the dip is expelled through the pipeline faster for water than for oil.
- The duration time for experimentation and the front and peak velocities increase with rise in liquid volume accumulated.

- 
- With an increase in gas velocity the peak holdup increases slightly.
  - The peak holdup increases with increasing liquid volume accumulated in the dip.
  - Peak holdup decreases as pipe inclination increases.

The shape of the waves created did not reach a steady state condition. It is probable that these waves do reach a steady state with time or remain unstable for long periods as thin liquid films in long conduits.[27, p. 25]

### **2.6.1.3 Surges generated by pump**

These experiments were carried out due to the absence of a steady state for the dip generated waves. Straight geometry was used to initiate the waves with a 4° inclination. The liquid pump was strategically turned on and off to induce the waves. Front and tail velocities showed no much difference which showed that they do not change shape. The peak and shape of holdup curve also did not change much along the test section with respect to time and position.[27, p. 28-29]

### **2.6.1.4 Sequential Double Surges**

Two surges in sequence were tested experimentally to observe the effect of the thin liquid film from the first wave on the following. An observation was made of the effect on the following wave velocity. The pipe geometry as used in pump generated surges was employed. The pump was turned on to initiate a positive surge and then turned off after some time to bring a new surge in the flow. The hold up and front velocity for the first surge behaves as the surges in the section describing long surge wave behaviors. The velocity of the following surge was slightly lower than the first. The differences were however insignificant and the wetness of the pipe is concluded to not be a big influence.

## **2.6.2 Master Thesis two-phase Surge Wave Experiments**

The scope of the thesis by Steinar Grøhdahl [18] is a basis for this current work, as seen in chapter 4. Laboratory experiments were performed on surge waves at the NTNU multiphase flow laboratory at the department of Energy and Process Engineering. The surges were induced by ramp down and ramp up of gas flow rates for a selected range of liquid rates. The liquid used was water. The pipeline length for the flow test section was 57.84 metres. Conductance probes measurements were used to calculate the hold up and perform calibrations on the rig. Six probes were placed out along the pipeline to measure the volume fraction of water. The probes were positioned at 6,44 m, 15,88 m, 29,92 m, 38,54 m, 45,12 m and 54,02 m downstream of the inlet nozzle.[18, p. 37]. Cameras were placed along the pipeline at 6,85 m, 30,54 m and 55,02 m downstream of the inlet nozzle.[18, p. 40]

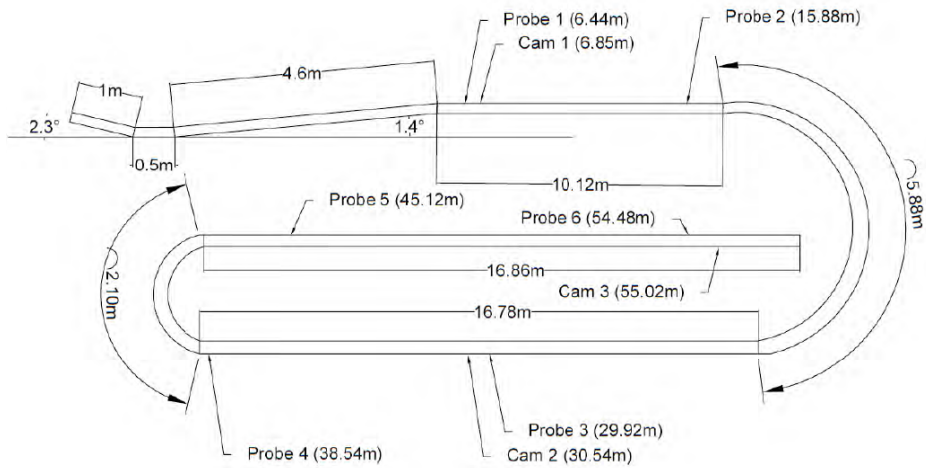


**Figure 2.31:** Schematic layout showing geometry of the test rig at NTNU multiphase laboratory used for the master thesis.

The experiments performed were summarized and presented in eight cases using the test matrix in the figure below.

Case:	Initial air flow rate		Initial air valve opening [% of full opening]	Water flow rate	
	$U_{sg}$ [m/s]	$\dot{m}$ [kg/s]		$U_{sl}$ [m/s]	$\dot{m}$ [kg/s]
1	13,4	0,045	27	0,0113	0,032
2	10,9	0,037	25	0,0113	0,032
3	8,5	0,029	23	0,0113	0,032
4	7,6	0,026	22	0,0113	0,032
5	13,4	0,045	27	0,0264	0,075
6	10,9	0,037	25	0,0264	0,075
7	8,5	0,029	23	0,0264	0,075
8	7,4	0,025	22	0,0264	0,075

**Figure 2.32:** The test matrix employed in the master thesis work.

Cameras at different positions were used to capture images of the surge waves passing through the test section. On **Fig.2.33** a visual of a series of images showing a passing surge wave are seen.

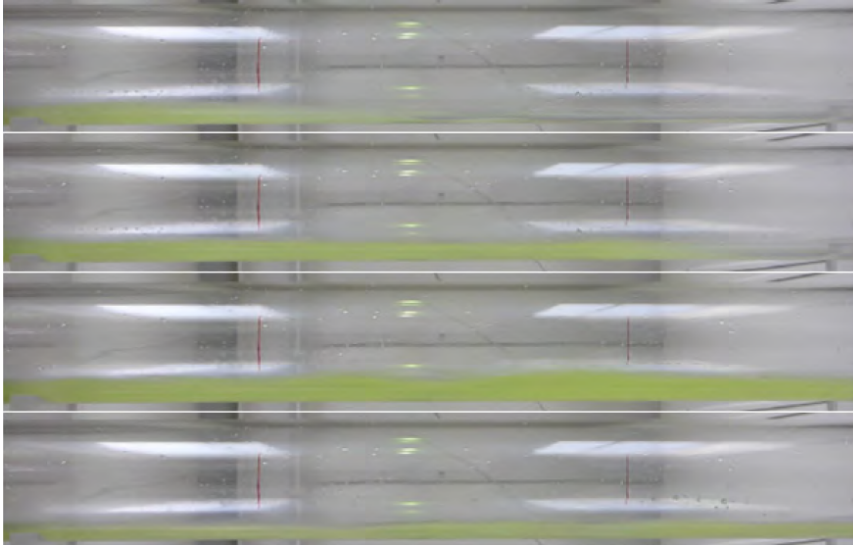


**Figure 2.33:** Screenshots of Case 2 [ $U_{SG} = 10.9$  m/s  $U_{SL} = 0.0113$  m/s] showing surge wave passing through test section at first camera at position 6,44m [18, p. 43]

Plots were then made to observe changes in hold up along the pipeline as measured at different probes and in order to observe the wave shape changes and rates of these shape changes, see **Fig. 2.34** and **Fig. 2.35a**. Comparisons were also made between wave propagation velocity between the probes, see **Fig. 2.35b**.

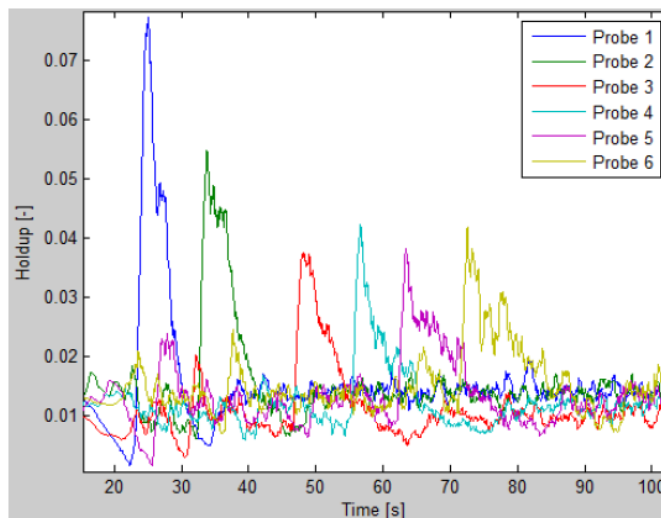
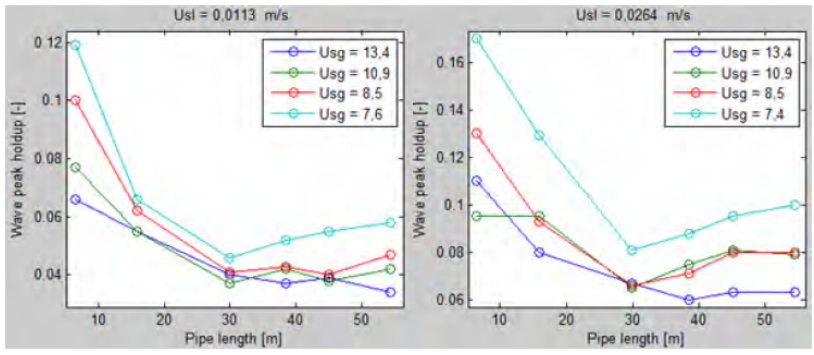


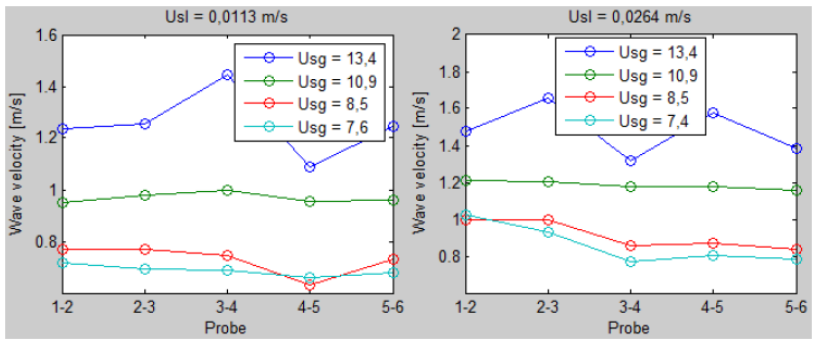
**Figure 2.34:** A plot showing the wave shape changes and hold up behavior for a case in the previous master thesis work

Simulations were also performed for all 8 cases in **Fig. 2.32** using dynamic simulators

OLGA and Leda Flow. The OLGA model used was OLGA7.1. Results for both simulators were compared and analyzed based on mesh size and various models in the simulators. Two variables were observed which were wave holdup and wave velocity. OLGA simulations were found to match well with the experimental data findings. The results from the OLGA 7.1 simulations will be compared with results in this thesis.



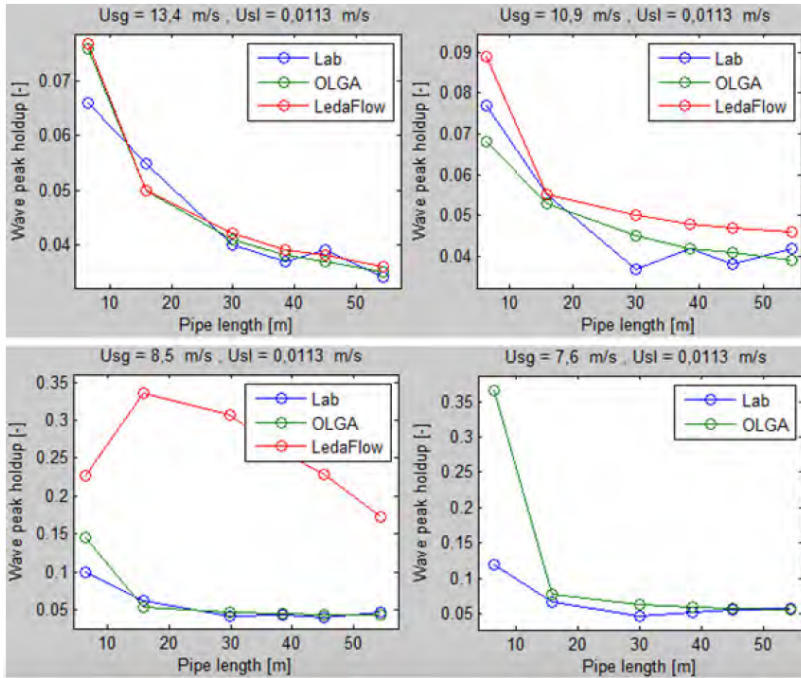
(a) A plot showing the differences in wave peak hold up along the test section versus the pipe length for changing gas velocities



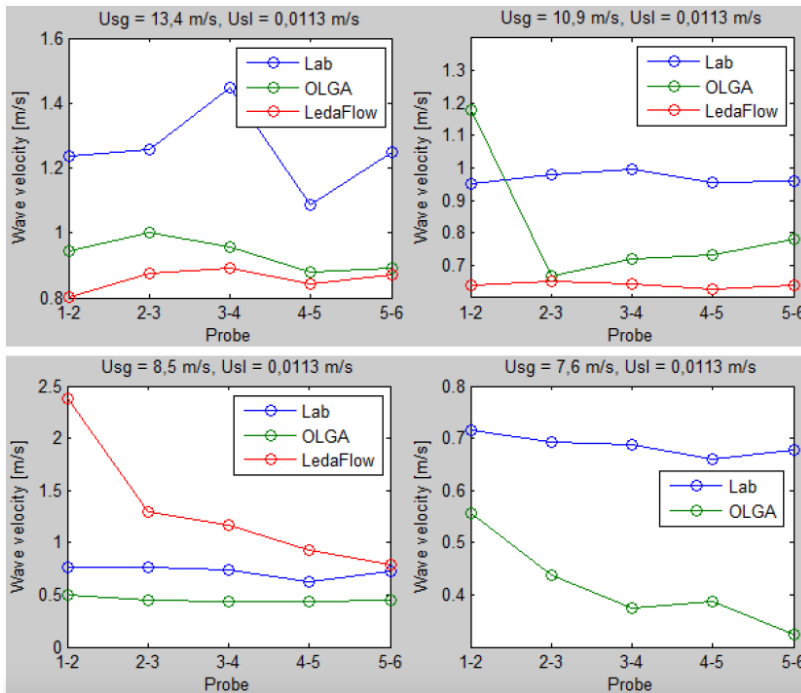
(b) A plot showing the differences in wave velocity along the test section at different probe positions for changing gas velocities.

**Figure 2.35:** Excerpts of plots from previous master thesis [18, p. 45-46]

Leda Flow did not correlate well with the experimental data for both hold up and wave velocity. Conclusively, the surge waves were formed in the laboratory and shared characteristics with those observed in the field. The waves were smooth, non-breaking fronts traveling in stratified flow regime. The waves changed in shape along the pipeline and varied in rates of change. The rate slowed down as the pipe section came to its end. The waves were also assumed able to flow for longer distances than the test pipeline in the lab. three-phase experimentation was not observed.



(a) Comparison plot of wave hold up between the simulators and lab results

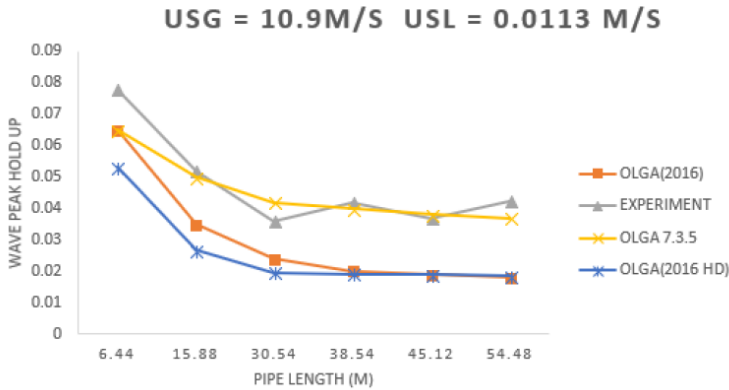


(b) Comparison plot of wave velocity between the simulators and lab results

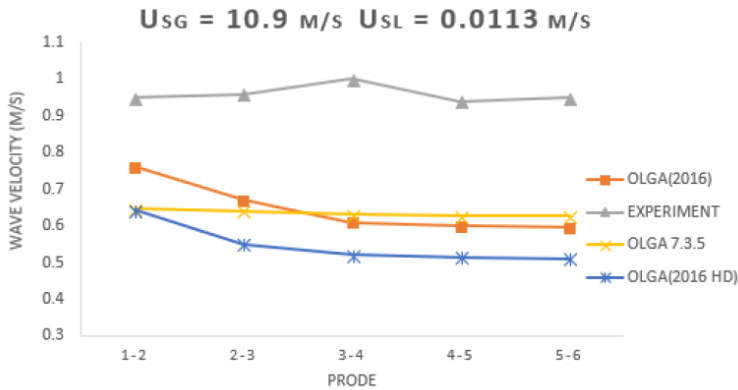
**Figure 2.36:** Excerpts of plots from previous master thesis [18, p. 68,71]

### 2.6.3 Master Thesis Numerical Simulation of Surge Waves

Simulations of the experiments discussed in 2.6.2 performed by Steinar [18] were repeated in a thesis by Linge Dan [14] to observe the differences brought about by newer versions of OLGA and Leda flow. The OLGA models used were OLGA2016.2.1 and OLGA7.3.5.



(a) Comparison plot of wave hold up between the simulators and lab results



(b) Comparison plot of wave velocity between the simulators and lab results

**Figure 2.37:** Excerpts of plots showing comparisons of simulator performance to experimental data from previous master thesis [14, p. 45-46]

It was found that though surge waves could be simulated by OLGA2016.2.1, there was a considerably large difference with the experimental data. OLGA7.3.5 performed better when matched with experimental data, as seen in **Fig. 2.37**. There was a larger deviation with wave velocity than with wave hold up.



## 2.6.4 Project Work two-phase Surge Wave Experiments

The experiments performed by Steinar [18] were repeated to review surge wave formation in two-phase. Similar experiments were also performed in three-phase. There were some differences with the pipe geometry. Three probes were placed on the pipeline and were positioned at three spots on the pipeline; 6.4 m, 26.7 m and 52.3 m. A layout of this can be seen on **Fig.2.38**

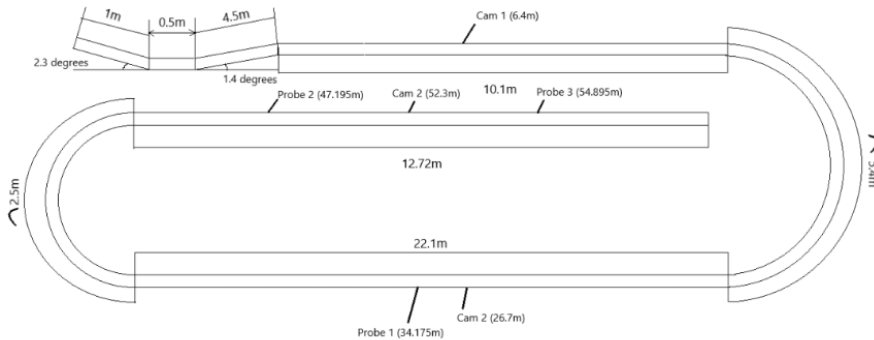


**Figure 2.38:** Schematic layout of rig used in project work

The test matrix employed for the two-phase experiments was similar to that used for the experiments discussed in section 2.6.2. Eight cases were performed with varying air and water rates. It can be seen in **Fig.2.39**

Case	Initial Air Flow rate		Initial air valve opening	Water Flow Rate	
	Usg[m/s]	g[kg/s]		Usl[m/s]	l[kg/s]
1	13.37	0.045	25	0.0113	0.033
2	12.01	0.040	23.5	0.0113	0.033
3	8.88	0.0298	21	0.0113	0.033
4	7.69	0.0258	20	0.0113	0.033
5	13.37	0.045	24.2	0.0265	0.075
6	11.46	0.0385	23.5	0.0265	0.075
7	8.89	0.03	21	0.0265	0.075
8	7.69	0.0258	20	0.0265	0.075

**Figure 2.39:** The air-water test matrix employed in the project work

The readings from the conductance probes were translated into hold up and were plotted against time for each case. The resulting waves were quite different from but showed the same trends, see **Fig.2.40** below. It was suggested that change of lab equipment could be a reason for difference in results.

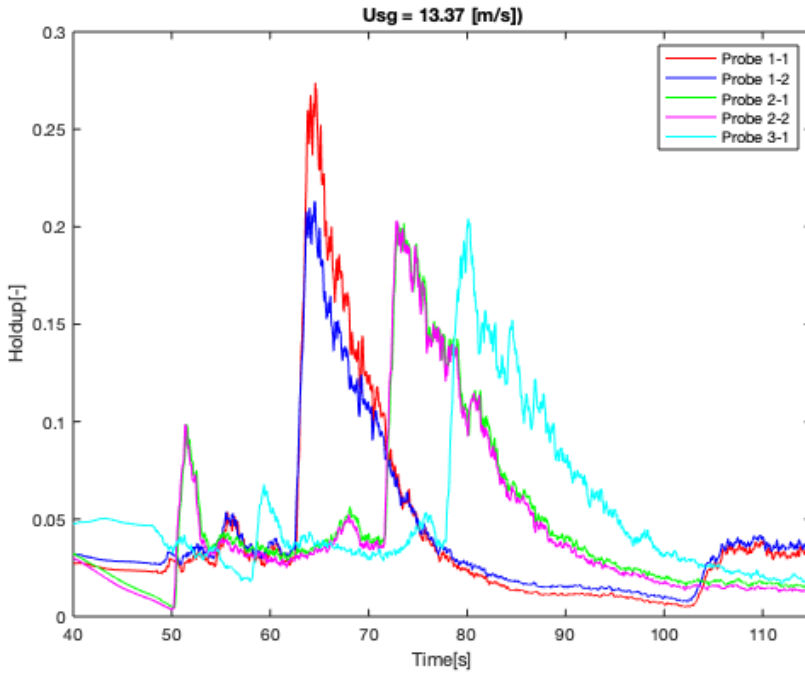


**Figure 2.40:** Laboratory data showing hold up vs time for case 1  $U_G = 13.4$  m/s  $U_L = 0.0113$  m/s at Probe 1,2 and 3

The test matrix used for the three-phase experiments was generated from the two-phase test matrix. The water volume fraction was used as total liquid volume fraction for the three-phase cases, with oil and water as the two liquids. The liquid superficial velocity increased when two liquids were used.

Case	Initial Air Flow rate		Initial air valve opening	Liquid Flow Rate	
	$U_{sg}$ [m/s]	$g$ [kg/s]		$U_{sl}$ [m/s]	$l$ [kg/s]
1	13.37	0.045	25	0,0128	0,033
2	12.01	0.036	23.6	0,0128	0,033
3	8.88	0.028	21.8	0,0128	0,033
4	7.69	0.026	21	0,0128	0,033
5	13.37	0.045	25.3	0.0283	0.075
6	11.46	0.036	23.6	0.0283	0.075
7	8.89	0.029	21.8	0.0283	0.075
8	7.69	0.026	21	0.0283	0.075

**Figure 2.41:** The air-water-oil test matrix employed in the project work

This was analysed through camera images and video footage since the proper equipment for hold up measurement is not available at the multiphase laboratory. It was found that the volume fractions employed for two-phase could not create good surge waves in

---

three-phase. More experimentation was needed in order to find optimum volume fractions for three-phase cases. The test matrix for three-phase in this project work was used as a basis for creation of a new test matrix for this master thesis.



# Experimental Work and Analysis

## 3.1 Laboratory facilities and methodology

Laboratory experiments on surge waves have been conducted in the multiphase flow laboratory at the Department of Energy and Process Engineering at NTNU. The main goal of these lab experiments was to perform a visual inspection and analysis of surge waves in three phase flow (two liquids) for stratified gas-liquid flow in a test section with a dip. The waves were initiated by choking the gas flow, causing liquid accumulation in the dip, and then ramping up the gas flow to its initially set rate to blow the accumulated liquid through the pipeline as a surge wave. To achieve this it was important to have comparatively higher gas velocities flowing with low liquid volumes in the flowline. The behavior of the surge waves through the test pipeline was then to be studied. The horizontal pipeline test section has a total length of 57,84 meters.

Larger scale experiments have been performed based on three phase flow instabilities for some real cases. Similar small scale lab experiments on three phase flow surge waves as those performed for this master work are not known to be conducted previously. The results of these experiments will possibly contribute to further understanding of the surge wave phenomenon in three phase flows.

### 3.1.1 The multiphase flow laboratory at NTNU

There are three main loops at the multiphase flow lab at NTNU; one for air, one for water and one for oil. These loops are illustrated in **Fig. 3.1**, **Fig. 3.2** and **Fig. 3.3** respectively. They can be connected to an S-riser test section, a horizontal test section or a vertical section. The horizontal test section can be tilted to create different angles at different positions to create different flow phenomenons through the sections. As well, different pipes with different inner diameters can be used. The test fluids are tap water, atmospheric air and a given oil at ambient room temperature. The oil used for these experiments have a density ranging from 750-800 kg/m<sup>3</sup>. A density of 800 kg/m<sup>3</sup> was applied.

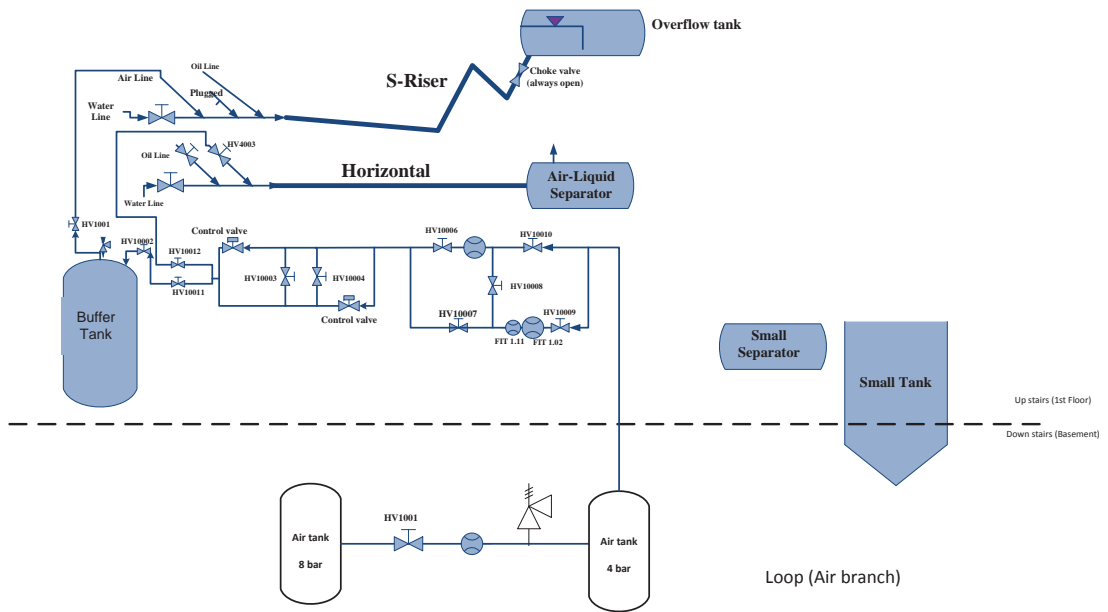


**Figure 3.1:** A schematic illustration of the air loop at the multiphase flow lab at NTNU. [Provided by NTNU]

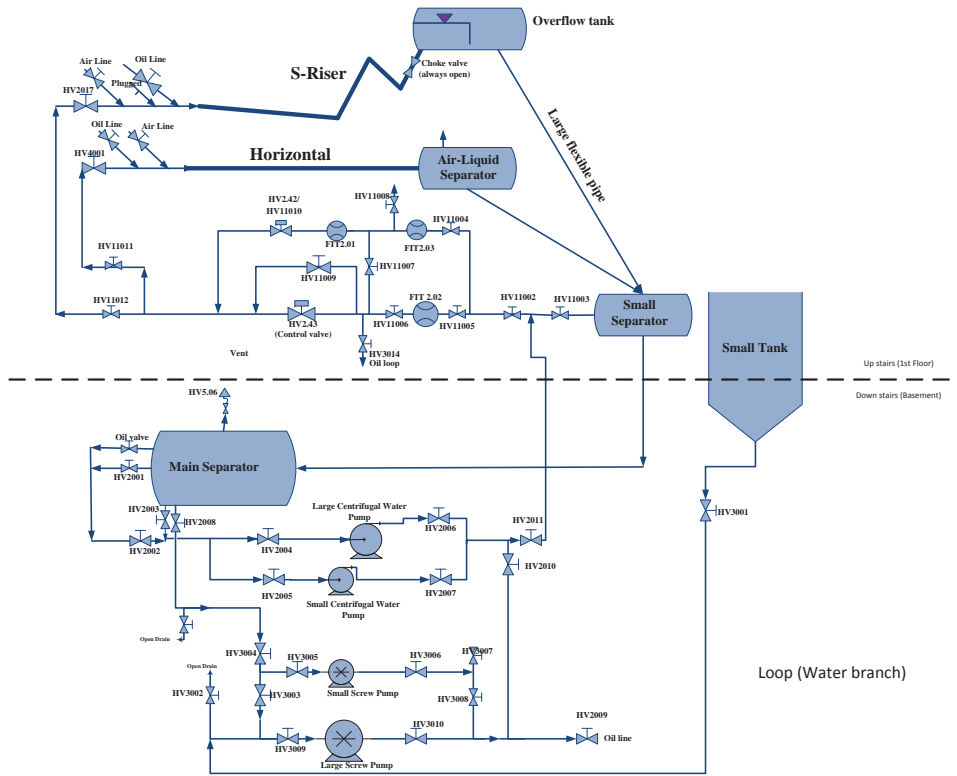


**Figure 3.2:** A schematic illustration of the water loop at the multiphase flow lab at NTNU. [Provided by NTNU]

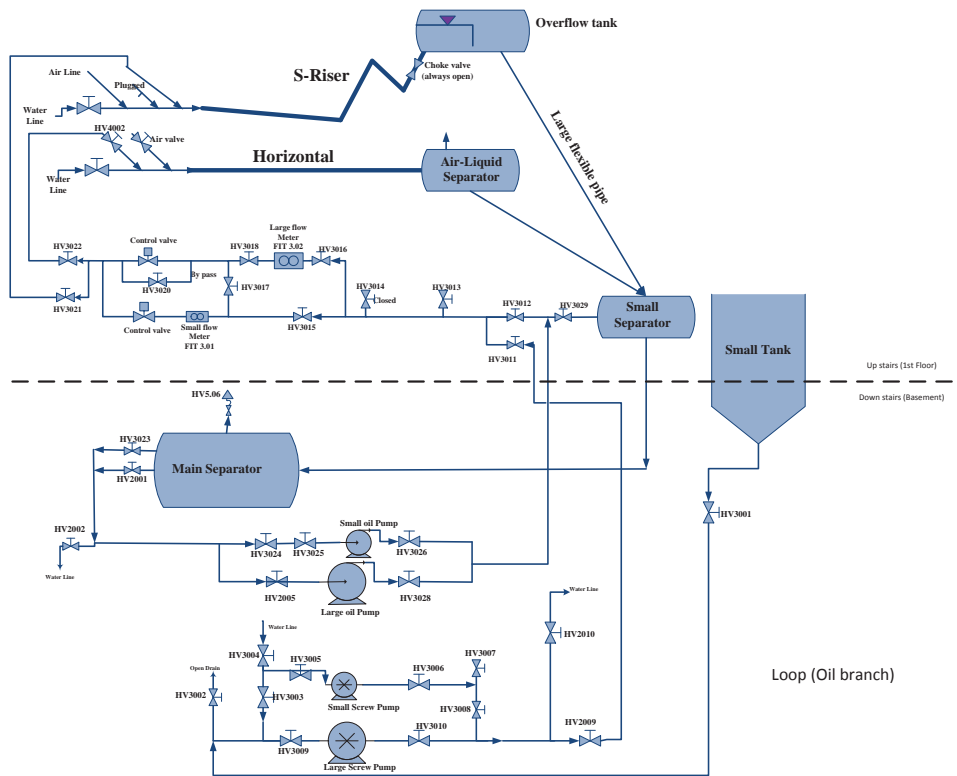


**Figure 3.3:** A schematic illustration of the oil loop at the multiphase flow lab at NTNU. [Provided by NTNU]

All three setups were utilized in order to perform the experiments for this work. Maintenance has been done on the test sections since the earlier mentioned experiments were performed. These changes include replacement of equipment and varying orientation of the pipes and probes. This may lead to significant differences in comparison to the earlier performed experiment reports.



## 3.2 Experimental Setup

The inner diameter of the flowline used for these experiments was 60mm. The horizontal test section has a total pipe length of about 57,84 metres. The S-riser nozzle and the horizontal section were used over the duration of experimentation. The S-riser nozzle brought in the oil flow during the three phase experiments. This nozzle was connected to a plexi-pipe connected to a flexible hose. The flexible hose is used to allow easier manipulation of dips and elevation at the start of the flow section. These manipulations in orientation of the flowline assist in initiating phenomena such as surge waves in the flow.

A dip is positioned 1 metre from the start of the plexi-pipe at an angle of  $2.3^\circ$  from the S-riser nozzle. The flexible hose is straight for about 0.5 metres and elevates at an angle of  $1.3^\circ$  for a distance of 4.5 metres. The hose then connects to a horizontal section of plexi-pipe. The dip geometry in the test section is significant for liquid accumulation when air flow rate is decreased.

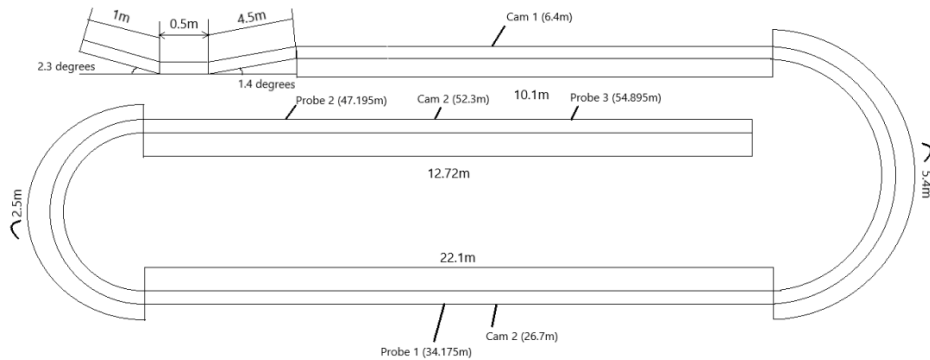


**Figure 3.4:** Schematic layout of the test rig at the NTNU multiphase laboratory employed for the experimentation of this project work. This shows the distances and positioning of equipment and specific geometry manipulations to achieve initiation of surge waves

The remainder of the flow section was horizontal with two  $180^\circ$  bends, which ultimately form the loop. A horizontal separator stands at the end of the flowline. It receives all fluids run through the test section and send them back to their respective storage facilities. The liquids are directed through a flexible hose at the bottom of the separator to a large horizontal separator placed in the basement. A schematic outline of the test flowline is shown in **Fig. 3.4**

Air and liquid valves were used to control the fractions flowing through the pipeline. In order to create the desired surge waves through the flowline, The large air valve was employed to obtain sufficient high air flow rate to create stable, stratified flow through the pipeline. Measurements of the air flow rate were made by the air flowmeter (FIT 1.02). The small centrifugal water pump was used to regulate the amount of water through the small water valve with small water flow rates. The small centrifugal oil pump was used to regulate the amount of oil through the small oil valve with small oil flow rates. Measurements of the liquid flow rate were made by the flowmeters for water flowline and oil flowline respectively (FIT 2.01 and FIT 3.01). The main concept was to have high air

---

flow rates and low liquid flow rates.

The behavior of the waves could be influenced by the 180° bends on the loop. For this reason, it is important to take them into consideration during analysis of the results. The plexi-pipe roughness is 0,05 mm; a slightly different pipe roughness must be expected to apply for the flexible hoses that were applied to make the turns. [18]

### 3.2.1 Calibration and measurement

Three conductance probes were positioned at 34,175m, 47,195m, and 54,895m along the flowline. Each probe had two wires connected. These probes would measure the conductance and log the values in large excel files. It is necessary to know the liquid and vapor fractions flowing through the flowline in order to properly analyse the flow behavior. The liquid fraction, also known as 'Hold Up' and denoted by the symbol [H], can be measured using conductance probes placed at locations on the flow section. Conductance probes are not efficient at determining liquid fractions when there are two liquids flowing since it is mainly responsive to water flow. This means the hold up of oil cannot be accurately accounted for. The conductance readings obtained are instead used to observe the trends of a passing wave.

The instrumentation has to be calibrated before the experiments are carried out. The calibration was done by logging the conductance along the pipeline when the pipeline was completely filled with water and when it was completely dry, in order to obtain an average value for both completely filled pipeline,  $C_f$ , and completely dry pipeline,  $C_e$ . The desired experiments were then conducted. The variable  $C_n$  stands for a normalized value of conductance calculated using each individual conductance reading,  $C$ , as seen in the equation(3.1) . This normalized conductance value is then used to observe the waves.

$$C_n = \frac{C - C_e}{C_f - C_e} \quad (3.1)$$

A gamma densitometer can be employed to measure hold ups in the flow line. This instrumentation was not used for this work.

### 3.2.2 Data handling and presentation

The data obtained from the large excel files require extensive sorting in order to obtain desired variables. The variables obtained assist with data analysis and representation depending on what is to be analysed. For this thesis several variables were extracted from the large data files such as time, conductance, flow rate and pressure. The normalized conductance values calculated using equation (3.1) were relocated to a separate file for easier use. After the excel file was properly arranged, the data was imported to Matlab. Matlab is a useful programming tool with several functions.

The raw data from the probes is very noisy. This noise is due to the instability at the interface of the air and the liquids. When air and liquid are flowing together in stratified flow in a conduit, the air drags the liquid surface leading to a wavy motion of liquid along the flowline. This produces readings with a lot of fluctuations, making it difficult to analyse the data as it is. Matlab was then used to smooth the data, making it easier to perceive the characteristic trend of the wave. The function used for this is a curve smoothing filter. The data is read by the Matlab from excel sheet and a vector is created in Matlab.

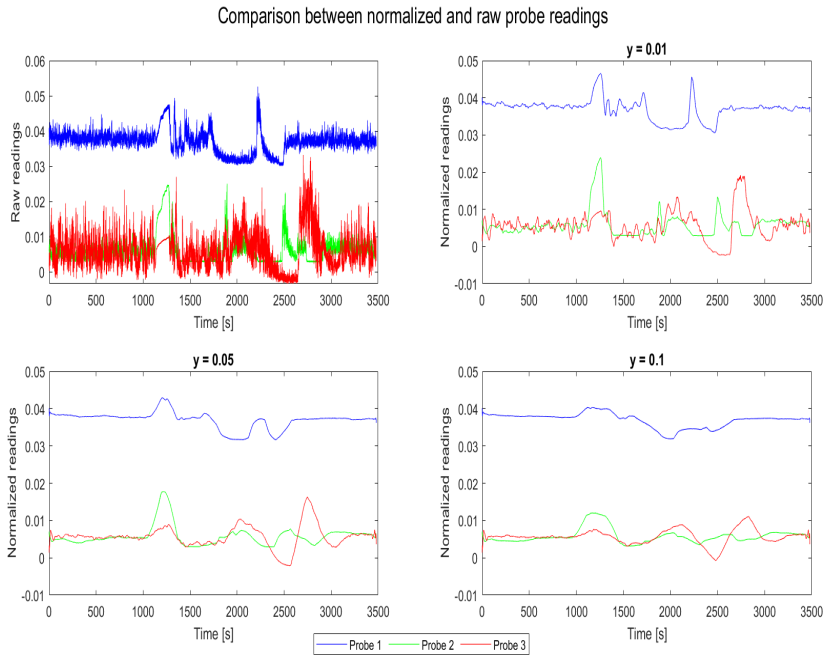


**Figure 3.5:** Plots showing the effect of curve smoothing with different filters 0.01,0.05 and 0.1

The data from the conductance probes will be useful when estimating a possible velocity of the travelling waves. Their level of accuracy to the simulations will be determined. It is expected to have inaccuracies since the oil is not taken to consideration.

### 3.2.3 Camera Recording

Cameras were placed at three positions along the pipeline: 6.4m, 26.7m and 52.3m. They were positioned strategically to observe the wave propagation along each long side of the flowline, as seen in **Fig.3.4**. For each case measured, a series of snapshots and videos were recorded and observed. The orientation for each camera is as follows;

- Camera 1: Flow moves Left to Right
- Camera 2: Flow moves Right to Left
- Camera 3: Flow moves Left to Right

## 3.3 Performed Experiments

A total of seven lab cases will be included in the appendix of this thesis. A selected number will be discussed for this thesis. Analysis was made of the data and camera recordings collected. Analysis of the surge waves relied mostly on video-based surge wave characterization since hold up calculation was not applicable. The laboratory was not equipped

with instrumentation to measure the hold ups for flows with both oil and water accurately. The air flow rates and liquid flow rates are different for each case since the main goal was to find liquid volumes which showed good surge waves formation in the pipeline.

### 3.3.1 Test procedures

The test procedures applied to initiate the surge waves is provided in accordance to the one used for previous experiments[18]

- (i) The test section geometry was set up.
- (ii) Steady state stratified flow was established through the entire pipeline, with fixed air and liquid flow rates.
- (iii) The data logger and cameras were turned on.
- (iv) The air valve was choked down to 12 percent of the total opening,  $U_{sg} = 3,6$  m/s ( $\dot{m} = 0,012$  kg/s), and ramped up to its initial value after 10 seconds, and in some cases with lower liquid volume rates, 20 seconds.
- (v) The liquid volume accumulated in the dip, during the choking of the air flow, was expelled through the pipeline in a surge wave and steady state stratified flow was re-established through the entire pipeline.

### 3.3.2 Selected Three Phase Cases

These seven cases were selected based on their ability to create clear surge waves. The volumes for each case were selected after a series of several experiments were performed in the lab. The starting point was from the test matrix used in the project work detailed in 2.6.4. This test matrix can be seen in **Table.3.2** below.

**Table 3.1:** Table showing the test matrix values for air,water and oil experiments employed for this work

Case	Initial Air Flow rate		Initial air valve opening	Liquid Flow Rate			
	$U_{SG}$ [m/s]	$\dot{m}_g$ [kg/s]		Water Rate [l/s]	Oil Rate [kg/h]	$U_{SL}$ [m/s]	$\dot{m}_l$ [kg/s]
1	8.95	0.030	22.0	0.015	60	0.0144	0.036
2	8.37	0.028	21.8	0.015	74	0.0127	0.032
3	8.52	0.029	21.8	0.01	72	0.0124	0.030
4	8.52	0.029	22.0	0.005	72	0.0106	0.025
5	8.52	0.029	22.0	0.015	6	0.0060	0.017
6	7.65	0.026	20.9	0.01	6	0.0043	0.012
7	8.52	0.029	21.9	0.005	6	0.0025	0.007

**Table 3.2:** Table showing the test matrix values for air,water and oil experiments employed for this work

The cases are arranged in descending order of liquid flow rate.

### 3.3.3 Varying Water cuts

Experiments were performed with varying water cuts for one chosen case in order to observe possible differences in flow behavior. Altering the volume flow rates of the liquids changes the liquid superficial velocity. Experiments were performed for all seven cases maintaining the liquid mass flow for each water cut applied. Tables detailing the experiments are shown below from **Tables 3.3 to 3.9**

**Table 3.3:** Table showing the test matrix used for Case 1 experiments with varying water cut

Case 1 - $\dot{m}_l = 0.036$						
Air Flow [kg/s]	Water Flow [l/s]	Oil Flow [kg/h]	Liquid Mass Flow [kg/s]	Water Cut [%]		
0.03	0.000	128.04	0.036	0		
0.03	0.015	74.00	0.036	37		
0.03	0.020	57.35	0.036	50		
0.03	0.031	16.30	0.036	85		
0.03	0.036	0.00	0.036	100		

**Table 3.4:** Table showing the test matrix used for Case 2 experiments with varying water cut

Case 2 - $\dot{m}_l = 0.032$						
Air Flow [kg/s]	Water Flow [l/s]	Oil Flow [kg/h]	Liquid Mass Flow [kg/s]	Water Cut [%]		
0.028	0.000	114.04	0.032	0		
0.028	0.015	60.00	0.032	42		
0.028	0.0177	51.00	0.032	50		
0.028	0.0278	14.20	0.032	85		
0.028	0.032	0.00	0.032	100		

**Table 3.5:** Table showing the test matrix used for Case 3 experiments with varying water cut

Case 3 - $\dot{m}_l = 0.030$						
Air Flow [kg/s]	Water Flow [l/s]	Oil Flow [kg/h]	Liquid Mass Flow [kg/s]	Water Cut [%]		
0.0286	0.000	108.00	0.030	0		
0.0286	0.010	72.00	0.030	29		
0.0286	0.017	48.00	0.030	50		
0.0286	0.026	13.00	0.030	85		
0.0286	0.030	0.00	0.030	100		

**Table 3.6:** Table showing the test matrix used for Case 4 experiments with varying water cut

Case 4 - $\dot{m}_l = 0.025$						
Air Flow [kg/s]	Water Flow [l/s]	Oil Flow [kg/h]	Liquid Mass Flow [kg/s]	Water Cut [%]		
0.0286	0.000	90.00	0.025	0		
0.0286	0.005	72.00	0.025	17		
0.0286	0.014	40.00	0.025	50		
0.0286	0.022	11.48	0.025	85		
0.0286	0.025	0.00	0.025	100		

**Table 3.7:** Table showing the test matrix used for Case 5 experiments with varying water cut

Case 5 - $\dot{m}_l = 0.017$						
Air Flow [kg/s]	Water Flow [l/s]	Oil Flow [kg/h]	Liquid Mass Flow [kg/s]	Water Cut [%]		
0.0286	0.000	60.040	0.017	0		
0.0286	0.006	39.100	0.017	30		
0.0286	0.009	26.680	0.017	50		
0.0286	0.015	6.000	0.017	88		
0.0286	0.017	0.000	0.017	100		

**Table 3.8:** Table showing the test matrix used for Case 6 experiments with varying water cut

Case 6 - $\dot{m}_l = 0.012$						
Air Flow [kg/s]	Water Flow [l/s]	Oil Flow [kg/h]	Liquid Mass Flow [kg/s]	Water Cut [%]		
0.0257	0.000	60.04	0.012	0		
0.0257	0.004	39.10	0.012	30		
0.0257	0.006	26.68	0.012	50		
0.0257	0.010	6.00	0.012	83		
0.0257	0.012	0.00	0.012	100		

**Table 3.9:** Table showing the test matrix used for Case 7 experiments with varying water cut

Case 7 - $\dot{m}_l = 0.007$						
Air Flow [kg/s]	Water Flow [l/s]	Oil Flow [kg/h]	Liquid Mass Flow [kg/s]	Water Cut [%]		
0.0286	0.000	24.00	0.007	0		
0.0286	0.004	10.70	0.007	50		
0.0286	0.004	15.60	0.007	71		
0.0286	0.007	0.00	0.007	100		

---

## 3.4 Observations

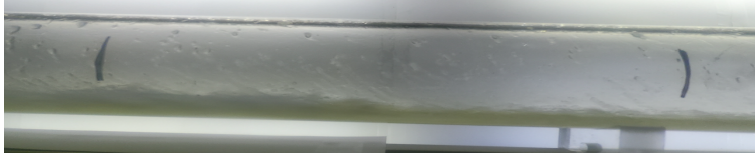
Surge waves were created in the lab with the seven cases detailed in the section above. Several experiments had to be carried out to narrow down mass flows that produce surge waves in the lab. For some of the cases, small roll waves could occur just after ramp up. This did not repeat throughout the straight section of the pipe. It should also be mentioned that the 180° curves at either end pipe geometry affect the flow behavior.

In the three phase experiments done during the project work [26] it was noticed that liquid rates similar to Steinars' in **Fig. 2.32** combined with higher air velocities created several roll waves along the pipeline, which was not desired. All cases for this thesis have air superficial velocities ranging from 7.65 m/s to 8.95 m/s, which are between cases 3-4 and 7-8 seen in the master thesis two phase case experiments [18]. All cases have much lower liquid superficial velocities as well. This significantly improved the performance of the experiments.

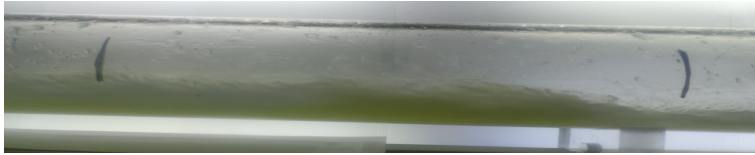
The images below show a wave passing through Camera 1 for case 1. Case 1 had the highest liquid superficial velocity. An initial wave which lasts about 3 seconds is seen in **fig.3.6a** before a larger wave passes with a visible higher hold up peak in **fig.3.6b**. The bigger wave lasts for about 7s. The duration of both waves seems to be about 10 to 12 seconds. Water, which is colored bright green, is more visible towards the end of the wave which is indicative of oil preceding water when air rate increases. This could be due to the difference in densities of the two liquids. The flow is very wavy however does not fill the pipe and thus can be classified as stratified wavy visually. There is also a foamy appearance when the wave passes which seems to cast a shadow when a wave passes. This is a result of the mixing of oil and water after ramp up. The flow does not remain clearly separated after ramp up. Once the wave passes the flow returns uniform after a certain period.

At camera 2 the wave passes with a clear front and lasts about 13s. Water is more visible at the end of the wave indicating water lagging behind compared to oil. This can also be seen in other cases like Case 3 **5.7e** and section A.3. Camera 3 records a number of smaller waves before a clear wave is seen that has travelled from the start of the pipe, see appendix A. The velocity of the wave has largely declined and the wave is diffused. At camera 2 and camera 3 it is comparatively difficult to detect the front of the wave for those cases with lower liquid velocities though waves are still visible.

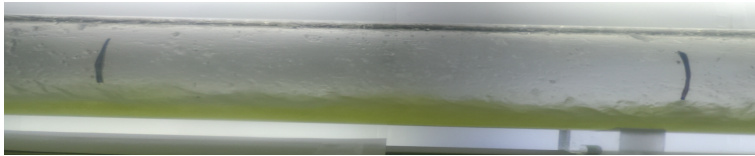
Case 4 differed from the rest as it had a 20s ramp down period. In this case, even with low gas velocity, the surge wave is seen clearly on all cameras 1,2 and 3. This case had an oil flow which was much higher than water flow and thus it was expected that water would not be as clearly visible as in case 3. However, the water was more visible than the other cases with higher water volume rate. As seen in case 7, water lags behind oil coming in a separate peak. It can be noted that there are separate waves at the beginning of the pipe, as seen on camera 1. These waves are in turn seen as a single wave in the second and third cameras with the liquids mixed but with the lighter liquid dominant in the front and the heavier liquid dominant at the tail. See Appendix A.4.



(a) Initial wave passes through the observation section



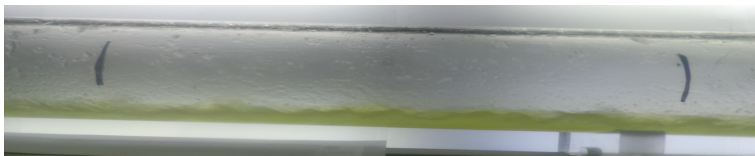
(b) Larger wave following the first wave, more messy and foamy at the top. Liquid distribution is unclear



(c) The wave continues through the observation section decreasing in hold up



(d) Larger wave following the first wave, more messy and foamy at the top. Liquid distribution is unclear



(e) The wave has passed and stability is regained shortly after

**Figure 3.6:** Images showing Case 1 [ $U_{SG} = 8.95$  m/s,  $U_{SL} = 0.0144$  m/s] at Camera 1 position at the 6.4m

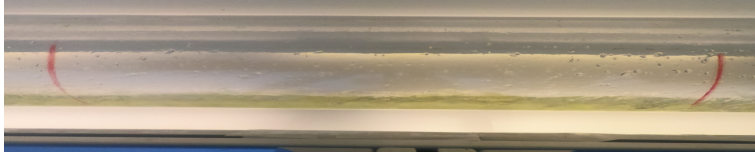
Cases 5,6 and 7 performed well showing surge waves in all cameras quite clearly despite extremely low liquid volume. Though fronts were not clearly visible, clear surge waves are seen flowing through the observation section. All three cases had low oil rates flowing in the liquid mixture, with water volume rate decreasing with case 5, 6 and 7 respectively. This may be an indication that surge waves are easily formed when there is higher water cut.

Some cases, like case 2, did not perform very well in spite of a surge wave passing through the pipe. this is because in camera 2 and 3 the waves were almost undetectable.

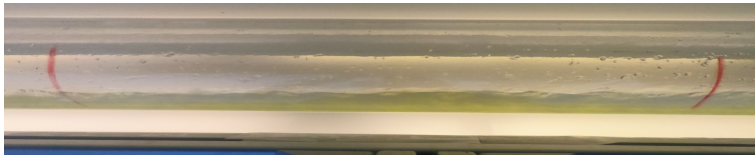


---

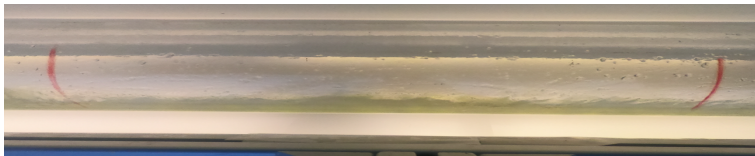
Though the fronts and ends are not very visible, a miniature wave is known to pass through by keen observation. See Appendix A.2.



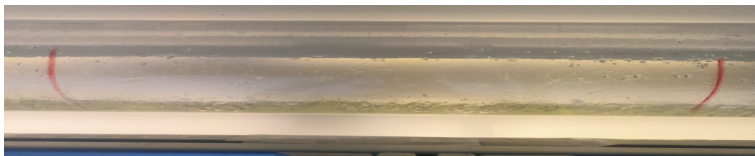
(a) Stable flow before wave passes



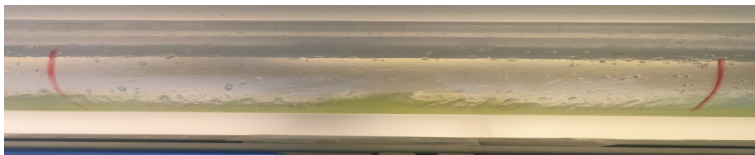
(b) Wave enters the frame with foamy-like substance at the top. Peak holdup visible



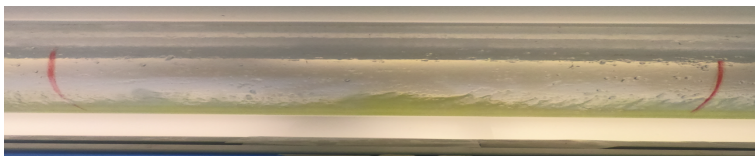
(c) Hold up gradually decreases



(d) The wave has passed and seems like normal flow will restore



(e) More waves seem to pass, mostly likely lagged behind water



(f) The peaks continue showing non-uniformity before the flow begins to stabilize again

**Figure 3.7:** Images showing Case 1 [ $U_{SG} = 8.95$  m/s,  $U_{SL} = 0.0144$  m/s] at Camera 2 position at 26.7m

---

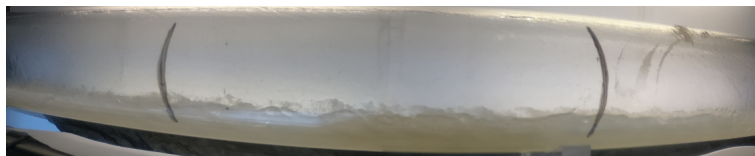
### 3.4.1 Case Study: Varying water cut experiments

Experiments were also carried out with varying water cuts. The liquid mass flow rates remained the same for different water cuts which indicates a change in the  $U_{SL}$ . The water cuts that will be discussed are those for 0%, 50% and 100%. The water cut for Case 1, which was discussed above is 37%. Case 1 [ $U_{SG} = 8.95$  m/s,  $U_{SL} = 0.0144$  m/s], will be analysed.

At 0% water cut, the waves are miniature in comparison to the waves seen in the above figures for Case 1. At the first camera position, two waves are seen passing through with very smooth fronts. The wave tail is seen to be quite messy as well. The wave period should range between 10 to 15 seconds. This could be longer since it is difficult to accurately point out where the wave ends. The plots for this can be seen in **fig.??**



(a) Stable flow before wave passes



(b) Wave enters the frame, Peak holdup slightly visible



(c) The wave continues through the observation section



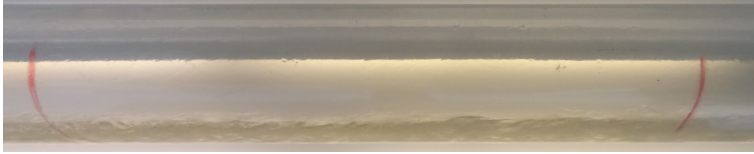
(d) The wave has passed and normal flow is restoring

**Figure 3.8:** Images showing Case 1 at 0% water cut at Camera 1 position (6.4m)

At the second camera (26.7m) the waves are obviously diminished in amplitude however continue to travel through the pipe. An initial wave passes before a second larger wave passes. The wave length is difficult to accurately determine due to low amplitude, but roughly is about 20 to 25 seconds. **fig.3.9**



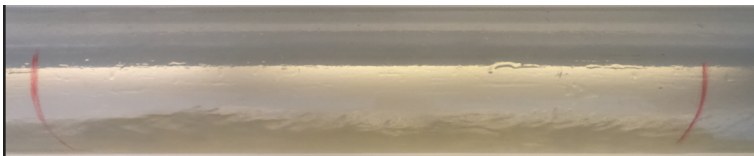
(a) Stable flow before wave passes



(b) Wave enters the frame with foamy-like substance at the top. Peak holdup visible



(c) Hold up gradually decreases



(d) The wave has passed and seems like normal flow will restore

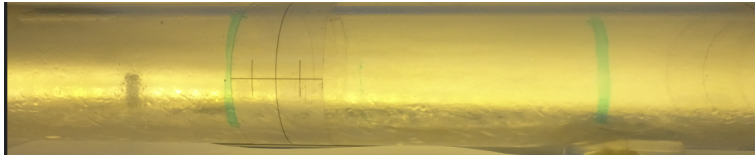


(e) The wave has passed and seems like normal flow will restore

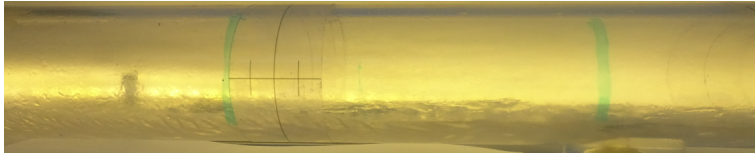
**Figure 3.9:** Images showing Case 1 at 0% water cut at Camera 2 position (26.7m)

The third camera shows the wave passing with difficulty since it has diminished from the last position. Hence the best way to see the wave is by observing for hold up increase.

At 50% water cut an initial with a smooth front passes through the observation section with a foamy top. The foam at the top layer of the liquid is indicative of mixing of oil and water. After the initial wave a larger wave passes with a sharper front visible. This is a trend observed at both cameras 1 2. At camera 3, it is difficult to observe a distinct front. Observation of hold up increase is employed. See **fig.5.25,5.26 fig.5.27**.

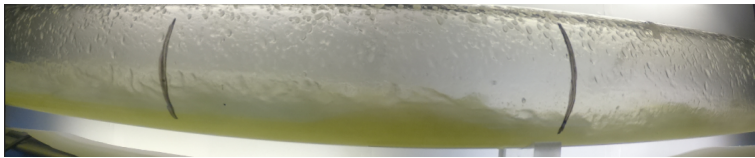


(a) Stable flow before wave passes



(b) Wave enters the frame with foamy-like substance at the top. Peak holdup visible

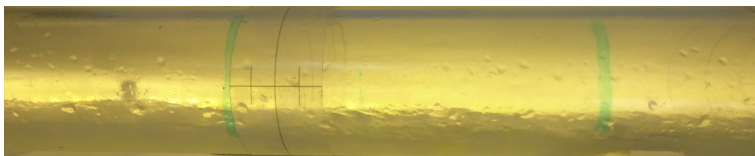
**Figure 3.10:** Images showing Case 1 at 0% water cut at Camera 3 position (52.3m)



(a) Main wave at Camera 1 Orientation: left to right



(b) Main wave at Camera 2 Orientation: right to left

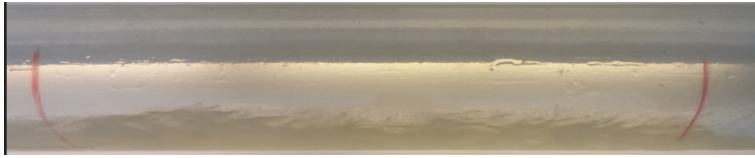


(c) Main wave at camera 3, Orientation: left to right

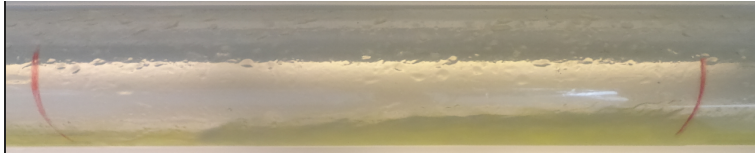
**Figure 3.11:** Images showing comparison of main waves for Case 1 at 50% water cut at all camera positions

At 100% water cut similar phenomenon is observed where two waves are observed passing through the observation section. An initial smaller wave and a latter larger adjoining wave. At farther camera positions, the two waves join together and appear as a single longer wave. The peak of the wave diminishes with time. See **fig.5.28,5.29 fig.5.30**

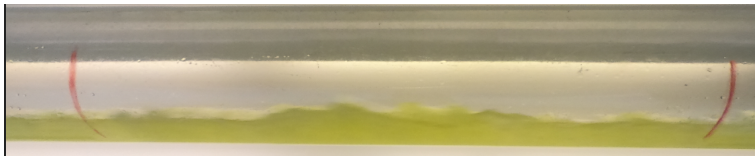
From visual inspection of these cases with varying water cuts, it seems that the higher water cut, the larger the wave flowing through the section. This is especially visible in camera 2. A comparison of the peaks is made below.



(a) Main wave 0% water cut Case 1



(b) Main wave 50% water cut Case 1



(c) Main wave 100% water cut Case 1

**Figure 3.12:** Images showing comparison of main waves for Case 1 at 0%, 50% and 100% water cut at camera 2 position (26.7m) Orientation: right to left

### 3.5 Limitations

- The experiments were carried out within a very short period of time. This results in a smaller range of successful cases at lower air and liquid flow rates. Further experimentation could reveal a larger range of better options.
- Some equipment in the lab was not available which contributed to the difficulty in proper analysis to the work presented. One such equipment is the gamma ray densitometer which helps with determination of the hold up flowing in the pipe.

---

# Computational Simulation and Analysis

The numerical simulations of surge wave are another part of this Master thesis. The latest version of OLGA is applied (OLGA2019.1). The simulations are divided into two parts.

Firstly, to reproduce the previous experiments done by Steinar[18] in the simulation program, adjust the parameters in the software and observe for changes. These results will also be compared to similar simulations done by Linge Dan [14].

The latter is to simulate the surge waves in three phase in the small scale lab setup and observe the propagation of waves and whether there is any correspondence with experimental data. As an extension of the second part, to simulate a particular case with varying water cuts and research the influence of water content in the 3-phase flow on the wave propagation. The simulations were carried out in gas-liquid-liquid three phase flow.

The tab file used to simulate the two phase cases was provided by SINTEF. The tab files used to simulate the three phase cases were created on google colaboratory platform with a code provided by Even Solbraa from Equinor ASA.

## 4.1 OLGA Multiphase Dynamic Simulator

The OLGA dynamic multiphase flow simulator is a modelling tool used to model transient flow of multiple phases in order to maximize production potential in the oil and gas industry [2]. The acronym OLGA is short for 'oil and gas simulator' [5]. It was initially created to simulate slow transients in relation with mass transportation. Main development of the software that is used today is a result of a research project started by the Institute of Energy Technology (IFE) and SINTEF with the support of several oil and gas companies. It is applied extensively in the oil and gas industry to study transients in pipelines and well bores for both offshore and onshore developments [9].

Transient simulation with the OLGA simulator provides an additional dimension to steady-state analysis by predicting system dynamics such as time-varying changes in flow

---

rates, fluid compositions, temperature, solids deposition and operational changes [2].

OLGA is a three fluid model and consists of separate continuity equations for the gas, oil and water as continuous liquid phases as well as one for oil and gas droplets. Three momentum equations are applied, with one for each continuous liquid phase and one for the combination of gas with liquid droplets. A slip relation helps in determining the velocity of the liquid droplets entrained in the gas phase. A general mixture energy equation is also applied with the assumption of a uniform temperature for all phases. Conclusively, a total of seven conservation equations and one equation of state are applied [34]. It is termed as an extended two fluid model [9].

### 4.1.1 Basic Equations

#### I. Conservation of Mass Equations

For gas phase,

$$\frac{\partial}{\partial t}(V_G \rho_G) = -\frac{1}{A} \frac{\partial}{\partial z}(AV_G \rho_G v_G) + \psi_G + G_G \quad (4.1)$$

For the liquid phase at the wall, the liquid being oil or water,

$$\frac{\partial}{\partial t}(V_L \rho_L) = -\frac{1}{A} \frac{\partial}{\partial z}(AV_L \rho_L v_L) - \psi_G \frac{V_L}{V_L + V_D} - \psi_e + \psi_d + G_L \quad (4.2)$$

For liquid droplets,

$$\frac{\partial}{\partial t}(V_D \rho_L) = -\frac{1}{A} \frac{\partial}{\partial z}(AV_D \rho_L v_D) - \psi_G \frac{V_D}{V_L + V_D} + \psi_e - \psi_d + G_D \quad (4.3)$$

where

- $V_G, V_L, V_D$  are volume fractions for gas, liquid film and liquid droplets respectively.
- $\rho$  stands for density,  $v$  stands for velocity,  $p$  stands for pressure and  $A$  stands for pipe cross sectional area.
- $\psi_G, \psi_e$  and  $\psi_d$  stand for the mass transfer rate between phases, the entrainment rates and deposition rates respectively.
- Assuming  $f$  is any specified phase,  $G_f$  is a possible mass source of phase  $f$ .

#### II. Momentum Conservation Equations

For a combination of gas phase and liquid droplets,



$$\begin{aligned}
\frac{\partial}{\partial t}(V_G \rho_G v_G + V_D \rho_L v_D) = & -(V_G + V_D) \left( \frac{\partial p}{\partial z} \right) - \frac{1}{A} \frac{\partial}{\partial z} (AV_G \rho_G v_G^2 + AV_D \rho_L v_D^2) \\
& - \lambda_G \frac{1}{2} \rho_G |v_G| v_G \frac{S_G}{4A} - \lambda_L \frac{1}{2} \rho_L |v_L| v_L \frac{S_L}{4A} + (V_G \rho_G + V_D \rho_L) g \cos \theta \\
& + \psi_G \frac{V_L}{V_L + V_D} v_a + \psi_e v_i - \psi_d v_D
\end{aligned} \tag{4.4}$$

For liquid at the wall,

$$\begin{aligned}
\frac{\partial}{\partial t}(V_L \rho_L v_L) = & -V_L \frac{\partial p}{\partial z} - \frac{1}{A} \frac{\partial}{\partial v} (AV_L \rho_L v_L^2) - \lambda_L \frac{1}{2} \rho_L |v_L| v_L \frac{S_L}{4A} + \lambda_i \frac{1}{2} \rho_G |v_r| v_r \frac{S_i}{4A} \\
& + V_L \rho_L g \cos \alpha - \psi_G \frac{V_L}{V_L + V_D} v_a + \psi_e v_i - \psi_d v_D \\
& - V_L d(\rho_L - \rho_G) g \frac{\partial V_L}{\partial z} \sin \alpha
\end{aligned} \tag{4.5}$$

where

- $\alpha$  = pipe inclination with the vertical
- $S_G, S_L$  and  $S_i$  stand for the wetted perimeters of the gas, liquid, and interface respectively.
- $G_f$  is assumed to enter at a  $90^\circ$  angle to the pipe wall, carrying no net momentum.

A pressure equation formulated by OLGA before discretization of differential equations is solved simultaneously with momentum equations to determine pressure and phase velocities. A single equation for pressure and phase fluxes can be seen in (4.6) below

$$\begin{aligned}
\left[ \frac{V_G}{\rho_G} \left( \frac{\partial \rho_G}{\partial p} \right)_{T, R_s} + \frac{1 - V_G}{\rho_L} \left( \frac{\partial \rho_L}{\partial p} \right)_{T, R_s} \right] \frac{\partial p}{\partial t} = & \frac{1}{A \rho_G} \frac{\partial AV_G \rho_G v_G}{\partial z} - \frac{1}{A \rho_L} \frac{\partial AV_L \rho_L v_L}{\partial z} \\
& - \frac{1}{A \rho_L} \frac{\partial AV_D \rho_L v_D}{\partial z} + \psi_G \left( \frac{1}{\rho_G} - \frac{1}{\rho_L} \right) + \\
& G_G \frac{1}{\rho_G} + G_L \frac{1}{\rho_L} + G_D \frac{1}{\rho_L}
\end{aligned} \tag{4.6}$$

---

### III. Mixture Energy Conservation Equation

$$\begin{aligned}
\frac{\partial}{\partial t} \left[ m_G(E_G + \frac{1}{2}v_G^2 + gh) + m_L(E_L + \frac{1}{2}v_L^2 + gh) + m_D(E_D + \frac{1}{2}v_D^2 + gh) \right] \\
= -\frac{\partial}{\partial z} \left[ m_G v_G (H_G + \frac{1}{2}v_g^2 + gh) + m_L v_L (H_L + \frac{1}{2}v_L^2 + gh) \right. \\
\left. + m_D v_D (H_D + \frac{1}{2}v_D^2 + gh) \right] + H_s + U
\end{aligned} \tag{4.7}$$

where

- E is the internal energy per unit mass
- h is the elevation
- $H_S$  stands for the enthalpy from mass sources G,L or D
- U stands for heat transfer from pipe walls

### IV. Closure laws

Closure laws are used to find solutions to equations. In OLGA they are used to solve the equations for gas-liquid stratified flow. They consider variables such as wall friction, interphase friction, gas bubbles in liquid film, liquid/liquid dispersion and droplet entrainment/deposition [33, p. 9]

## 4.2 Simulation setup

As mentioned in the introduction of this chapter, OLGA2019.1 was used to carry out experiments. Several tab files were used to carry out the experiments in this thesis.

### 4.2.1 Geometric setup and Input conditions

The framework for an OLGA basic case was used and modified to fit the specifications for all simulations. Both parts employed the same geometry since the same pipeline was used for experimentation.

**Table 4.1:** Setup geometry applied for simulations

PIPE	x [m]	y [m]	Length [m]	Elevation [m]	Diameter [m]
Start	0	0			
PIPE-1	0.9992	-0.04	1	-0.04	0.06
PIPE-2	1.4992	-0.04	0.5	0	0.06
PIPE-3	6.09788	0.07	4.6	0.11	0.06
PIPE-4	57.8379	0.07	51.74	0	0.06

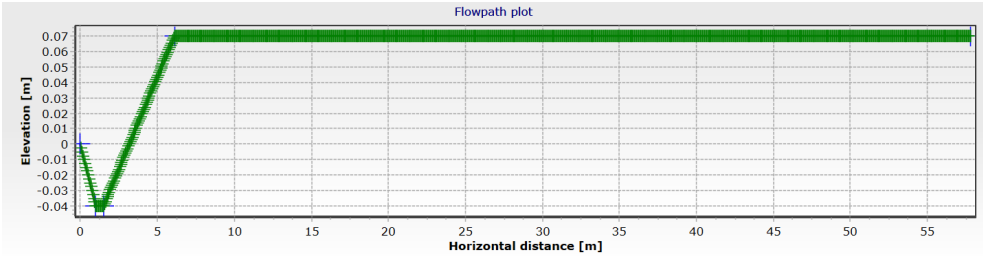


**Figure 4.1:** Geometry setup in OLGA

#### 4.2.1.1 Repetition of previous experiments

The geometry and input details were set up as they were in previous work by Steinar[18] and Linge Dan[14]. They are represented above, see 4.1. Two mass sources for water and air are placed on the first section of the pipe. The air-water tab file was provided by SINTEF. In order to ensure stabilization of the hold up before and after ramp down, the first simulation file is run using steady-state processor followed by another which uses the first file as a restart file with prior stable conditions. Ramp down is performed in the second simulation. The simulations were carried out in 1D mesh. All the hold up plots can be seen in appendix B.

The assumptions were as follows;

- Adiabatic model with no temperature calculations.
- All temperatures set to 20°.
- Outlet node pressure set to 1 atm.
- A straight pipeline with no turns is assumed.
- The pipeline is assumed to have a roughness of 0.05 mm for the entire layout.
- A maximum time step of 1 second is applied.
- A minimum time step of 1E-05 seconds is applied.
- SLUGVOID: SINTEF
- 1st order mass equation discretization is applied.
- An air-water PVT file provided by Jørn from SINTEF is used.

#### 4.2.1.2 Three phase cases

The geometry was setup as seen in **tab.4.1**. Two mass sources for liquid and air are placed on the first section of the pipe. The air-water tab file was created using a program run on google colaboratory provided by Even Solbraa, an expert in gas processing and flow assurance from Equinor. This will be shared in appendix C. In order to ensure stabilization of the hold up before and after ramp down, the first simulation file is run using steady-state

---

processor followed by another which uses the first file as a restart file with prior stable conditions. Ramp down is performed in the second simulation. For different water cuts, the liquid fraction was specified.

- Adiabatic model with no temperature calculations.
- All temperatures set to 20°.
- Outlet node pressure set to 1 atm.
- A straight pipeline with no turns is assumed.
- The pipeline is assumed to have a roughness of 0.05 mm for the entire layout.
- A maximum time step of 1 second is applied.
- A minimum time step of 1E-07 seconds is applied.
- SLUGVOID: SINTEF
- 1st order mass equation discretization is applied.
- An air-water PVT file provided by Jørn from SINTEF is used.

## 4.3 Analysis and Discussion

All OLGA simulated results are presented in Appendix C and D.

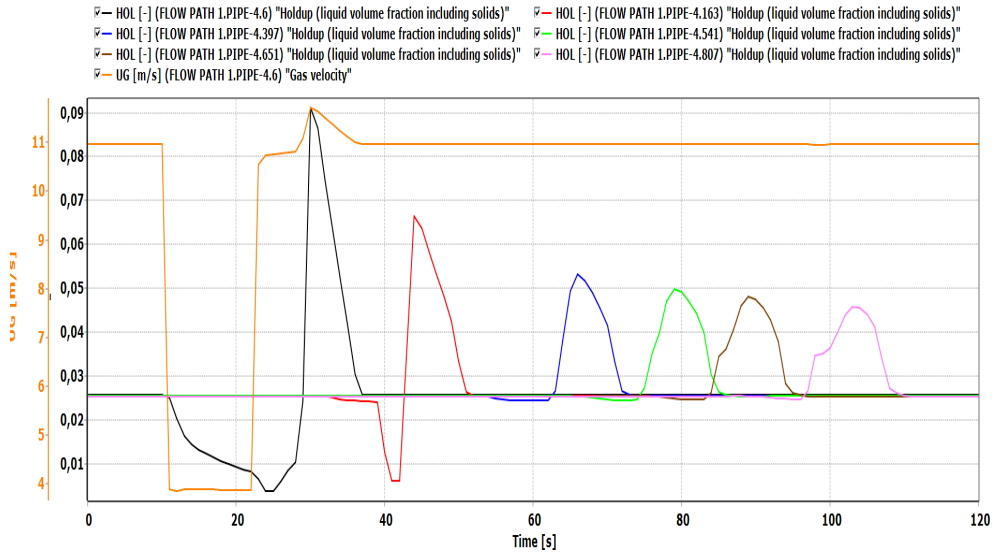
### 4.3.1 Repeated Two Phase Surge Wave Simulations

Previous simulations were made using various versions of OLGA. The earliest simulations were performed using OLGA 7.1 [18] and then later performed using OLGA 7.3.5 and OLGA 2016.2.1 [14]. It should be noted that significant differences may be observed due to different fluid file applied. The version used to produce the results discussed is OLGA 2019.1.

**Table 4.2:** Flow rate input used to initiate waves for Case 2 [ $U_{SG} = 10.9$  m/s  $U_{SL} = 0.0113$  m/s]

Time [s]	Air Flow Rate [kg/s]	Water Flow rate [kg/s]
0	0.037	0.032
10	0.037	0.032
11	0.013	0.032
22	0.013	0.032
23	0.037	0.032

Consider the results for Case 2,  $U_{SG} = 10.9$  m/s  $U_{SL} = 0.0113$  m/s. A table for the flow input is presented above in **tab.4.2**. It is seen from the resulting plot that surge waves are generated through the pipe and are of similar trend to the resulting waves seen in the lab experiments [18] and thus correlate rather well. The gas velocity is also plotted to illustrate the initiation of the waves.



File: Case2\_Steinar\_sintef\_RD.tpl

**Figure 4.2:** OLGA 2019.1 hold up plot for Case 2 [ $U_{SG} = 10.9$  m/s  $U_{SL} = 0.0113$  m/s]

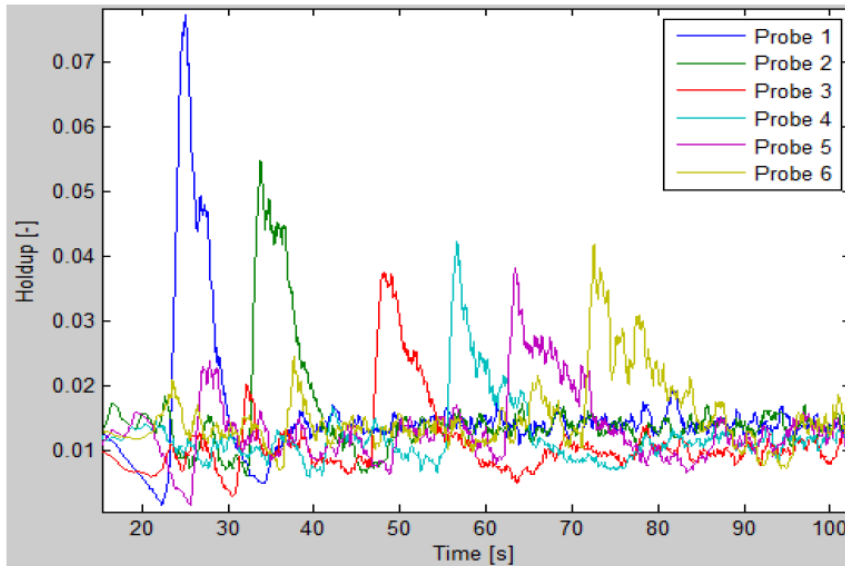


**Figure 4.3:** Experimental Results hold up plot for Case 2 [ $U_{SG} = 10.9$  m/s  $U_{SL} = 0.0113$  m/s] [18, p. 85]

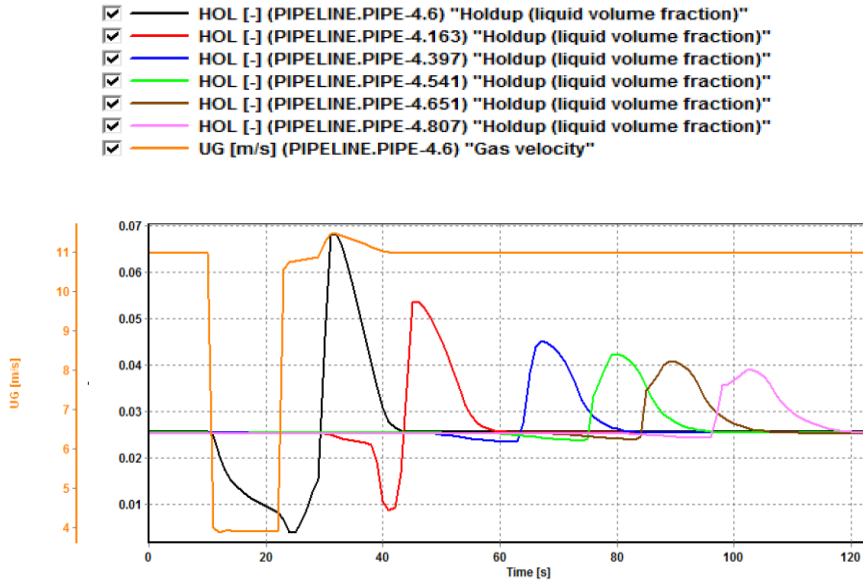


**Figure 4.4:** OLGA 7.1 hold up plot for Case 2 [ $U_{SG} = 10.9$  m/s  $U_{SL} = 0.0113$  m/s][18, p. 85]

The experimental hold ups are lower than the simulated hold up in OLGA 2019.1. It is common for simulators to predict higher values for some properties. Figures for the hold up plots for previously used versions OLGA 7.1[18], OLGA 7.3.5 and OLGA 2016.2.1[14] are presented in **fig.4.4**, **4.5** and **4.6** respectively. The fronts for the latest version are sharper and waves propagate faster in comparison despite the same input information to the simulator. Differences in simulator output could be a result of the computation models and calculation methods brought about with software updates. An alternative possibility could be the fluid file applied having a better match with the laboratory fluids.

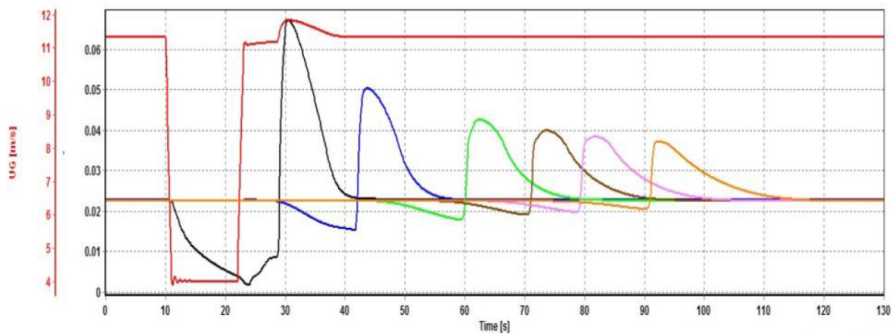


**Figure 4.5:** OLGA 7.3.5 hold up plot for Case 2 [ $U_{SG} = 10.9$  m/s  $U_{SL} = 0.0113$  m/s] [14, p. 44]

The result for OLGA2019.1 gives better results than OLGA2016.2.1 in comparison.

The waves from the third probe onward were smeared out and showed obvious hold up changes for the first and second probes only.

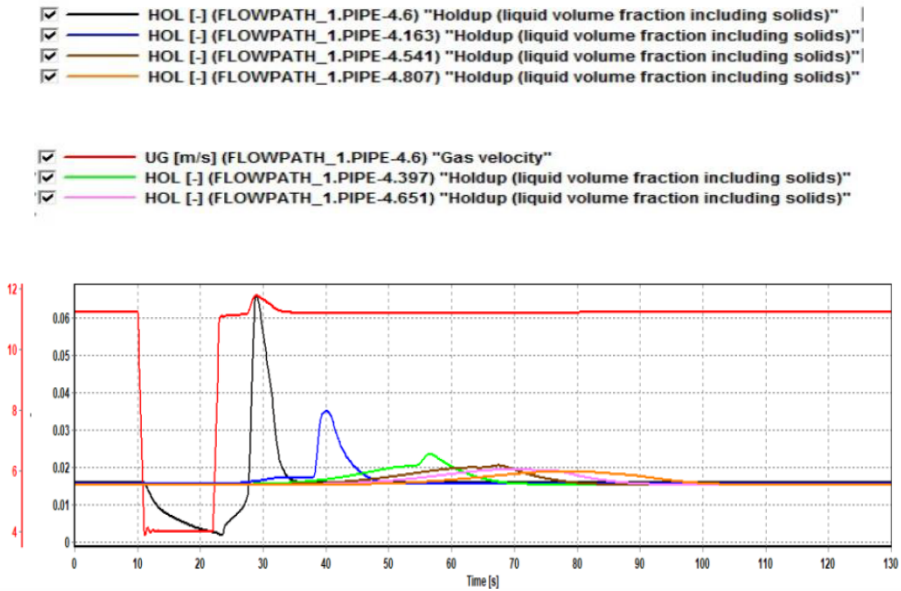


**Figure 4.6:** OLGA 2016.2.1 hold up plot for Case 2 [ $U_{SG} = 10.9$  m/s  $U_{SL} = 0.0113$  m/s] [14, p. 44]

Generally, the wave peak hold ups correlated well with simulation results for hold up. Wave velocities were also compared and showed more deviation with the experimental results. Comparison of wave peak hold ups and velocities for all experimental cases were made for Cases 1 through 8 [18, p. 45-46] and can be seen in **fig.2.35**. Plots comparing the two variables from lab data and simulators were also prepared [18, p. 68-69]. Some of these are seen in **fig.2.36** comparison of the wave peak hold ups and velocities for the different versions of OLGA for Case 2 were prepared [14, p. 45] and can be seen in **fig.2.37**. Wave peak hold up and wave velocity for OLGA2019.1 simulations are plotted in **fig.4.7 and 4.8** respectively and can be compared to previous results.

The wave hold up trend and values for Case 1 and 5 [ $U_{SG} = 13.4$  m/s] correspond rather well with the OLGA7.1 results with regards to the hold up range. OLGA2019.1 produces slightly higher value of hold up for Case 2 [ $U_{SG} = 10.9$  m/s  $U_{SL} = 0.0113$  m/s], however still correlates rather well. Cases 3 [ $U_{SG} = 8.5$  m/s  $U_{SL} = 0.0113$  m/s] and 4 [ $U_{SG} = 7.6$  m/s  $U_{SL} = 0.0113$  m/s] show increased hold up values up to 0.2 and 0.4. This is possibly because Case 3 and 4 were simulated with 2D mesh. The solutions were not able to converge with 1D mesh. Perhaps with 1D mesh it would have correlated better. The trends of the curves still relatively match well to OLGA7.1. Case 7 [ $U_{SG} = 8.5$  m/s  $U_{SL} = 0.0264$  m/s] corresponds well with OLGA7.1 from the second probe onward, but not with the first probe, spiking to hold up of 0.37. This is indicative of some kind of calculation error. Case 8 [ $U_{SG} = 7.6$  m/s  $U_{SL} = 0.0264$  m/s] behaved in a similar manner with spiked values at all probes. Cases 7 and 8 both used 2D mesh as well, which could

have contributed to the behavior of the curves. Case 6 [ $U_{SG} = 10.9$  m/s  $U_{SL} = 0.0264$  m/s] correlated well with OLGA7.1.

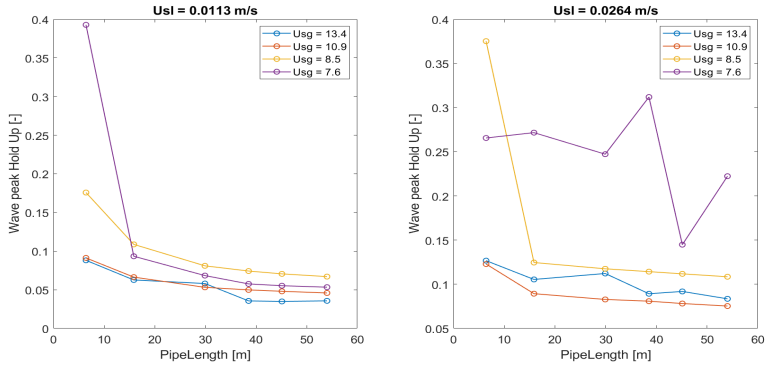


**Figure 4.7:** OLGA 2019.1 wave peak hold up comparison for Cases 1 through 8

The available plot for Case 2 showing contrast between experiment result and different versions of OLGA, see **fig.2.37a**, can be used to evaluate the presented wave peak hold up plots for OLGA2019.1. From this perspective, OLGA 2019.1 seems to correlate well with OLGA7.3.5 with slightly higher hold up values for this particular case. It has a larger deviation from OLGA 2016.2.1 result.

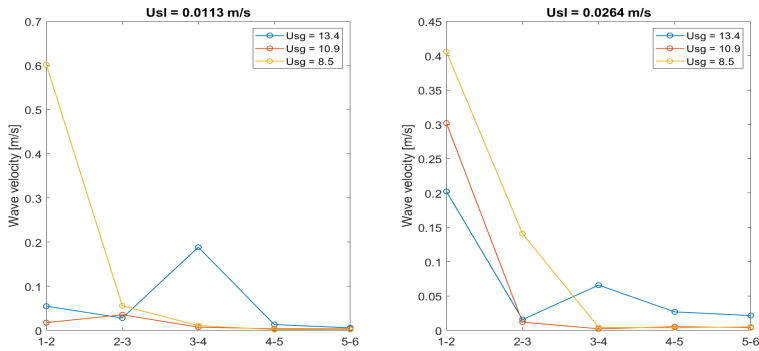


**Figure 4.8:** OLGA 2019.1 wave velocity comparison for Cases 1 through 8

Wave velocities generated for OLGA 2019.1 did not correlate with any of the wave velocities from the experimental data used in **fig.2.35b** for cases 1 to 8 [18]. Wave velocities were found to be above 0.8 m/s. The wave velocities calculated for OLGA 2019.1 simulations were found to range below 0.7 m/s for  $U_{SL} = 0.0113$  m/s and less than 0.45 for  $U_{SL} = 0.0264$  m/s. The wave velocities for OLGA 2016.2.1 HD **fig.2.37b** for Case 2 [14] had the closest correlation to OLGA 2019.1 wave velocities.

Cases 4 [ $U_{SG} = 7.6$  m/s  $U_{SL} = 0.0113$  m/s] and 8 [ $U_{SG} = 7.6$  m/s  $U_{SL} = 0.0264$  m/s] resulting plots were not considered when evaluating wave velocity due to uncertainty re-



garding the wave locations. Though waves are seen travelling downstream of the pipeline, there is difficulty in determining waves distinctly, see Appendix C. Observation of the flow regime identification for these cases showed that transitioning of stratified to slug flow takes place.

The gas velocity at the start of the pipe and the hold up for the first measuring point of Case 4 are fluctuating. **Fig. 4.9** shows some points of transition to slugging at the first probe location which explains this behavior. Other measuring points are also quite inconsistent leading to several peaks along the pipeline. It is a possibility that bigger mesh size scatters out the stand-out waves making it difficult to detect.

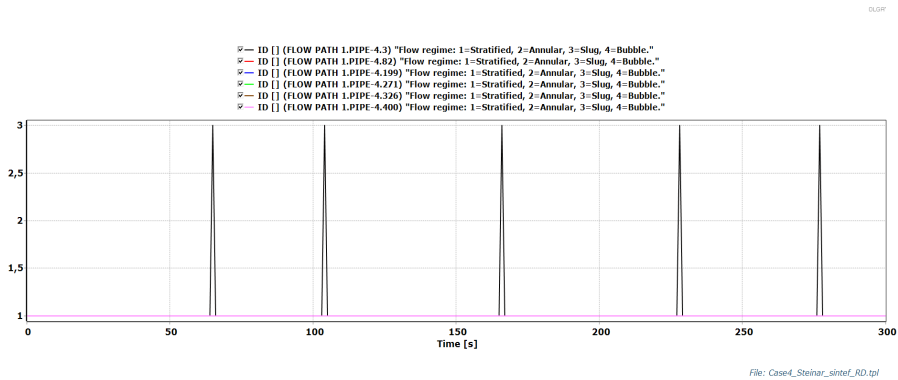


**Figure 4.9:** OLGA 2019.1 Flow Regime Identification for Case 4 [ $U_{SG} = 7.6$  m/s  $U_{SL} = 0.0113$  m/s]

Case 8 flow regime transitions from stratified to slug at several locations on the pipeline as seen in **fig. 4.10**.

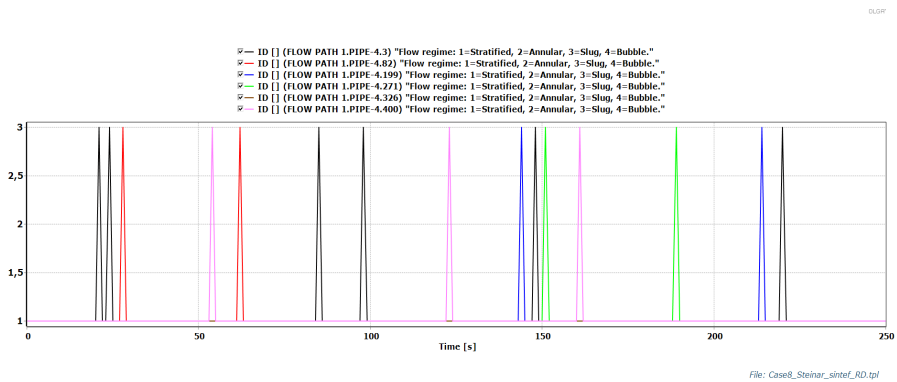


**Figure 4.10:** OLGA 2019.1 Flow Regime Identification for Case 8 [ $U_{SG} = 7.6$  m/s  $U_{SL} = 0.0264$  m/s]

---

### 4.3.2 Three Phase Simulations

Case 1 with  $U_{SG} = 8.95$  m/s and  $U_{SL} = 0.0144$  m/s was evaluated for this section of simulations due to time constraints. This case was one of the best experimental cases of three phase surge wave initiation for this work. Simulation of this case was adapted from the two phase cases set up, with very similar simulation input. The table below defines the mass flow input for the mass sources.

**Table 4.3:** Flow rate input used to initiate waves for Case 1 [ $U_{SG} = 8.95$  m/s  $U_{SL} = 0.0144$  m/s]

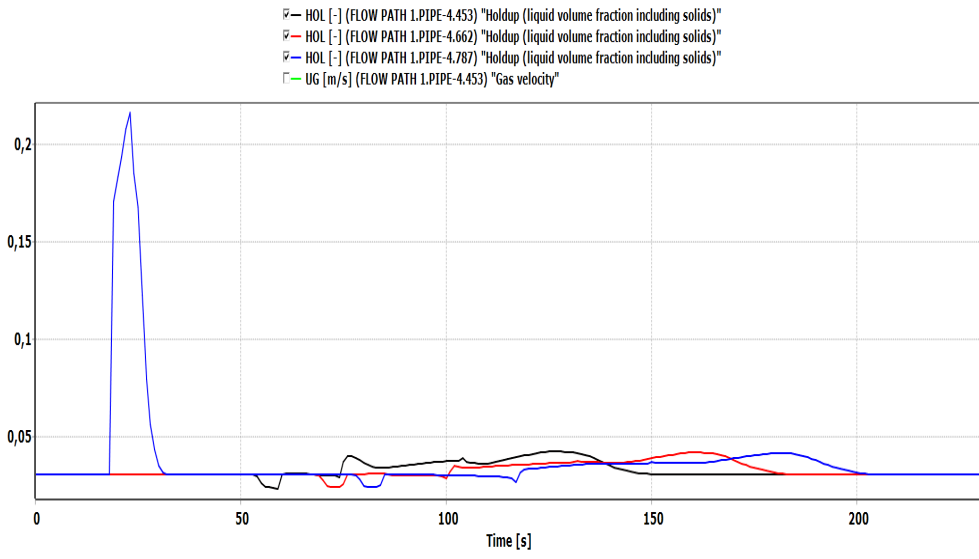
Time [s]	Air Flow Rate [kg/s]	Water Flow rate [kg/s]
0	0.030	0.036
10	0.030	0.036
11	0.012	0.036
22	0.012	0.036
23	0.030	0.036

#### 4.3.2.1 Mesh Size Effect

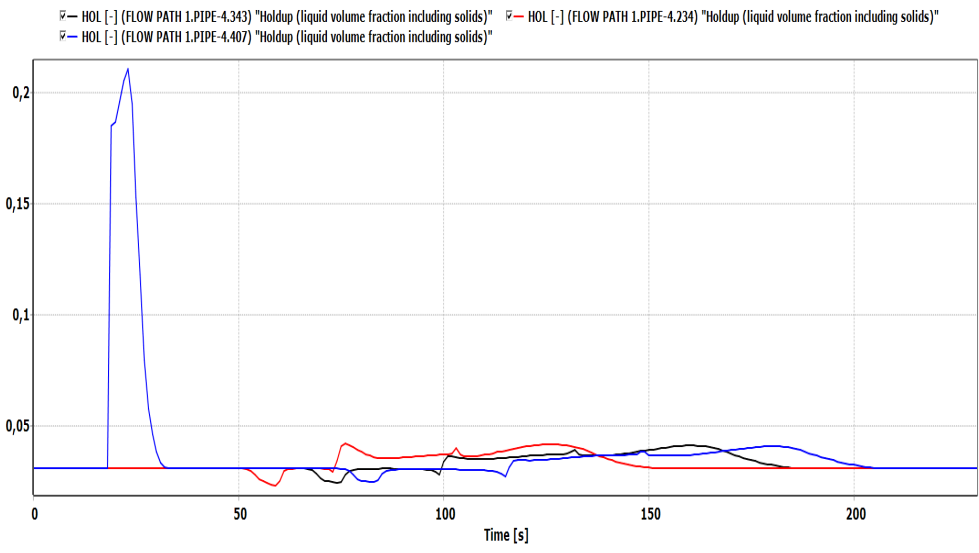
Mesh size influences numerical accuracy. It is said that the smaller the mesh size, the better the result. Computation time also increases with smaller mesh size. It is imperative to run a case with several mesh sizes to detect what mesh size is required to get a numerical solution to converge and eliminate numerical diffusion.

Instabilities and crashing is often an outcome of too fine mesh. Case 1 was run with four different mesh sizes ranging between  $\Delta = 1D - 10D$ , to observe the influence on the output. The plots are presented below. 1D mesh was the lowest mesh size applicable for this case and is recommended for OLGA simulations.

The larger mesh size smears out the resulting wave, increasing the period of the wave and decreasing the amplitude of the wave. This shows the effect of numerical diffusion increasing with increase in mesh size. The peak of the waves decrease significantly from 2D to 5D with 1D and 2D having only a slight difference in the waves. The hold up in all mesh sizes  $\Delta x = 1D - 10D$  remains below 0.05.

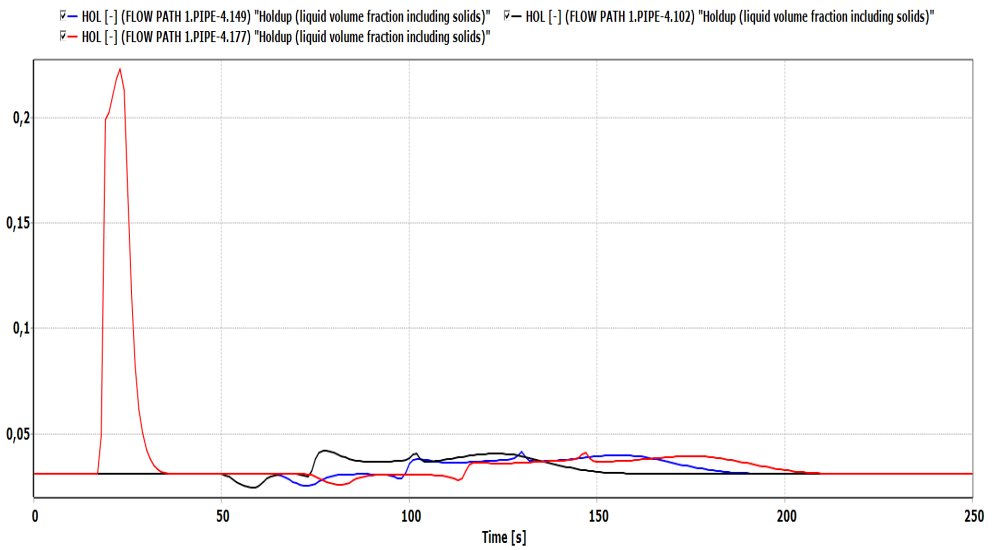


(a)  $\Delta x = 1$

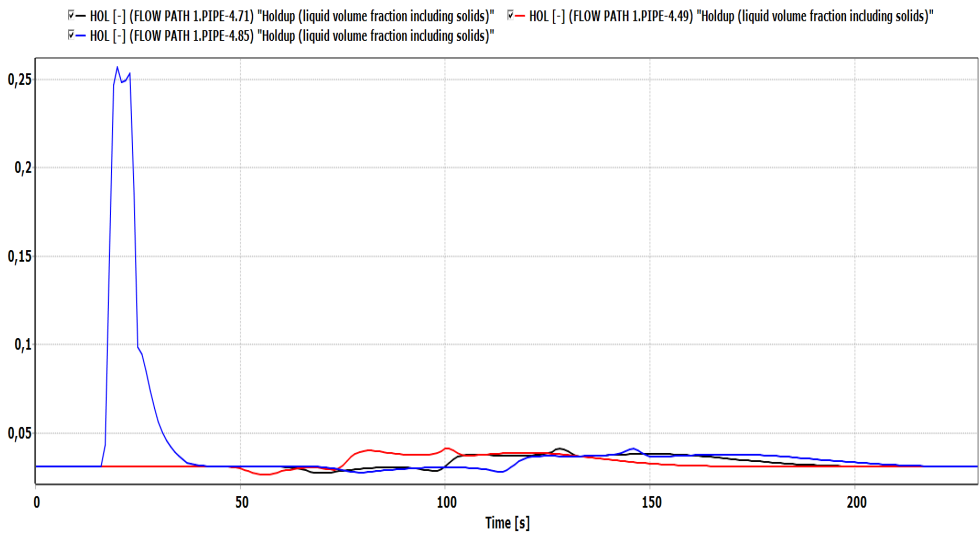


(b)  $\Delta x = 2$

**Figure 4.11:** Images showing influence of different mesh on the resulting wave,  $\Delta x=1D$  and  $\Delta x=2D$



(a)  $\Delta x = 5$



(b)  $\Delta x = 10$

**Figure 4.12:** Images showing influence of different meshes on the resulting wave,  $\Delta x=5D$  and  $\Delta x=10D$

The large peak at the beginning could represent an accumulation at the end of the pipe when air rate is ramped down, since it occurs at the last probe position, probe 3. This will

---

be discussed further in later sections.

### 4.3.2.2 Mass Discretization Scheme

The second order mass discretization scheme is an alternative to the 1st order scheme and incorporates a Total variation diminishing scheme in its calculation. It has less numerical diffusion and produces sharper fronts, as seen in **fig.4.13**. The front in comparison to **fig.4.11a** is sharper and well defined. After 50 seconds however, the oscillations are seen to be more defined. 2nd order scheme is known to highlight numerical instabilities in simulations.

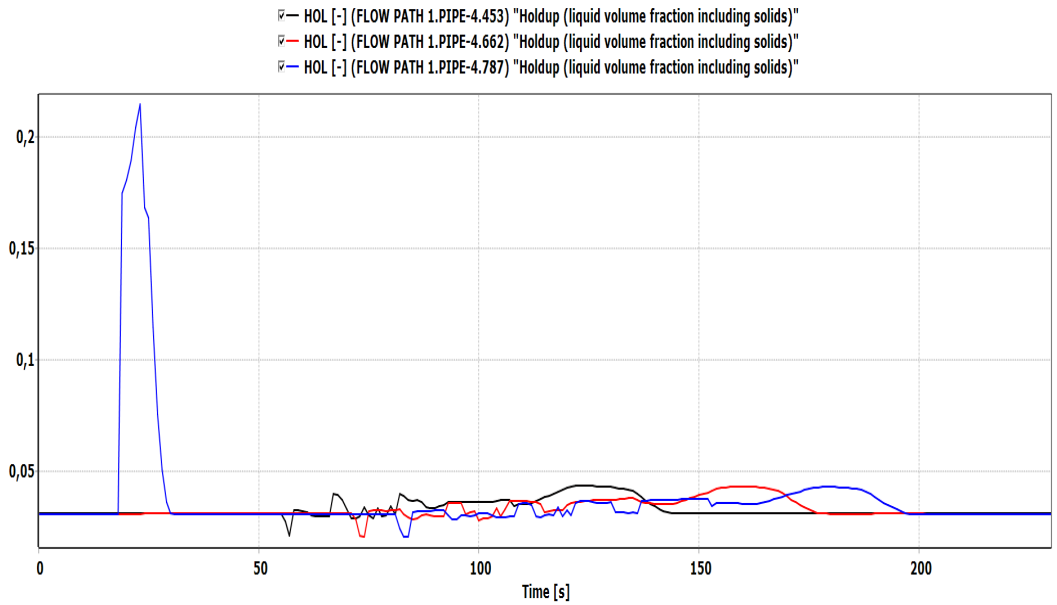


**Figure 4.13:** Case 1 simulation with 2nd Order scheme at  $\Delta x = 1D$

The diffusive behavior in the 1st order scheme reduces the unphysical numerical instabilities, is more robust and is preferred [34]. Thus, 1st order scheme will be used in this work.

---

### 4.3.2.3 Discussion

Case 1 had water flow of 54 kg/h and oil flow of 60 kg/h. In comparison with the rest of the cases, the liquid flow rates were almost equal. The air velocity was the highest of the seven cases, with a superficial velocity of  $U_{SG} = 8.95$  m/s. The flow was stratified for the duration of the simulation, see **fig.4.14**.

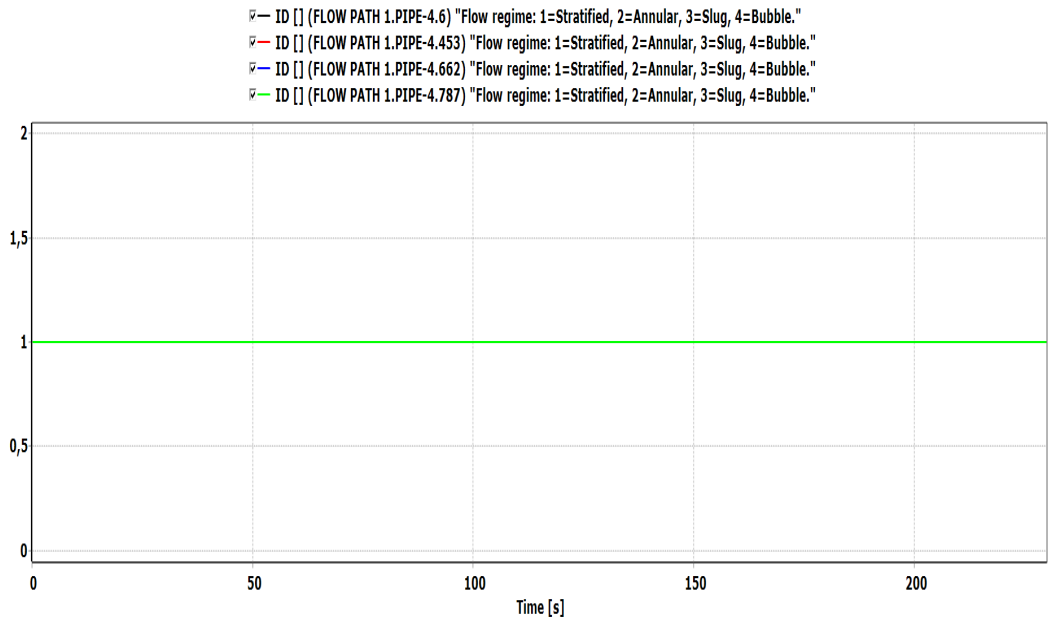


**Figure 4.14:** Flow regime identity for the flow path. A point at the very beginning of the pipe is included to show no formation of slugs

From the simulation result, waves are observed flowing through the pipe at the three probe positions on the pipeline. At probe 3 position, which is closest to the end of the pipe, quite a large spike in hold up is seen when the air rate is ramped down. This is highly possible since when the rate is abruptly ramped down, the flow does not remain completely immobile. The hold up seen at this point may be exaggerated since OLGAs is known to predict higher hold ups. Quickly after ramp up, the accumulation is drawn out and the wave formed at the start of the pipe is seen moving along the pipe. These observations can be seen in **fig4.15**.

This corresponds with experimental data where it is seen that there is an increase in the hold up during air rate ramp down before normal wave activity transpires. A figure showing the normalized conductance probe readings for Case 1 is shown below in **fig4.16**. The red line represents the conductance readings at probe 3. At about 170 seconds is where air rate ramp down is experienced at probe 2 (blue line) and it is seen that the curve is significantly rising at probe 3. At about 210 seconds the effect of the air rate ramp up is felt and the accumulation passes 3 before the actual wave comes.

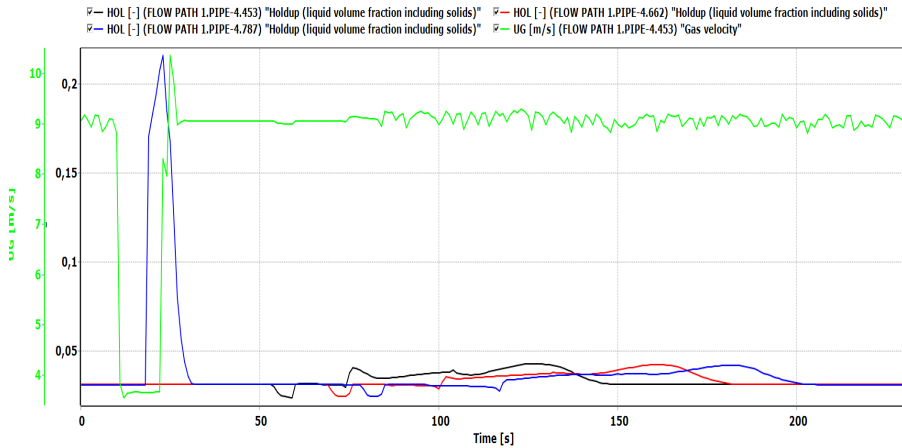


**Figure 4.15:** Case 1 simulated result showing flow behavior as a result of air flow manipulation

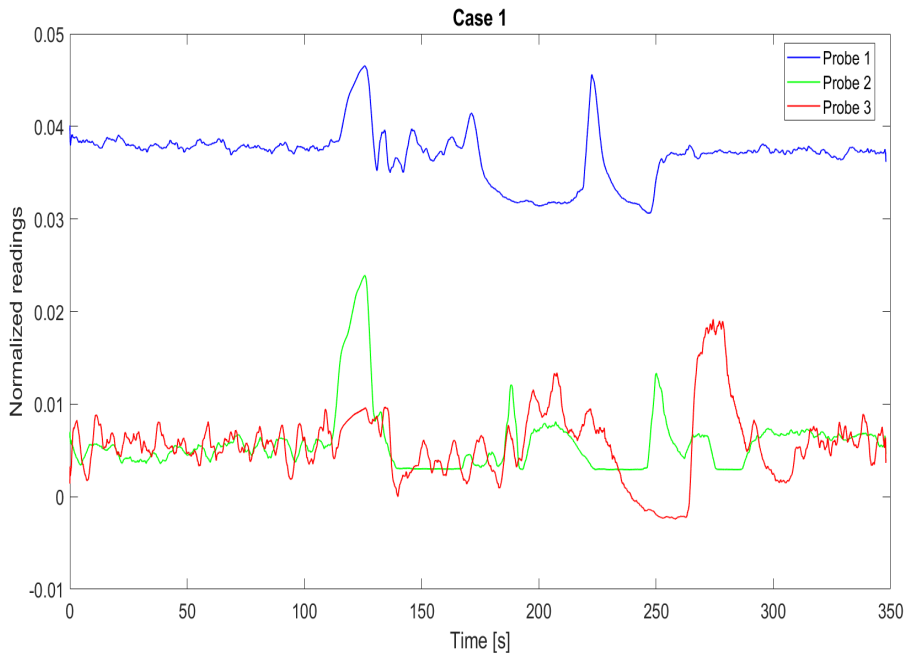


**Figure 4.16:** Case 1 experimental data - Conductance probe readings

The first wave lasts for a period of about 70 seconds while the last wave lasts for a period of about 85 seconds. This shows that the wavelength increases over time as it diminishes. The wave periods are longer than that in the recorded footage which is seen to

last for a period of about 15 - 20 seconds. However, the prediction of the wavelength of the waves produced in the lab was done by visual perception. It was difficult to predict the ends of the waves due to this. This makes it a possibility that the waves lasted for much longer durations of time.

The air velocity seen on **fig.4.15** is represented by a green line. It is seen to have a lot of small oscillations. This could be a result of the numerical computation of the software.

#### 4.3.2.4 Varying water cut effect

The same case was repeated with water cuts of 0%, 50% and 100%. The initial case has a water cut of 37%. The wave behavior changed significantly with change in water cuts.

For the case of 0% water cut (only oil) seen in **fig.4.17**, there are two wave peaks at each observation point. The wave does not seem to adjoin until the end of the pipe which means that the velocity of the first wave does not diminish enough for the second to catch up and become a single wave. Possibly a longer pipeline would show such a phenomenon since the wave peaks are seen diminishing at the third position (blue line) The wavelength of the waves is slightly shorter than those with more than one liquid flowing, about a minute long.

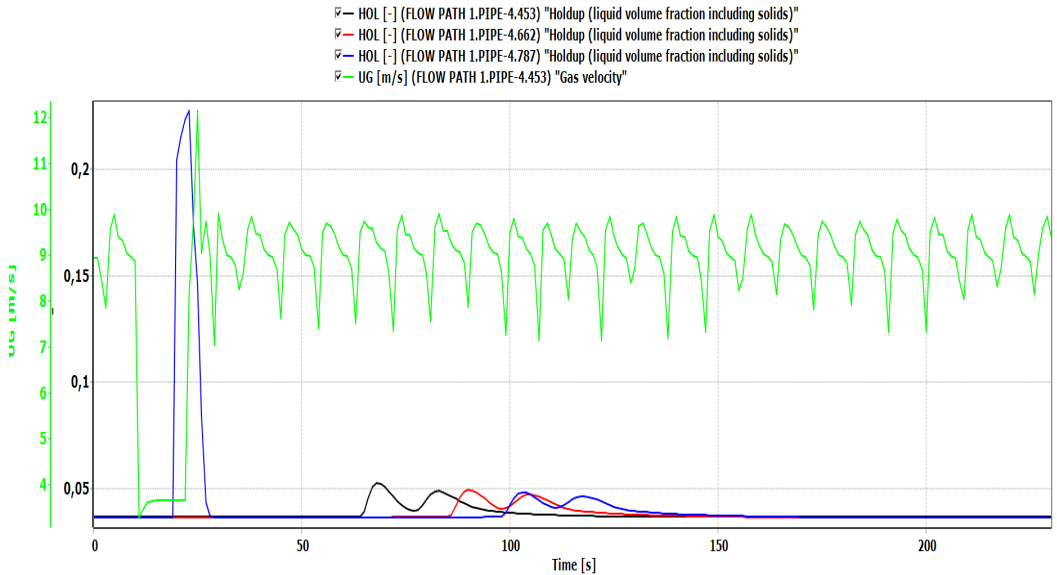


**Figure 4.17:** OLGA 2019.1 plot of Case 1 at 0% water cut

At 50% water cut the wave behavior shows an interesting observation. After the ramp up it seems there are two waves flowing through the pipe. Looking at **fig.4.18**, it is seen



that after an initial dip small wave passes before a larger dip is followed by a bigger wave. This is seen at all three positions along the pipe. The differences in densities of the two liquids is a huge factor that could explain this behavior. The phenomenon by which the oil and water is distributed as they flow is difficult to know at every position of the pipe. Thus it is possible that the denser fluid is held back while the other flows ahead, before it receives enough energy to be propagated through the pipe. This is seen in some of the images in appendix A and B, where it can be said that mixture flow with more oil precedes that with more water. This is more evident in flows with higher water cut.

It can also be noted that the wave length of the waves is much longer compared to the 0% and 37% water cut cases. Thus as water cut increases, the wave length gradually increases. The wave period also seems to increase ranging from 100 to 140 seconds in this plot. More time is needed for the flow to return as before.

OLGA

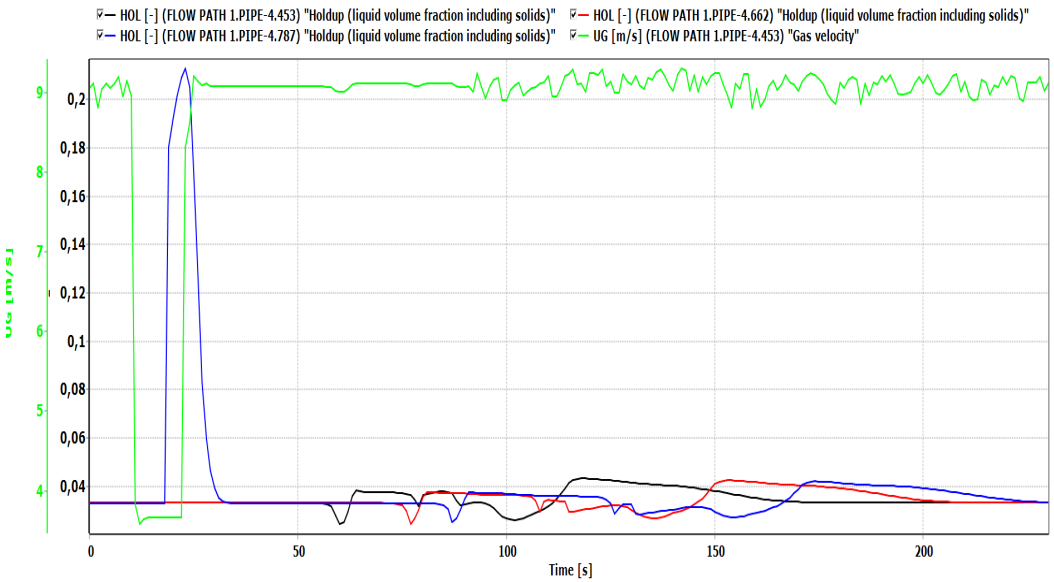


**Figure 4.18:** OLGA 2019.1 plot of Case 1 at 50% water cut

At 100% water cut it is observed that the flow behavior is completely different from three phase flow. Water takes a longer period to stabilize, needing more than 230s unlike the rest of the cases. The gas velocity is more stable with no oscillations. The waves seem to show a delayed response to the air rate alterations, with the first wave starting after 100 seconds. The density of the water is a major factor that can explain this behavior. From this it can be concluded that at higher water cuts, waves of this nature need a longer period of time to decay. The waves can thus travel for longer lengths of pipe. The behavior of the simulator does not show two peaks like it is seen from the experiments in **fig.5.28,5.29** and **5.30**.

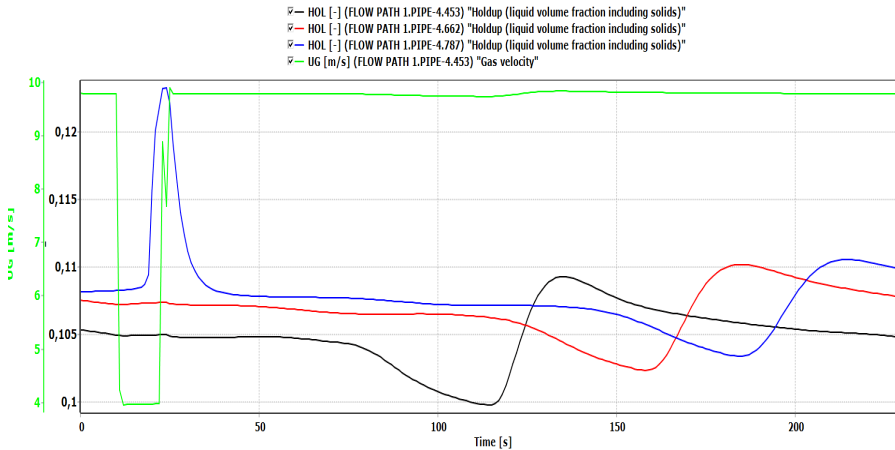


**Figure 4.19:** OLGA 2019.1 plot of Case 1 at 100% water cut

Wave velocities were calculated for this case from the experimental recorded data and the simulation data. The distance between probe 1 (34.175 m) and probe 2 (47.195 m) is about 13 metres. The distance between probe 2 and probe 3 (54.895 m) is about 6 metres. It is expected that the velocity from probe 2 to probe 3 will be lower due to the short distance between the two probes. It should be noted that there may be inaccuracies with the calculations for wave velocity from the experimental data because the conductance probes record only water flow and do not account for oil. This means that the peaks chosen to represent the actual waves in the plots from the experimental data may be imprecise to some degree, especially considering the observation that water is plentiful towards the end of the wave.

The results for 0% water cut case were not able to be used due to the nature of the readings. As explained above, oil flow is not detected by the conductance probes. This can be seen in **fig.4.20**

**Figure 4.21** shows the comparison between wave velocities for simulations and experimental data. The experimental data showed that wave moved faster from probe 1 to probe 2 and slowed down from probe 2 to probe 3 for all three cases, which is expected since the distances between the probes are not equal. The simulated data showed the same trend though the difference in velocity between probes 1 and 2 and probes 2 and 3 were smaller. Generally the experimental data lies above the simulated data, which indicates that the waves moved faster in the experiments than the simulations. This could be due to numerical errors as well as differences in fluid properties.

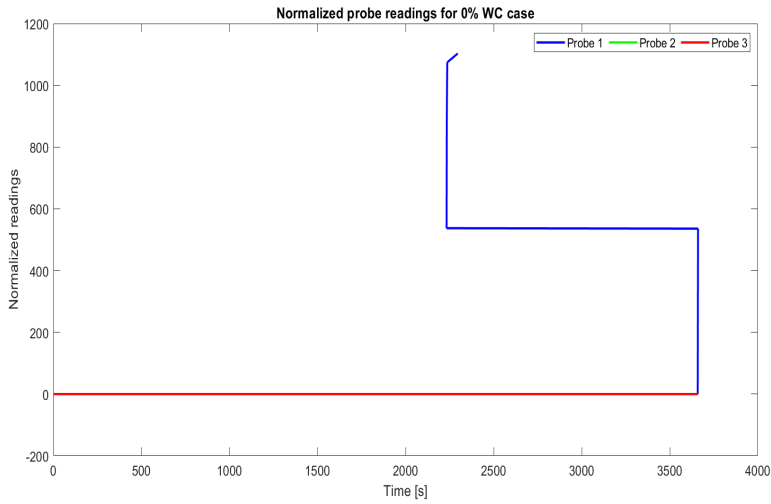


**Figure 4.20:** Conductance probe readings for 0% case

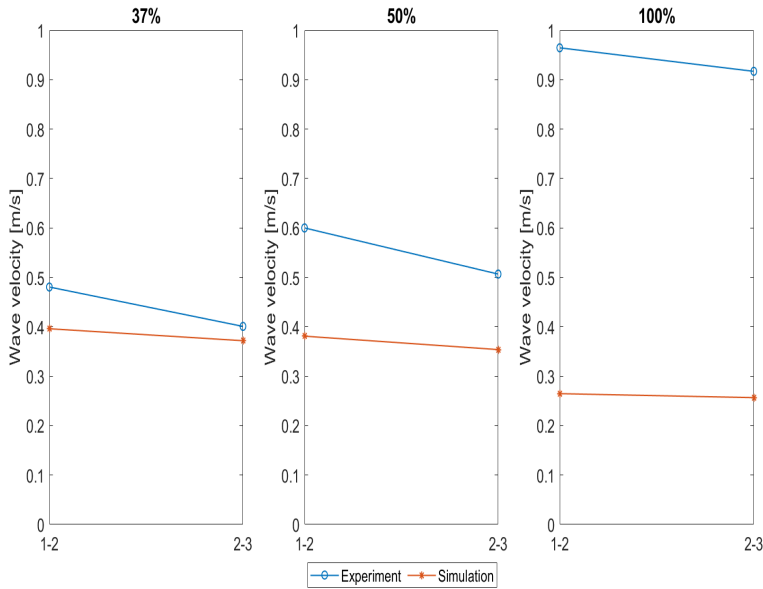


**Figure 4.21:** Plot showing comparisons of experiment and simulated results for wave velocity at 37%, 50% and 100%

The wave velocities for 37% water cut for the experimental and the simulated data were comparable with about 0.1 m/s difference between probe 1 and 2 and less than 0.1 m/s difference between probe 2 and 3. The gap widened for 50% water cut presented a larger deviation in values with about 0.2 m/s difference between probe 1 and 2 and about

---

0.15 m/s between probe 2 and 3. For 100% water cut, the gap between the simulated and experimental data becomes significantly larger with velocity difference greater than 0.6 m/s between both probe 1 and 2 and probe 2 and 3.

For two-phase flow with air and water it was seen in previous work that the wave velocity in real data deviated from the simulated data. The simulated data was characteristically lower than the real data. From this perspective, the 100% water cut wave velocity comparison may be more accurate than the 37% wave velocity comparison. Further analysis on this is needed.

### **4.3.3 Limitations**

- The density used for the experimental analysis was greater than that used in the simulations. The specified density used for lab analysis was  $800 \text{ kg/m}^3$  while that of the simulations ranged between 750 to  $755 \text{ kg/m}^3$ . Attempts to increase the density used for the fluid file were not successful. This can be a precaution in case further work is done on this topic.
- The determination of the wave velocity for experimental data may not be accurate. This is because the waves represented in the data plots are for water flowing in the conduit and not oil flow. The oil flow is seen to distort the readings meaning that actual wave peaks and occurrence times may differ.

# Conclusion

## 5.1 Concluding Remarks

Experiments were performed in the NTNU multiphase laboratory to make a study on surge waves in three-phase flow. Similar experiments to this were done previously during project work. In the project work, with two-liquid flows [26], it was found that the propagation of waves at higher air velocities formed roll waves in comparison to only water flows. Assurance of formation of three-phase surge waves in the laboratory was with lower air velocities and lower amounts of liquid.

Several tests were carried out with varying amounts of oil and water in order to find cases which created good surge waves in the flow path. The waves were created by manipulating the air flow. Air flow rate was ramped down, accumulations occurred at the lower points of the pipe, and then subsequently ramped up. This caused waves to propel along the pipe line. Seven cases were selected and are highlighted in this work. The cases were arranged in descending order of the liquid mass flow rate with Case 1 having the highest liquid mass rate and case 7 having the lowest liquid mass rate. Surge waves were able to be formed successfully with regard to the previous attempt during the project work [26].

As a general trend, most cases would have two waves - an initial smaller wave with a smooth front and a larger wave that followed with a some what sharper front. There was difficulty in distinctly predicting the end of the waves since visual perception was used for determination. It was found that the waves would last between 10 to 25 seconds, with the period increasing as the wave propagated towards the end. In real cases, surge waves are known to last even for over an hour. The waves would gradually decrease in amplitude as they flowed along the pipe, which was expected. It was found that cases with higher amounts of water in the liquid mixture distinctly showed water towards the end of the wave. This means that the oil precedes the water in the flowing waves. From the camera at the start of the pipe, the two phases would often appear as separate waves with their own peaks. At the latter cameras, camera 2 and camera 3, the peaks would diminish and almost seem as one. It was not possible to determine this numerically due to absence of equipment to measure liquid phase hold up.

---

Case 1 [ $U_{SG} = 8.95$  m/s  $U_{SL} = 0.0144$  m/s] was applied in observing the three phase flow behavior for varying water cuts on the experimental side. It was found that with increasing water cut, the waves would increase in size. This means that the oil wave was much smaller than the water wave.

OLGA 2019.1 was the version of the software used for evaluation. Simulations performed in previous work by different versions of OLGA were replicated using this latest version. The previous simulations were done using OLGA 7.1[18], OLGA 7.3.5[14] and OLGA 2016.2.1[14]. The main difference between the replicated simulations and those done previously was the fluid file used. This fluid file was provided by Jørn Kjølås from SINTEF. The wave hold up results from the latest version corresponded most with those from OLGA 7.1 and OLGA 7.3.5. The results from OLGA 2016.2.1 did not comply. For wave velocity results, there was very little correlation with all the versions of OLGA. The closest correspondence was with OLGA 2016.2.1 HD results.

Case 1 [ $U_{SG} = 8.95$  m/s  $U_{SL} = 0.0144$  m/s] was the three phase case applied for simulations. The initial case that was selected in the lab had a water cut of 37%. One stand-out characteristic of the resulting plots was a large accumulation towards the end of the pipe during ramp down which was discharged soon after ramp up. This is a possible phenomenon as ramp down does not completely immobilize the liquid flowing in the pipe. Thereafter, the waves travel along the flow path with wavelength increasing after each position. Two peaks were visible on the wave front, with the first one smaller than the next. The two peaks blended in with each other as they moved along the pipe. This accounts for the two waves seemingly flowing after ramp up in the experimental results. The simulated waves lasted much longer than the experiment wave periods, ranging from 60 seconds to 85 seconds. This could mean that the waves observed in the lab lasted much longer than what was perceived. Simulations, however, are known to produce rather exaggerated values.

Case 1 [ $U_{SG} = 8.95$  m/s,  $U_{SL} = 0.0144$  m/s] was also simulated for different water cuts 0%, 50% and 100%. At 0% water cut, two peaks were well defined and did not merge into one throughout the pipe. At 50% water cut, two peaks were also visible. The first peak was smaller than the latter. The wavelength increased significantly. The behavior of the waves is indicative of the them being able to last for longer lengths of pipeline. In reality, gas-condensate pipelines span for great lengths, up to thousands of metres.

Wave velocities for both experimental and simulated results were compared. It revealed a significant deviation in result. The experimental wave velocities were higher than the simulated wave velocities. Lower water cuts showed better correlation in wave velocity than higher water cut **fig4.21**. However, the results of this need to be verified since the conductance probes may have not properly represented the surge waves. This is because the equipment is responsive to water flow and not oil flow.

Generally the simulated data highlighted similar trends from the experimental data such as the double peaks with a smaller wave before a larger wave. Not much can be said regarding the hold ups since it could not be determined experimentally. There was a difference in the wave period between the experiments and simulated results with simulated waves lasting for much longer periods up to 85 seconds.

---

## **5.2 Suggestions for further work**

For further experimental work, it would be very useful to carry out research on surge waves with instrumentation for rapid three phase fraction measurements. This would be helpful in expanding to a wider range of research that in relation to surge wave phenomenon in small scale.

Improved simulations would also be helpful to see whether waves can be accurately predicted by dynamic simulators in small scale.

Upon establishment of a better framework for three-phase surge waves in small scale, the design of a separator to accommodate these surges could be researched.

---



# Bibliography

- [1] Field: SNØHVIT. Library Catalog: [www.norskpetroleum.no](http://www.norskpetroleum.no).
- [2] OLGA Dynamic Multiphase Flow Simulator. Library Catalog: [www.software.slb.com](http://www.software.slb.com).
- [3] *A-to-Z Guide to Thermodynamics, Heat and Mass Transfer, and Fluids Engineering: AtoZ*, volume M. Begellhouse, 2006.
- [4] Multiphase Flow, June 2020.
- [5] OLGA (technology), Apr. 2020. Page Version ID: 952458545.
- [6] M. Açikgöz, F. França, and R. Lahey. An experimental study of three-phase flow regimes. *International Journal of Multiphase Flow*, 18(3):327–336, May 1992.
- [7] A. Bannwart, O. Rodriguez, F. Trevisan, F. Vieira, and C. de Carvalho. Experimental investigation on liquid–liquid–gas flow: Flow patterns and pressure-gradient. *Journal of Petroleum Science and Engineering*, 65(1-2):1–13, Mar. 2009.
- [8] D. H. Beggs and J. P. Brill. A Study of Two-Phase Flow in Inclined Pipes. *Journal of Petroleum Technology*, 25(05):607–617, May 1973. Publisher: Society of Petroleum Engineers.
- [9] K. H. Bendiksen, D. Maines, R. Moe, and S. Nuland. The Dynamic Two-Fluid Model OLGA: Theory and Application. *SPE Production Engineering*, 6(02):171–180, May 1991. Publisher: Society of Petroleum Engineers.
- [10] D. Biberg, H. Holmås, G. Staff, T. Sira, J. Nossen, P. Andersson, C. Lawrence, B. Hu, and K. Holmås. Basic flow modelling for long distance transport of wellstream fluids. *14th International Conference on Multiphase Production Technology*, pages 463–477, Jan. 2009.
- [11] M. Bonizzi, P. Andreussi, and S. Banerjee. Flow regime independent, high resolution multi-field modelling of near-horizontal gas–liquid flows in pipelines. *International Journal of Multiphase Flow*, 35(1):34–46, Jan. 2009.
- [12] O. Bratland. *Pipe Flow 2: Multi-phase Flow assurance*. Number 2 in Pipe Flow. 2nd edition, Sept. 2013.

- 
- [13] Cadarao. Lecture Notes TEP 10 - Reservoir. Oct. 2008.
- [14] L. Dan. Numerical simulation of surge wave instability of long distance transport of multiphase flow. Master's thesis, Norwegian University of Science and Technology, Trondheim, Norway, 2018.
- [15] A. De Leebeeck. *A roll wave and slug tracking scheme for gas-liquid pipe flow*. PhD thesis, NTNU, 2010.
- [16] S. Evje and K. Fjelde. Fjelde K.K.: Relaxation schemes for the calculation of two-phase flow in pipes. *Math. Comput. Model.* 36, 535-567. *Mathematical and Computer Modelling*, 36:535–567, Sept. 2002.
- [17] K. K. Fjelde and K. H. Karlsen. High-resolution hybrid primitive–conservative upwind schemes for the drift flux model. *Computers & Fluids*, 31(3):335–367, Mar. 2002.
- [18] S. I. Grøhdahl. Small scale multiphase flow experiments on surge waves in horizontal pipes. Master's thesis, Norwegian University of Science and Technology, June 2014.
- [19] H. Holm. Tanzania Gas Development-Flow Assurance Challenges. In *BHR-2019-409*, page 16, BHR, Dec. 2019. BHR Group. Journal Abbreviation: BHR-2019-409.
- [20] K. Holmås, G. Lunde, G. Setyadi, P. Angelo, and G. Rudrum. Prediction of liquid surge waves at Ormen Lange. pages 45–58, Jan. 2013.
- [21] R. I. Issa. Prediction of turbulent, stratified, two-phase flow in inclined pipes and channels. *International Journal of Multiphase Flow*, 14(2):141–154, Mar. 1988.
- [22] J. M. Jansen. Evaluation of a Flow Simulator for Multiphase Pipelines. *128*, 2009. Accepted: 2014-12-19T11:52:03Z Publisher: Institutt for energi- og prosesssteknikk.
- [23] G. S. Landsverk, G. Flaten, M.-A. Svenning, D. Pedersen, and B. H. Pettersen. Multiphase Flow Behaviour at SnøHvit. 2009.
- [24] R. W. Lockhart and R. C. Martinelli. Proposed correlation of data for isothermal two-phase, two-component flow in pipes. *Chemical Engineering Program*, 45:39–48, 1949.
- [25] G. G. Lunde, G. Rudrum, P. Angelo, K. Holmas, and G. R. Setyadi. Ormen Lange Flow Assurance System (FAS) - Online Flow Assurance Monitoring and Advice. In *OTC Brasil*, Rio de Janeiro, Brazil, 2013. Offshore Technology Conference.
- [26] S. Lyimo. Project: Multiphase Flow Transients in wet gas pipelines. Technical report, Norwegian University of Science and Technology, Trondheim, Norway, Jan. 2020.
- [27] M. Langsholt, O. Sendstad, and T. Sira. Surge waves in gas-liquid pipe flow Experiments and analysis,”. Technical report, IFE, Kjeller Halden, 2004.
- [28] F. Matovu. Drift Flux Models. *NTNU Open*, 2014.
- [29] E. E. Michaelides, C. T. Crowe, and J. D. Schwarzkopf, editors. *Multiphase Flow Handbook*. CRC Press, 2 edition, Oct. 2016.
-

- 
- [30] O. J. Nydal. Multiphase Transport Lecture Notes. 2008.
- [31] O. J. Nydal. Multiphase Transport Lecture Notes: Stratified Flow. 2019.
- [32] B. Pettersen, M. Nordsveen, and E. Thomassen. Liquid Inventory and Three Phase Surge Wave Data From the Midgard Gas Condensate Fields in the North Sea. In *BHR-2013-F2*, page 12, BHR, June 2013. BHR Group.
- [33] A. Scandpower. Lecture notes OLGA2000 NTNU. Apr. 2001.
- [34] . Schlumberger. OLGA 2019.1 User manual. Technical report.
- [35] G. R. Setyadi, K. Holm\ aas, G. G. Lunde, K. Vannes, A. Sengebusch, M. Nordsveen, and B. H. Pettersen. \AAsgard subsea compression and predictions of liquid surges. BHR Group, 2017.
- [36] H. Torpe, J.-M. Godhavn, S. T. Strand, M. Løvik, J. Tengedal, and B. H. Pettersen. Liquid Surge Handling at ÅSgard by Model Predictive Control. BHR Group, June 2009.
- [37] M. Wörner. A compact introduction to the numerical modeling of multiphase flows. Technical report, Karlsruhe, 2003. Medium: PDF.



---

# Appendix

This appendix will be split into 5 parts. The first part will show images of the initial cases that were selected to observe surge waves in three phase flow. The second part will show images of the surge waves for Case 1 at different water cuts of 0%, 50% and 100%. The third part will show the repeated two-phase simulations. The fourth part will show the simulations performed for the three-phase case. The fifth part will include any other useful information for this thesis work. The final part will include the Risk assessment report.

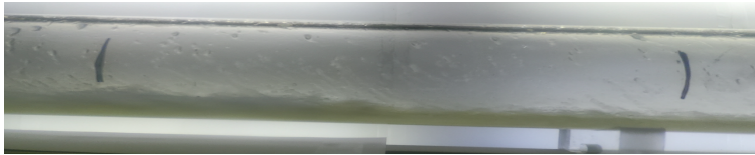
---

## A Camera Images: Initial Cases

Part 1 of Appendix A contains the images for cases 1 to 7 at different  $U_{SG}$  and  $U_{SL}$ . These are the cases that were selected out of a wider range of cases performed in the lab. They have varying oil and water rates constituting to the total liquid rate.

### A.1 Case 1 ( $U_{SG} = 8.95$ m/s $U_{SL} = 0.0144$ m/s)

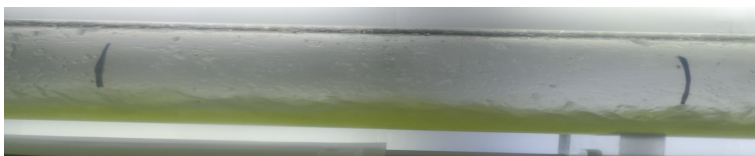
#### I. Camera 1



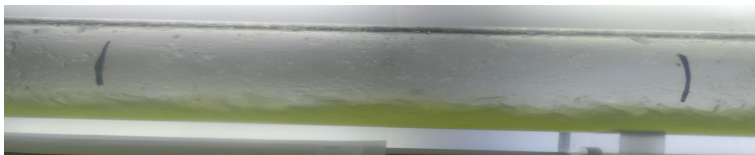
(a) Initial wave passes through the observation section



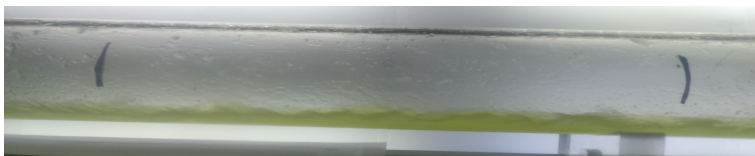
(b) Larger wave following the first wave, more messy and foamy at the top. Liquid distribution is unclear



(c) The wave continues through the observation section decreasing in hold up



(d) The tail of the wave continues to flow

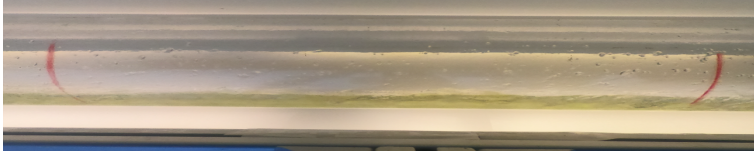


(e) The wave has passed and stability is regained shortly after

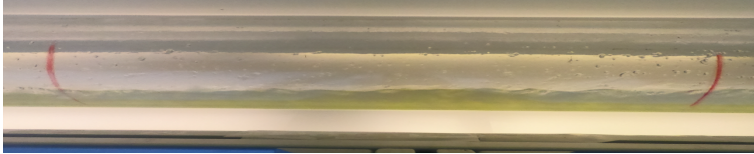
**Figure 5.1:** Images showing Case 1 [ $U_{SG} = 8.95$  m/s,  $U_{SL} = 0.0144$  m/s] at Camera 1 position at 6.4m

---

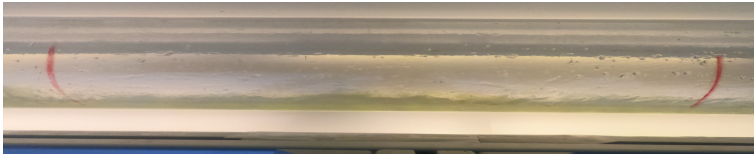
## II. Camera 2



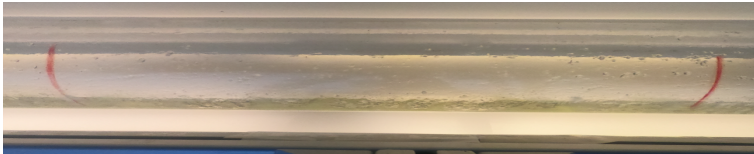
(a) Stable flow before wave passes



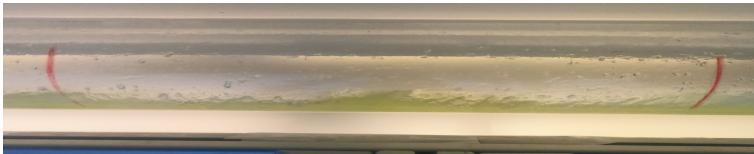
(b) Wave enters the frame with foamy-like substance at the top. Peak holdup visible



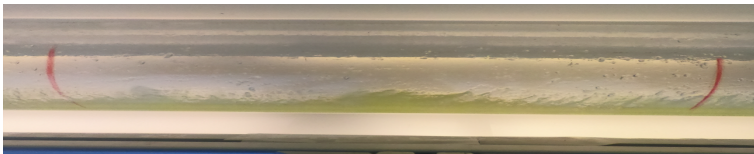
(c) Hold up gradually decreases



(d) The wave has passed and seems like normal flow will restore



(e) More waves seem to pass, mostly likely lagged behind water

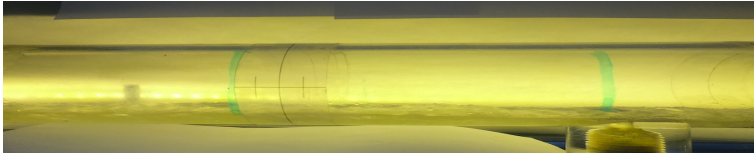


(f) The peaks continue showing non-uniformity before the flow begins to stabilize again

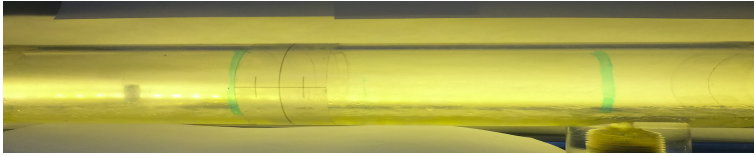
**Figure 5.2:** Images showing Case 1 [ $U_{SG} = 8.95$  m/s,  $U_{SL} = 0.0144$  m/s] at Camera 2 position at 26.7m

---

### III. Camera 3



(a) A severely diffused wave passes through the observation section. This is seen through an increase in hold up



(b) The wave has seemingly passed. This is not clearly detectable as the wave is diffused

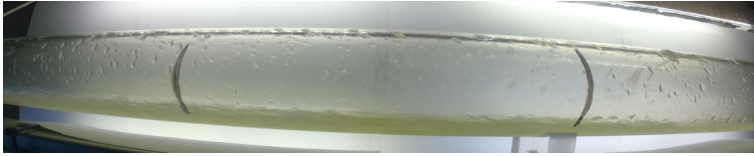
**Figure 5.3:** Images showing Case 1 [ $U_{SG} = 8.95$  m/s,  $U_{SL} = 0.0144$  m/s] at Camera 3 position at 52.3m



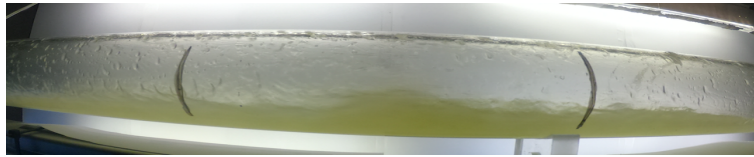
---

**A.2 Case 2 ( $U_{SG} = 8.37$  m/s,  $U_{SL} = 0.0127$  m/s)**

**I. Camera 1**



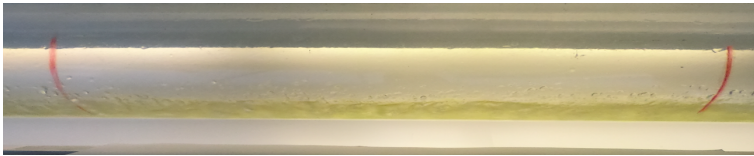
(a) Flow before ramp down



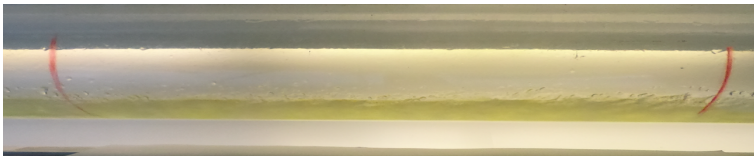
(b) A surge wave is seen passing through the observation section

**Figure 5.4:** Images showing Case 2 [ $U_{SG} = 8.37$  m/s,  $U_{SL} = 0.0127$  m/s] at Camera 1 position at 6.4m

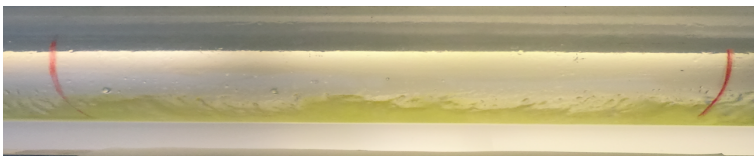
**II. Camera 2**



(a) Wave enters the observation section



(b) Wave is seen passing. The peak is not as eminent as other cases. A bit of foam is visible.

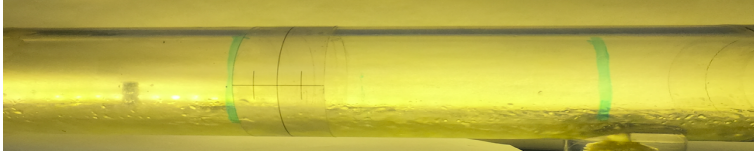


(c) The flow seems somewhat distorted with several small peaks passing

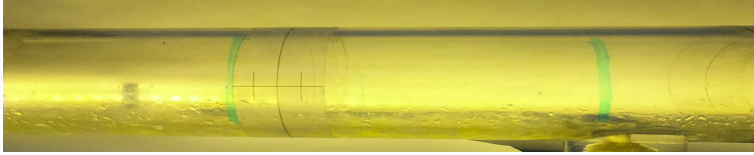
**Figure 5.5:** Images showing Case 2 [ $U_{SG} = 8.37$  m/s,  $U_{SL} = 0.0127$  m/s] at Camera 2 position at 26.7m

---

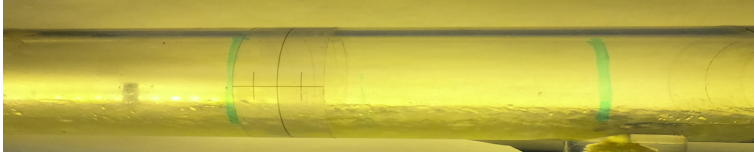
### III. Camera 3



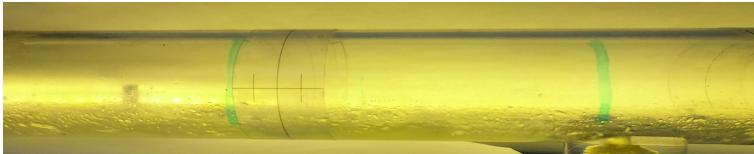
(a) Initial wave passes through the observation section visible as hold up increase, no clear front visible



(b) The wave continues through, though quite small. The wavelength is seemingly long



(c) The wave continues through the observation section with small increase in hold up



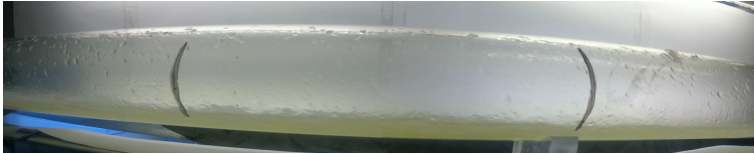
(d) The wave has seemingly passed

**Figure 5.6:** Images showing Case 2 [ $U_{SG} = 8.37$  m/s,  $U_{SL} = 0.0127$  m/s] at Camera 3 position at 52.3m

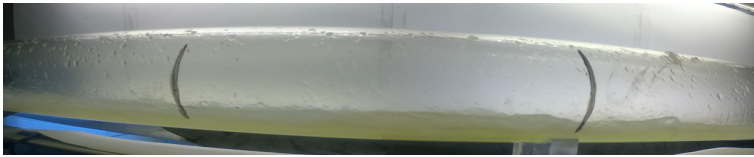
---

**A.3 Case 3  $U_{SG} = 8.52$  m/s,  $U_{SL} = 0.0124$  m/s**

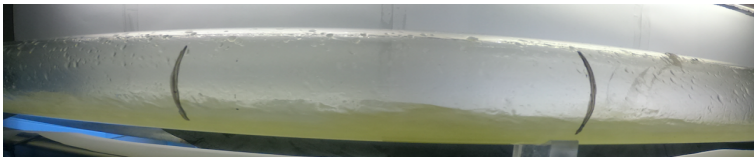
**I. Camera 1**



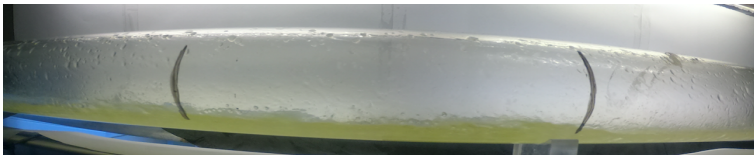
(a) Starting flow after ramp up before wave passes



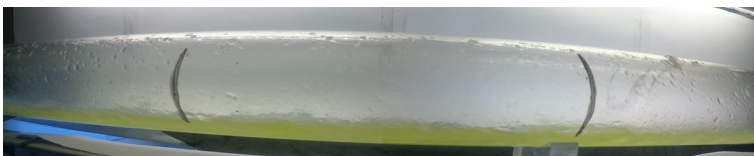
(b) Small wave passes begins first



(c) A surge wave with higher peak adjoins the initial wave, visually mixture of liquids



(d) A third smaller wave follows with more water in mixture

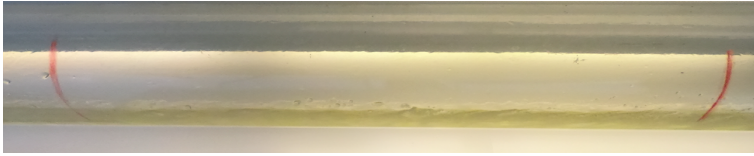


(e) The tail of the wave showing visibly more water in the mixture

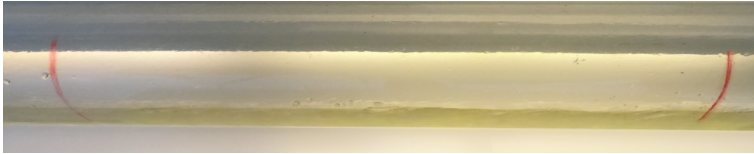
**Figure 5.7:** Images showing Case 3 [ $U_{SG} = 8.52$  m/s,  $U_{SL} = 0.0124$  m/s] at Camera 1 position at 6.4m

---

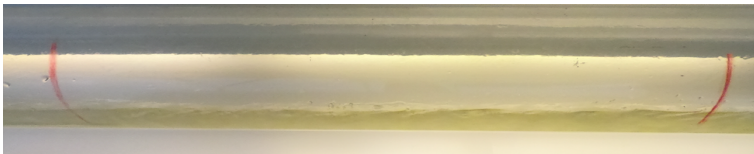
## II. Camera 2



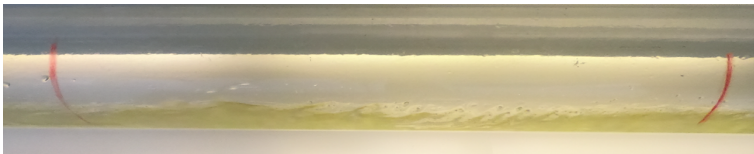
(a) The wave enters the frame at the first red mark. It is difficult to see the wave passing in still picture.



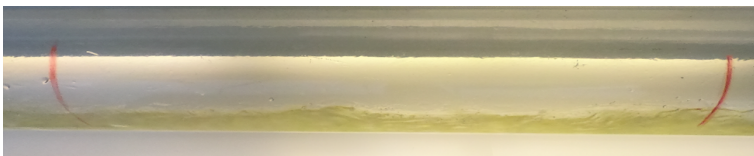
(b) Wave continues to pass, very diffused



(c) The wave continues through the observation section decreasing in hold up



(d) Breaks in the flow appear, more water is visible

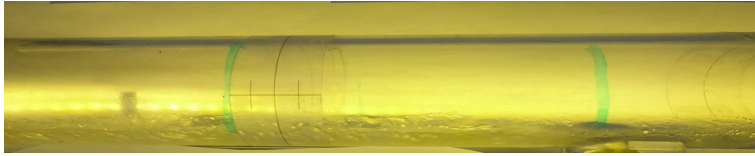


(e) After the wave has supposedly passed, some small peaks are seen that are presumed to contain more water than the start of the wave

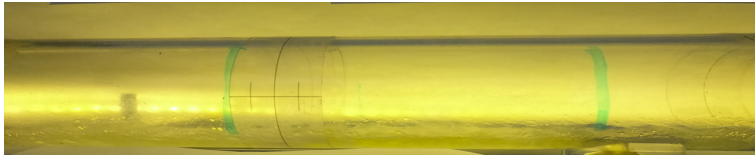
**Figure 5.8:** Images showing Case 3 [ $U_{SG} = 8.95$  m/s,  $U_{SL} = 0.0144$  m/s] at Camera 2 position at 26.7m

---

### III. Camera 3



(a) Wave passes through the observation section, visible through hold up increase



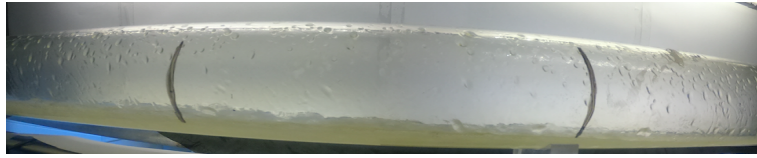
(b) The tail of the wave is not easily detectable

**Figure 5.9:** Images showing Case 3 [ $U_{SG} = 8.95$  m/s,  $U_{SL} = 0.0144$  m/s] at Camera 3 position at 52.3m

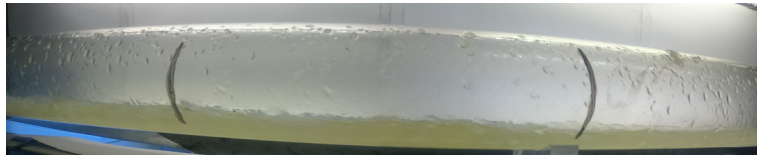
---

**A.4 Case 4  $U_{SG} = 8.52$  m/s,  $U_{SL} = 0.0106$  m/s**

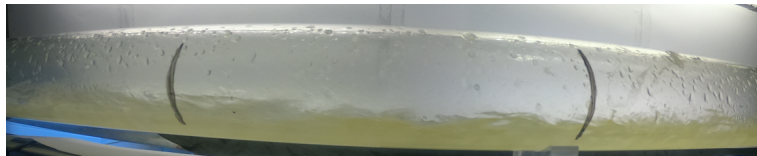
**I. Camera 1**



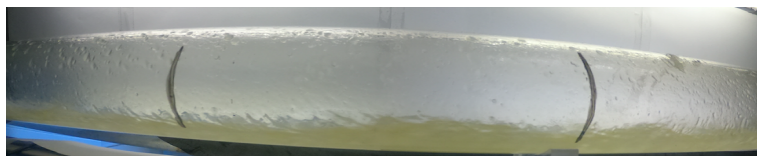
(a) The flow just after ramp up, wave has not passed



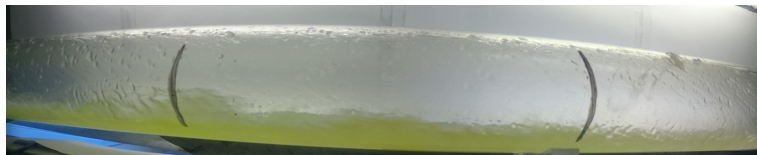
(b) Initial small wave passes through



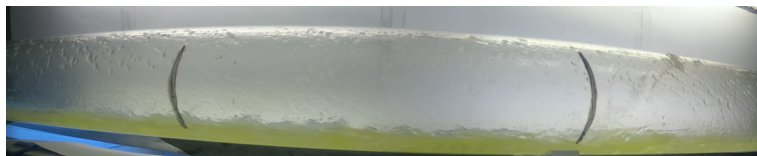
(c) Wave peak is visible, a bit rough due to more liquid held at dip



(d) The wave diminishes after the peak passes



(e) An adjoining wave of water, clearly visible

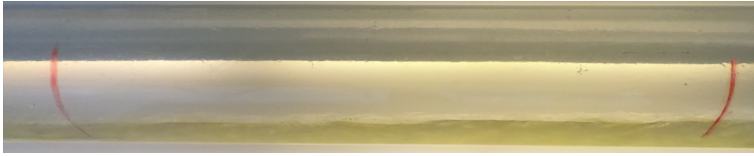


(f) The wave ends

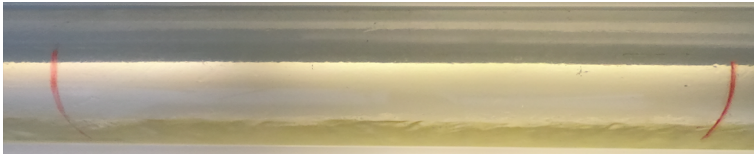
**Figure 5.10:** Images showing Case 4 [ $U_{SG} = 8.52$  m/s,  $U_{SL} = 0.0106$  m/s] at Camera 1 position at 6.4m

---

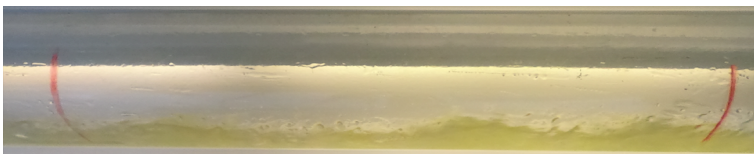
## II. Camera 2



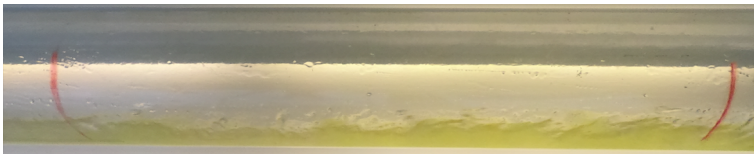
(a) Wave passes through the observation section



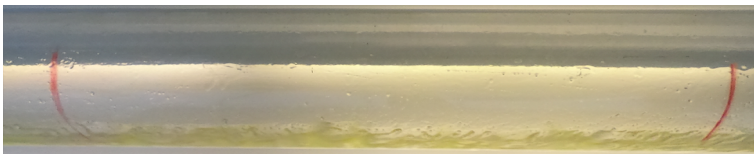
(b) It continues through the section



(c) Wave becomes distorted once more water becomes visible with small peaks passing



(d) Water is clearly visible in the passing wave

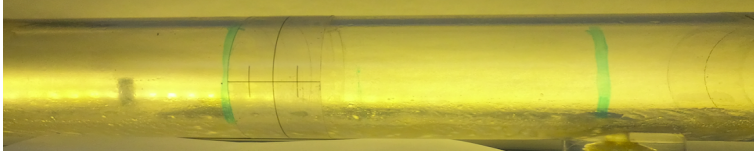


(e) The wave has passed

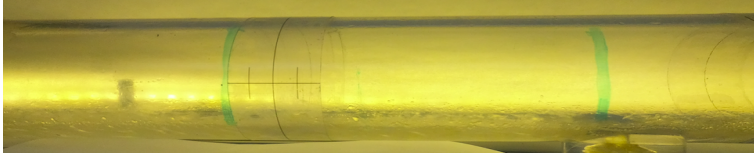
**Figure 5.11:** Images showing Case 4 [ $U_{SG} = 8.52$  m/s,  $U_{SL} = 0.0106$  m/s] at Camera 2 position at 26.7m

---

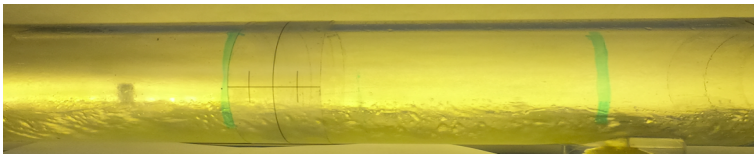
### III. Camera 3



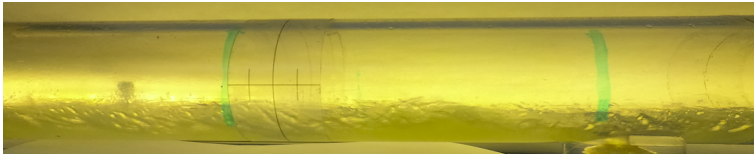
(a) Flow before the wave passes through the section



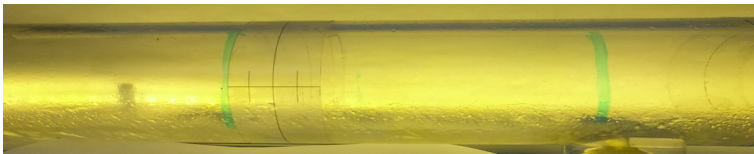
(b) A very diminished wave is seen as hold up increases



(c) The flow becomes distorted towards the end of the wave where water is predicted to be higher than oil in the mixture



(d) Water peaks are visible



(e) The wave has passed and the total flow has decreased before stabilization of flow

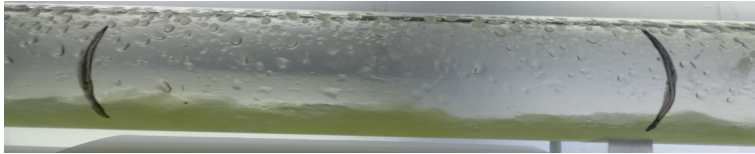
**Figure 5.12:** Images showing Case 4 [ $U_{SG} = 8.52$  m/s,  $U_{SL} = 0.0106$  m/s] at Camera 3 position at 52.3m



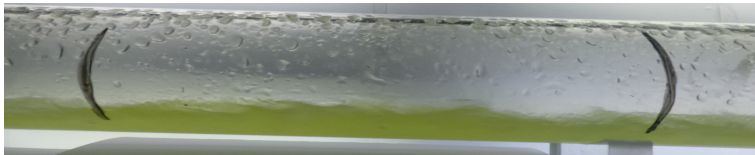
---

A.5 Case 5  $U_{SG} = 8.52$  m/s,  $U_{SL} = 0.0060$  m/s

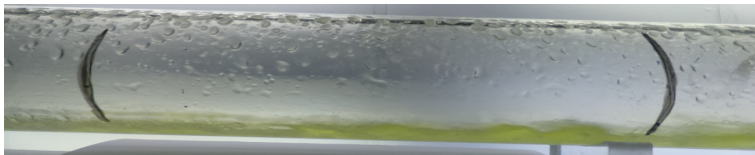
I. Camera 1



(a) The wave enters the observation section



(b) As the wave continues, water becomes more visible toward end

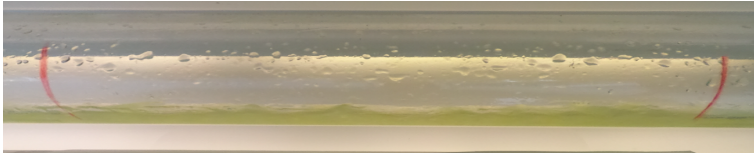


(c) The wave has passed

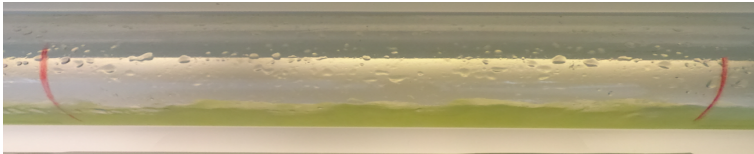
**Figure 5.13:** Images showing Case 5 [ $U_{SG} = 8.52$  m/s,  $U_{SL} = 0.0060$  m/s] at Camera 1 position at 6.4m

---

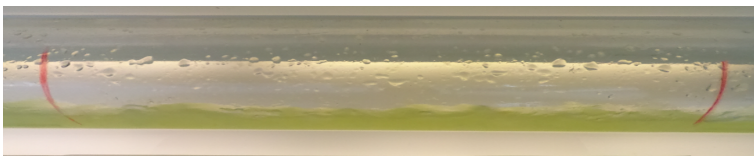
## II. Camera 2



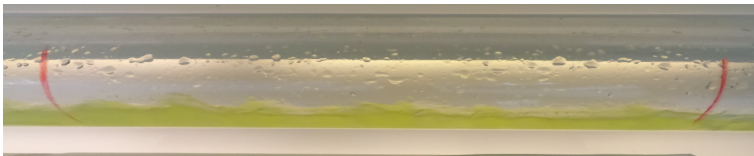
(a) A small wave front enters the frame



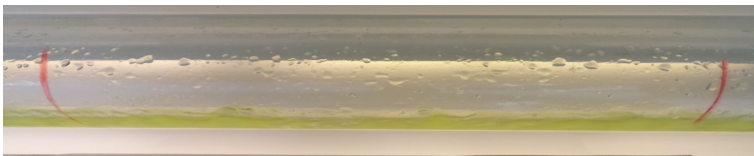
(b) The peak of the wave is visible as it flows through



(c) Wave continues through the section



(d) Water follows toward the end

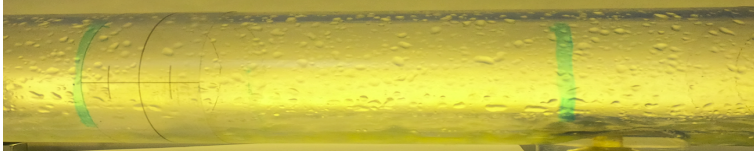


(e) The wave has passed

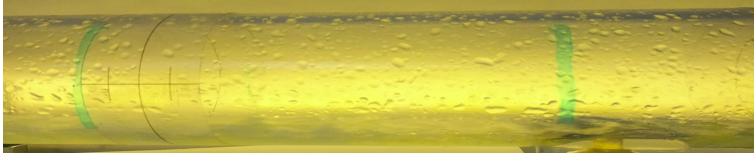
**Figure 5.14:** Images showing Case 5 [ $U_{SG} = 8.52$  m/s,  $U_{SL} = 0.0060$  m/s] at Camera 2 position at 26.7m

---

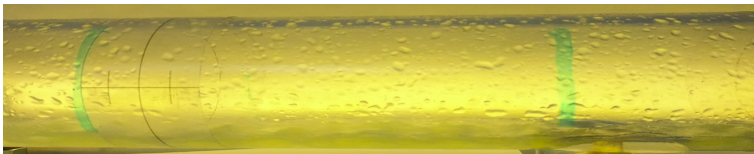
### III. Camera 3



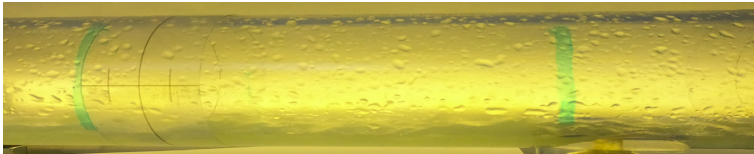
(a) Hold up starts to increase in the section



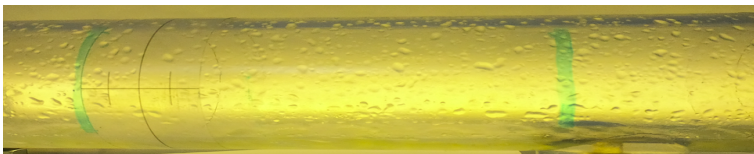
(b) Small peaks start to be visible indicating start of the wave



(c) The wave has possibly begun and is seen through hold up increase



(d) The wave peak passes through the section



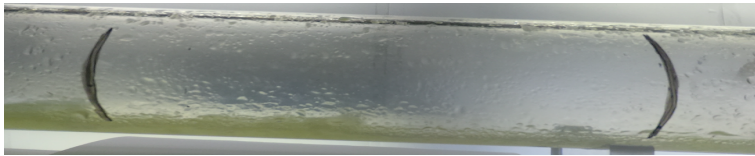
(e) The wave has passed

**Figure 5.15:** Images showing Case 5 [ $U_{SG} = 8.52$  m/s,  $U_{SL} = 0.0060$  m/s] at Camera 3 position at 52.3m

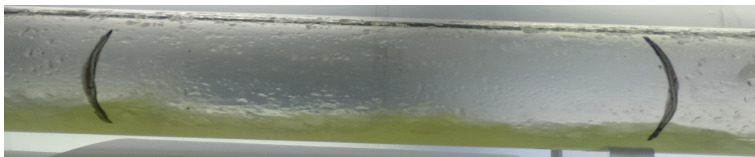
---

**A.6 Case 6  $U_{SG} = 7.65$  m/s,  $U_{SL} = 0.0043$  m/s**

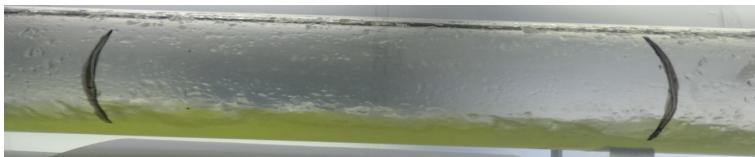
**I. Camera 1**



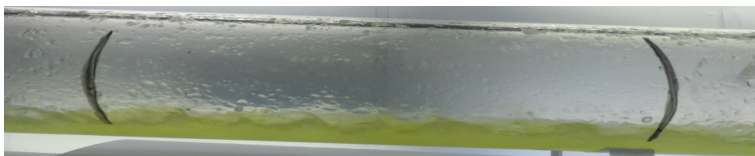
(a) Wave enters the observation section



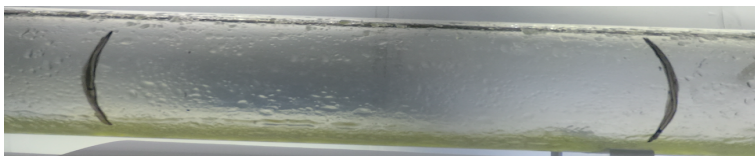
(b) The wave passes



(c) The wave continues through the section with more water becoming visible toward the end



(d) Water is dominant through the wave flowing

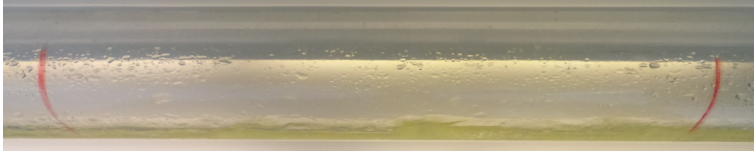


(e) The wave has passed

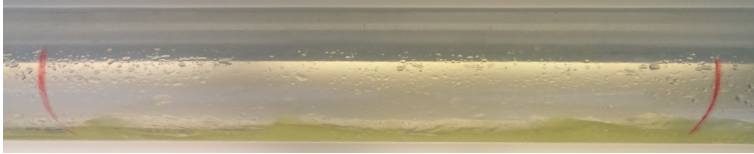
**Figure 5.16:** Images showing Case 6 [ $U_{SG} = 7.65$  m/s,  $U_{SL} = 0.0043$  m/s] at Camera 1 position at 6.4m

---

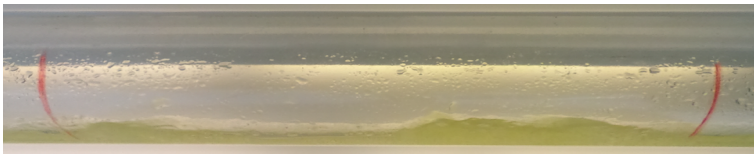
## II. Camera 2



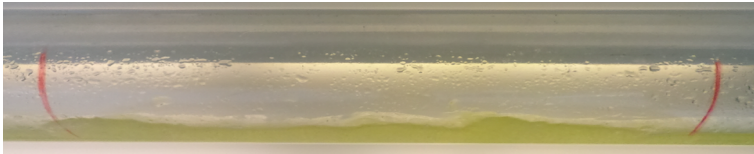
(a) The flow hold up starts to increase slowly



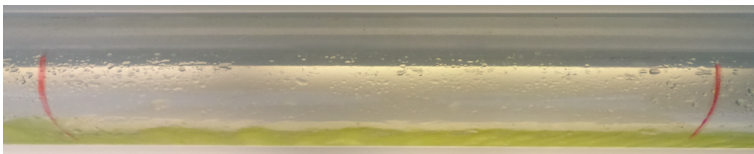
(b) The wave enters the observation section with a smooth front



(c) A small peak is seen passing



(d) The wave continues with a second smaller peak showing

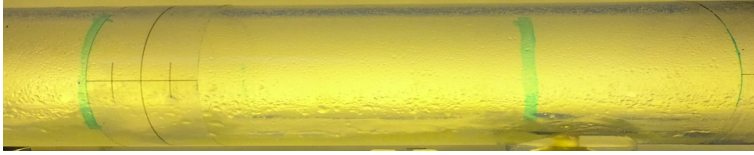


(e) The flow becomes uniform again, the wave has passed

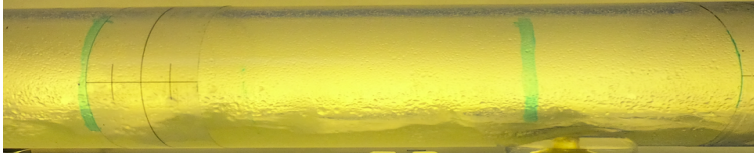
**Figure 5.17:** Images showing Case 6 [ $U_{SG} = 7.65$  m/s,  $U_{SL} = 0.0043$  m/s] at Camera 2 position at 26.7m

---

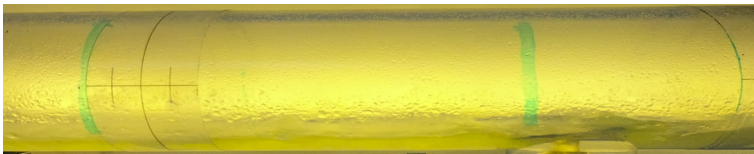
### III. Camera 3



(a) The wave enters the observation section



(b) The peak is diminished though the wave is still clear



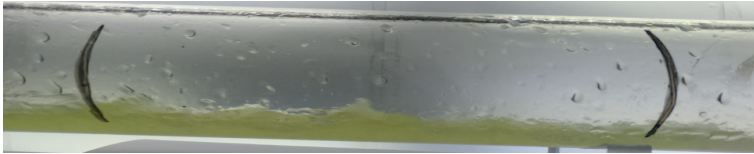
(c) The wave has passed

**Figure 5.18:** Images showing Case 6 [ $U_{SG} = 7.65$  m/s,  $U_{SL} = 0.0043$  m/s] at Camera 3 position at 52.3m

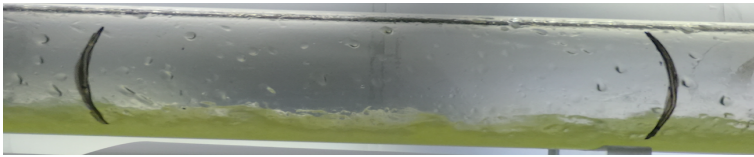
---

**A.7 Case 7  $U_{SG} = 8.52$  m/s,  $U_{SL} = 0.0025$  m/s**

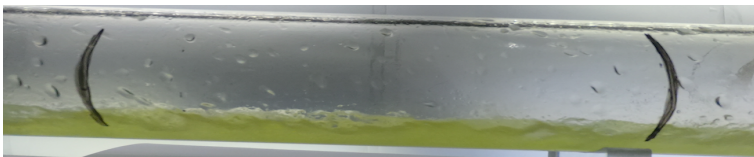
**I. Camera 1**



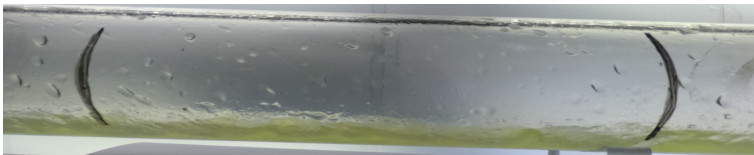
**(a)** The wave is flowing through the observation section



**(b)** The wave continues and is somewhat distorted



**(c)** The wave continues through



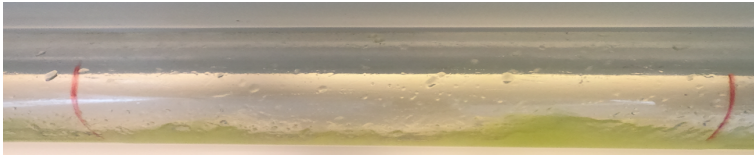
**(d)** The wave has passed

**Figure 5.19:** Images showing Case 7 [ $U_{SG} = 8.52$  m/s,  $U_{SL} = 0.0025$  m/s] at Camera 1 position at 6.4m

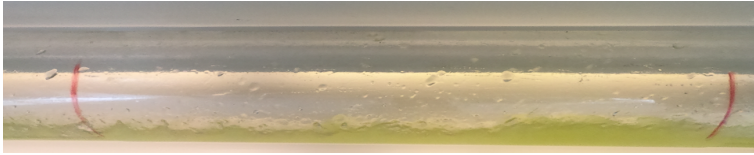
---

## II. Camera 2

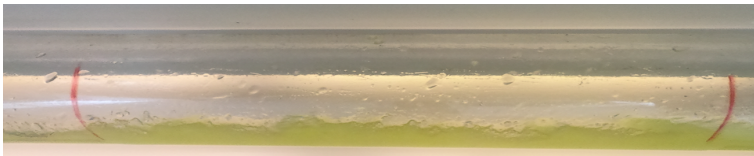




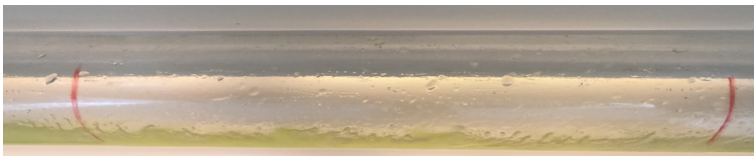
(a) The wave enters the section with a visible front



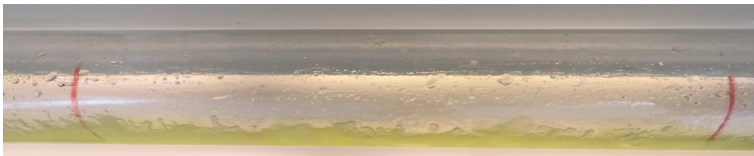
(b) There seems to be breaking in the flow then another wave passing



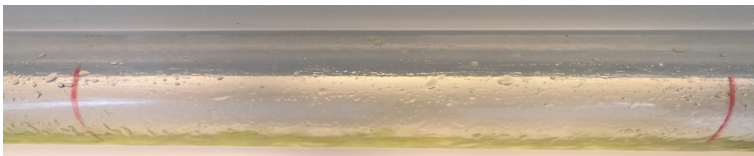
(c) The wave is seen continuing, more uniform



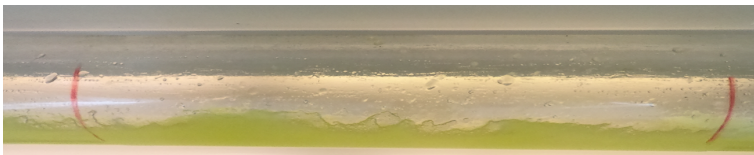
(d) The hold up decreases indicating end of wave



(e) Hold up fluctuates, increasing a bit in this frame



(f) Then the flow diminishes

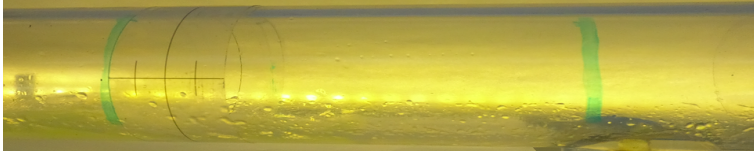


(g) Uncertainty whether this is a wave or restored flow in the pipe

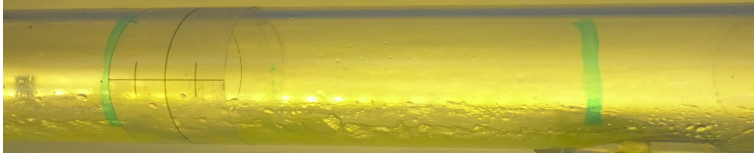
**Figure 5.20:** Images showing Case 7 [ $U_{SG} = 8.52$  m/s,  $U_{SL} = 0.0025$  m/s] at Camera 2 position at 26.7m

---

### III. Camera 3



(a) Wave front is seen entering the observation section



(b) The wave passes through the section. The tail/end of the wave was not easily detectable

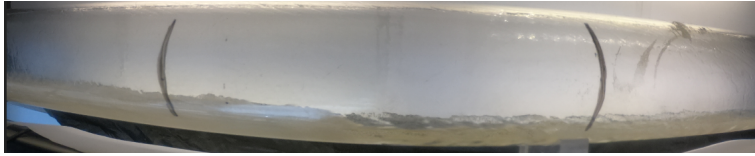
**Figure 5.21:** Images showing Case 7 [ $U_{SG} = 8.52$  m/s,  $U_{SL} = 0.0025$  m/s] at Camera 3 position at 52.3m

---

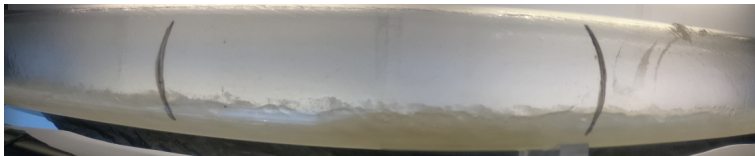
## B Camera Images: Varying Water Cuts

### B.1 Case 1 - 0% Water Cut

#### I Camera 1



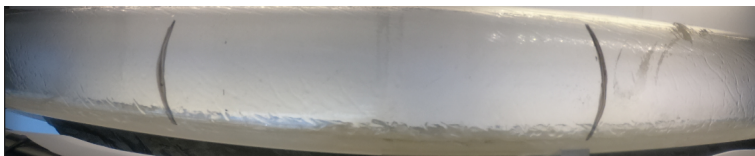
(a) Stable flow before wave passes



(b) Wave enters the frame, Peak holdup slightly visible



(c) The wave continues through the observation section

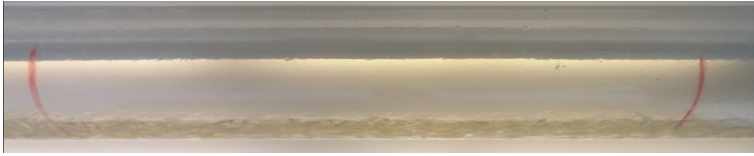


(d) The wave has passed and normal flow is restoring

**Figure 5.22:** Images showing Case 1 at 0% water cut at Camera 1 position (6.4m)

---

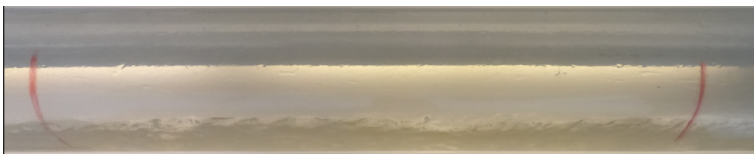
## II Camera 2



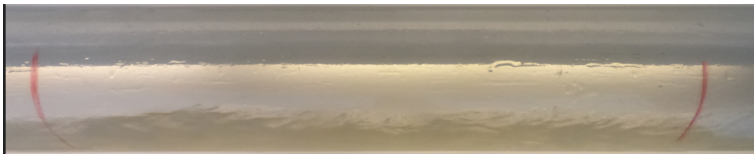
(a) Stable flow before wave passes



(b) An initial wave enters the observation section



(c) A second wave enters the observation section



(d) The wave peak passes

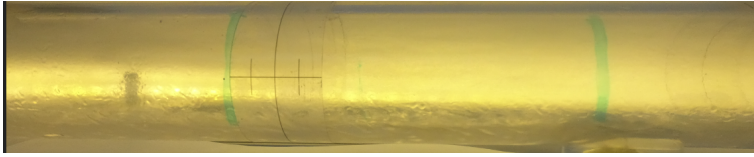


(e) The wave has passed

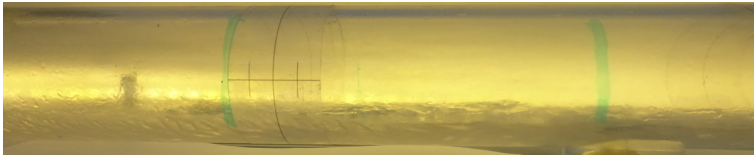
**Figure 5.23:** Images showing Case 1 at 0% water cut at Camera 2 position (26.7m)

---

### III Camera 3



(a) Wave enters the frame



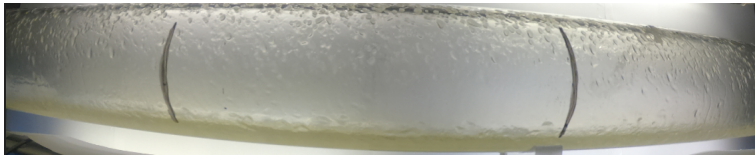
(b) An increase in hold up indicates wave passage

**Figure 5.24:** Images showing Case 1 at 0% water cut at Camera 3 position (52.3m)

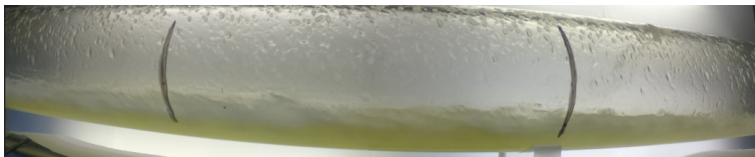
---

## B.2 Case 1 - 50% Water Cut

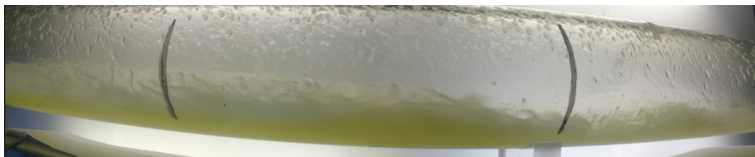
### I Camera 1



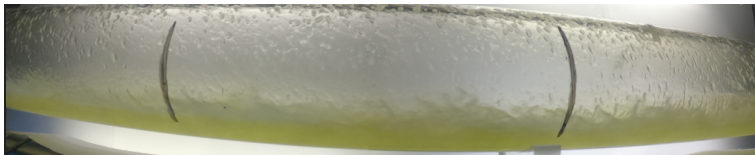
(a) Stable flow before wave passes



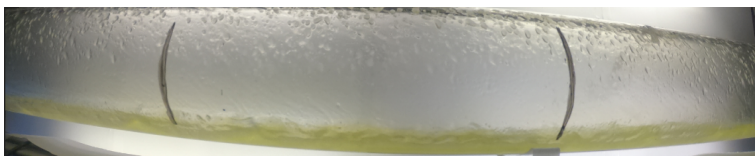
(b) Initial wave enters the frame with a smooth front



(c) Second larger wave with a sharper front passes through the observation section



(d) After-flow towards the tail of the wave

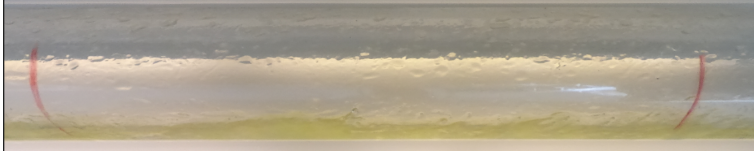


(e) The wave has passed

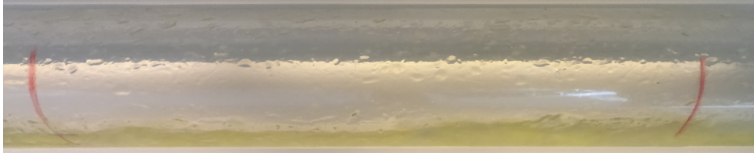
**Figure 5.25:** Images showing Case 1 at 50% water cut at Camera 1 position (6.4m)

---

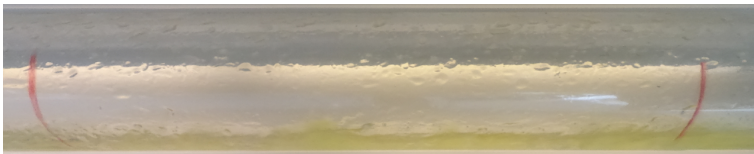
## II Camera 2



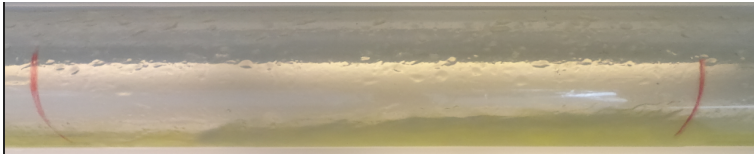
(a) Stable flow before wave passes



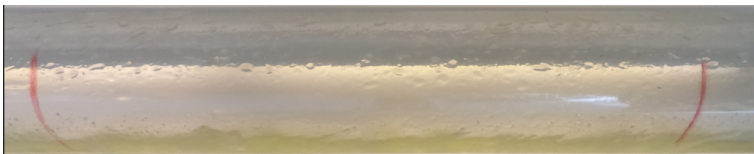
(b) An initial wave is seen entering



(c) Hold up gradually decreases, though the wave may still be flowing



(d) Second larger wave passes

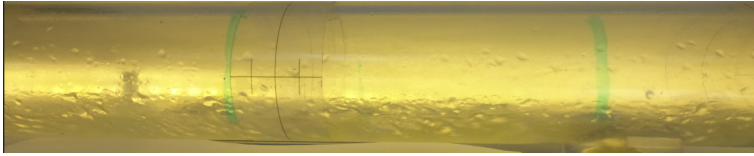


(e) The wave has passed

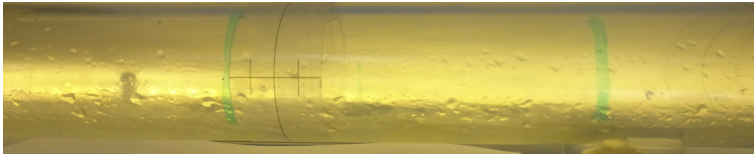
**Figure 5.26:** Images showing Case 1 at 50% water cut at Camera 2 position (26.7m)

---

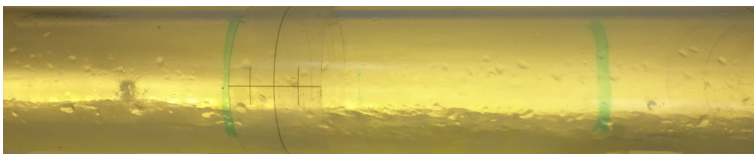
### III Camera 3



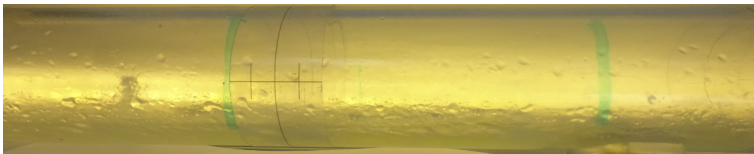
(a) Flow before a wave enters



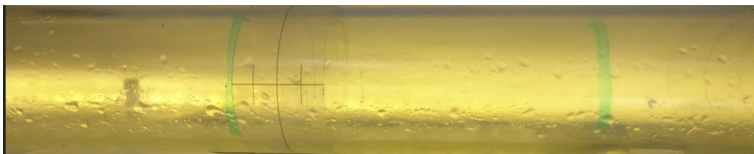
(b) Hold up gradually increases indicating wave passing, no clear front



(c) Wave peak is visible



(d) Water is seen clearly towards the end of the wave



(e) The wave has passed

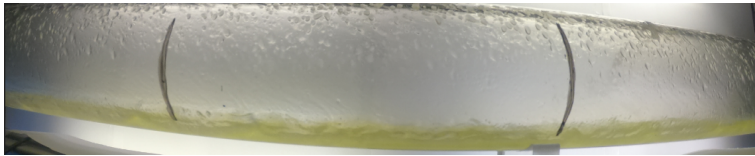
**Figure 5.27:** Images showing Case 1 at 50% water cut at Camera 3 position (52.3m)



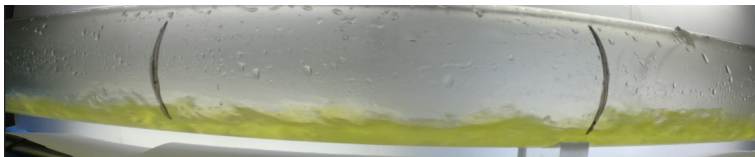
---

### B.3 Case 1 - 100% Water Cut

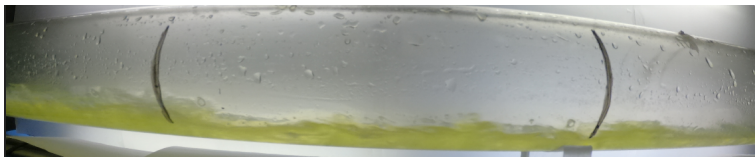
#### I Camera 1



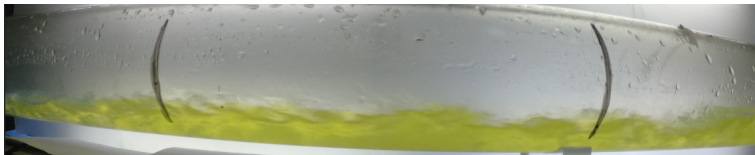
(a) A wave is seen incoming on the left



(b) Initial smaller wave enters the observation section



(c) Second larger wave enters the frame



(d) The wave peak passes

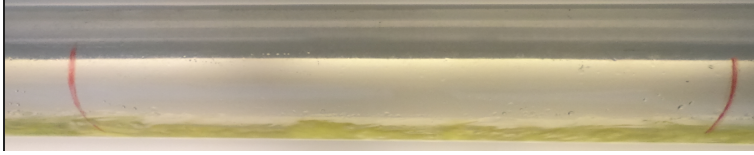


(e) The wave has passed and normal flow is restoring

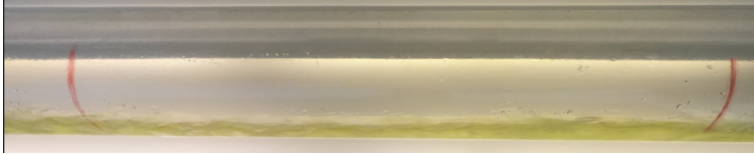
**Figure 5.28:** Images showing Case 1 at 100% water cut at Camera 1 position (6.4m)

---

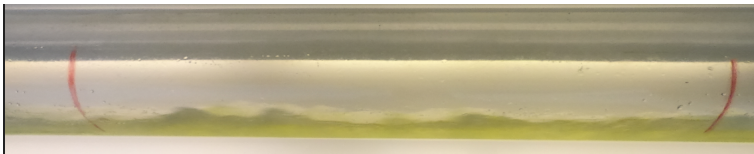
## II Camera 2



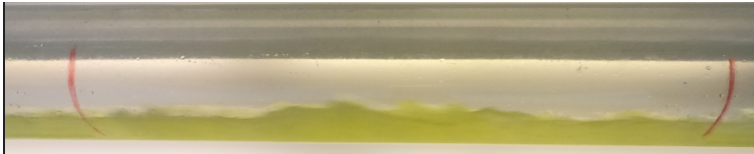
(a) Stable flow before wave passes



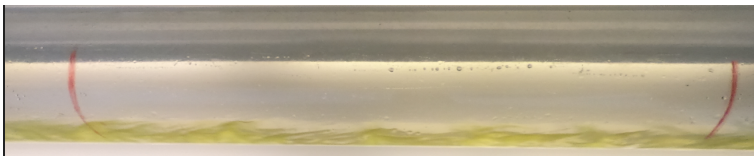
(b) Small initial wave enters the section



(c) Initial smaller wave passes with foamy-like substance at the top



(d) Peak of the wave is observed passing

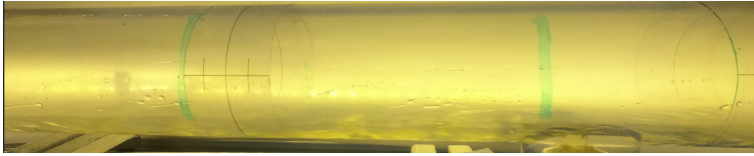


(e) The wave has passed

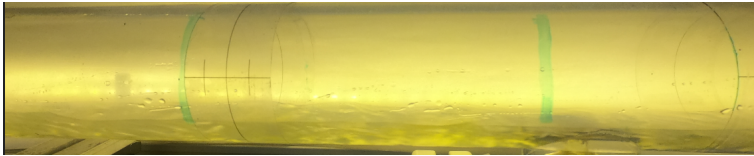
**Figure 5.29:** Images showing Case 1 at 100% water cut at Camera 2 position (26.7m)

---

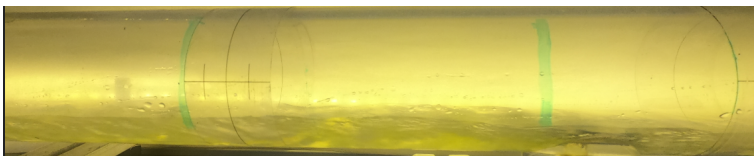
### III Camera 3



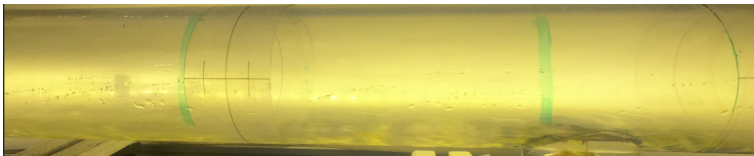
(a) Stable flow before wave passes



(b) Wave enters the section, seen by gradual hold up increase



(c) The wave continues through the section, peak holdup visible



(d) The wave has passed

**Figure 5.30:** Images showing Case 1 at 100% water cut at Camera 3 position (52.3m)

## C Simulation: Repetition of Two Phase Flow Surge Wave Simulations

This appendix will incorporate all the repeated two phase cases simulated with OLGA 2019.1.

### C.1 Case 1 [ $U_{SG} = 13.4$ m/s $U_{SL} = 0.0113$ m/s]

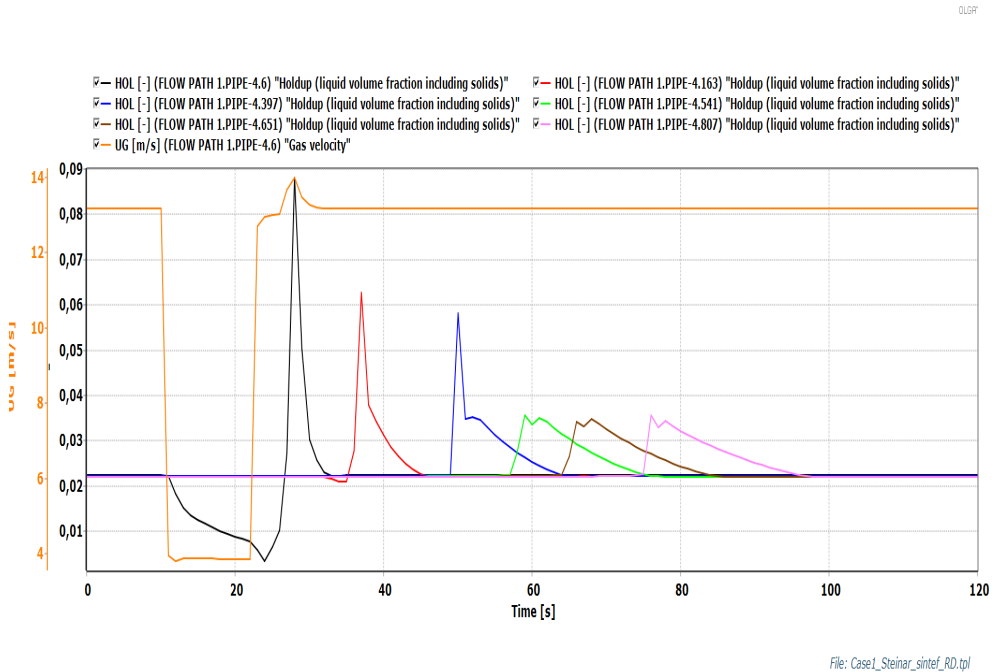


**Figure 5.31:** OLGA 2019.1 hold up plot for Case 1

**Table 5.1:** Flow rate input used to initiate waves for Case 1

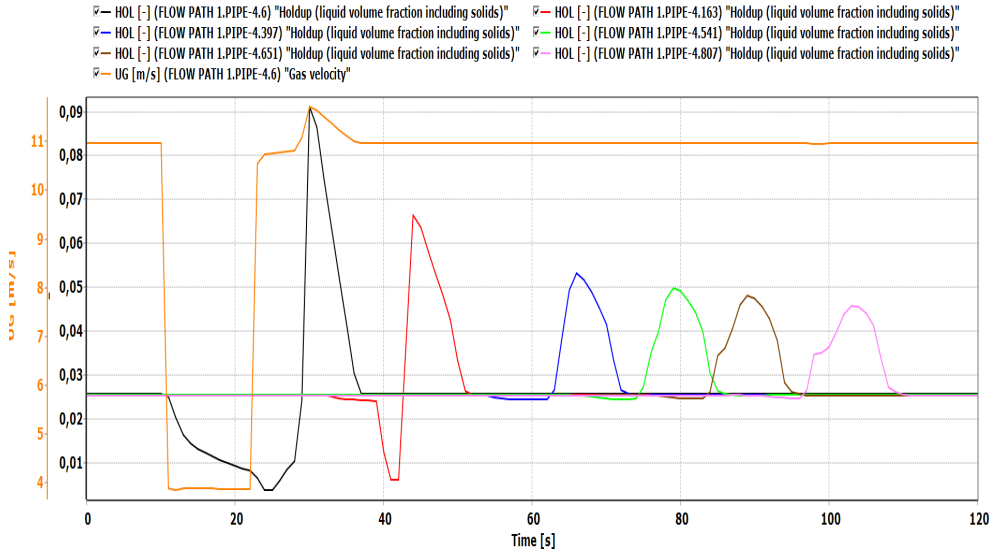
Time [s]	Air source Flow Rate [kg/s]	Water source Flow rate [kg/s]
0	0.045	0.032
10	0.045	0.032
11	0.013	0.032
22	0.013	0.032
23	0.045	0.032

**Table 5.2:** Additional Input Case 1

Integration time	120 seconds
Mesh	1D

**C.2 Case 2 [ $U_{SG} = 10.9 \text{ m/s}$   $U_{SL} = 0.0113 \text{ m/s}$ ]**

OLGA



File: Case2\_Steinar\_sintef\_RD.tpl

**Figure 5.32:** OLGA 2019.1 hold up plot for Case 2

**Table 5.3:** Flow rate input used to initiate waves for Case 2

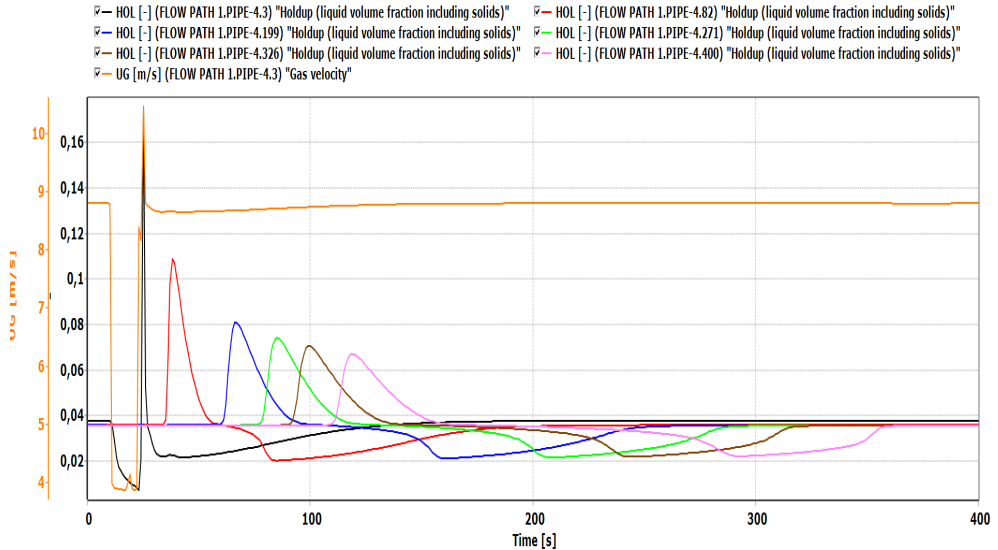
Time [s]	Air source Flow Rate [kg/s]	Water source Flow rate [kg/s]
0	0.037	0.032
10	0.037	0.032
11	0.013	0.032
22	0.013	0.032
23	0.037	0.032

**Table 5.4:** Additional Input Case 2

Integration time	120 seconds
Mesh	1D

### C.3 Case 3 [ $U_{SG} = 8.5 \text{ m/s}$ $U_{SL} = 0.0113 \text{ m/s}$ ]

OLGA



File: Case3\_Steinar\_sintef\_RD.tpl

**Figure 5.33:** OLGA 2019.1 hold up plot for Case 3

**Table 5.5:** Flow rate input used to initiate waves for Case 3

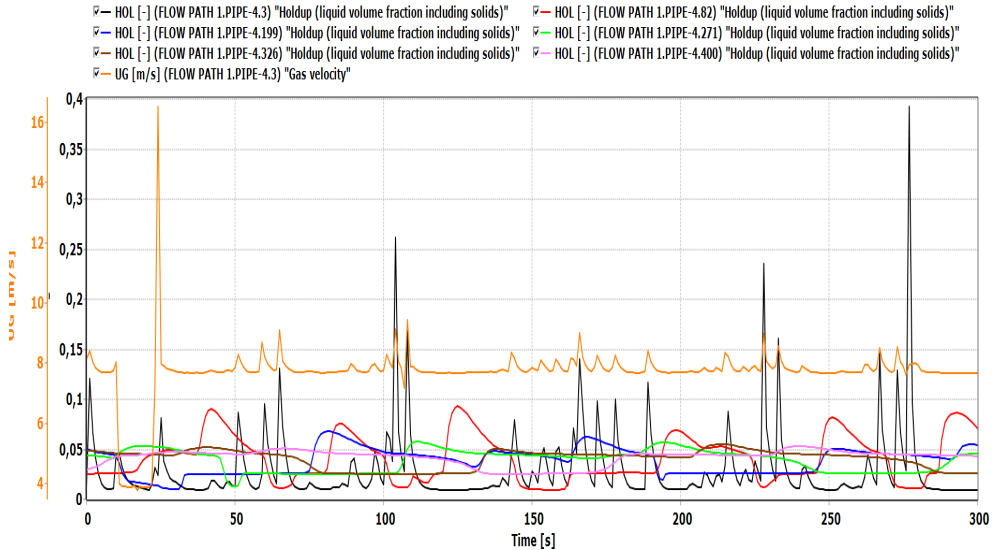
Time [s]	Air source Flow Rate [kg/s]	Water source Flow rate [kg/s]
0	0.029	0.032
10	0.029	0.032
11	0.013	0.032
22	0.013	0.032
23	0.029	0.032

**Table 5.6:** Additional Input Case 3

Integration time	400 seconds
Mesh	2D

## C.4 Case 4 [ $U_{SG} = 7.6 \text{ m/s}$ $U_{SL} = 0.0113 \text{ m/s}$ ]

OLGA



File: Case4\_Steinar\_sintef\_RD.tpl

**Figure 5.34:** OLGA 2019.1 hold up plot for Case 4

**Table 5.7:** Flow rate input used to initiate waves for Case 4

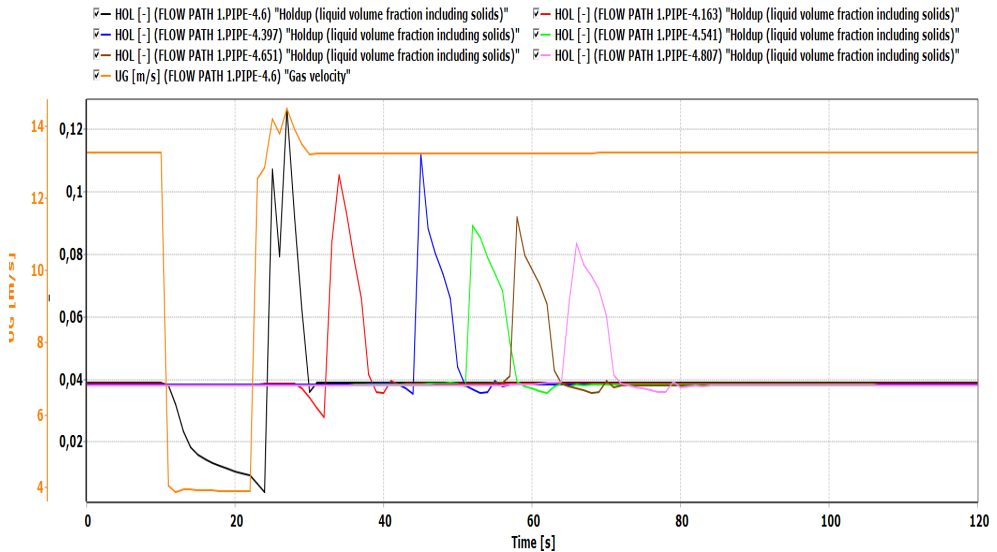
Time [s]	Air source Flow Rate [kg/s]	Water source Flow rate [kg/s]
0	0.026	0.032
10	0.026	0.032
11	0.013	0.032
22	0.013	0.032
23	0.026	0.032

**Table 5.8:** Additional Input Case 4

Integration time	300 seconds
Mesh	2D

**C.5 Case 5 [ $U_{SG} = 13.4 \text{ m/s}$   $U_{SL} = 0.0264 \text{ m/s}$ ]**

OLGA



File: Case5\_Steinar\_sintef\_RD.tpl

**Figure 5.35:** OLGA 2019.1 hold up plot for Case 5

**Table 5.9:** Flow rate input used to initiate waves for Case 5

Time [s]	Air source Flow Rate [kg/s]	Water source Flow rate [kg/s]
0	0.045	0.075
10	0.045	0.075
11	0.013	0.075
22	0.013	0.075
23	0.045	0.075

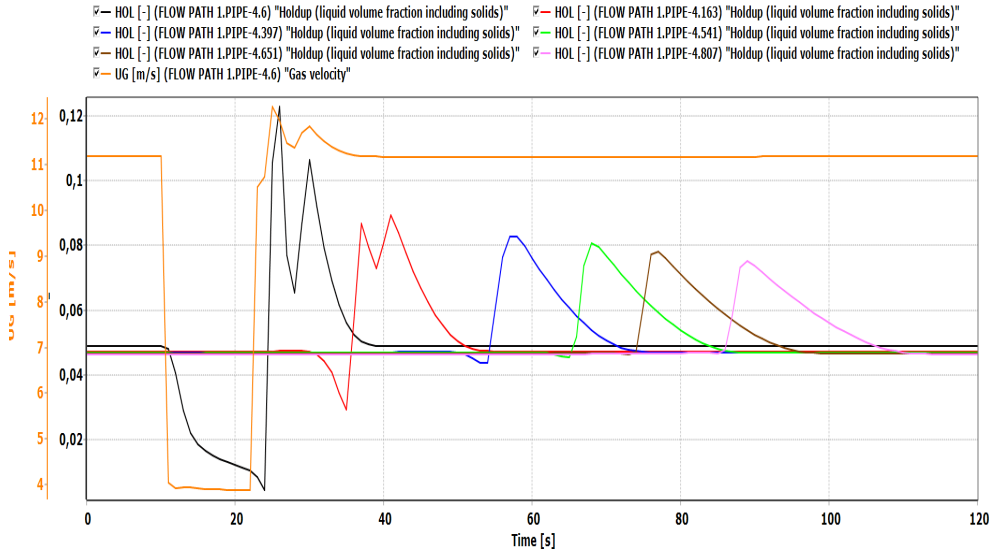
**Table 5.10:** Additional Input Case 5

Integration time	120 seconds
Mesh	1D



**C.6 Case 6 [ $U_{SG} = 10.9 \text{ m/s}$   $U_{SL} = 0.0264 \text{ m/s}$ ]**

OLGA



File: Case6\_Steinar\_sintef\_RD.tpl

**Figure 5.36:** OLGA 2019.1 hold up plot for Case 6

**Table 5.11:** Flow rate input used to initiate waves for Case 6

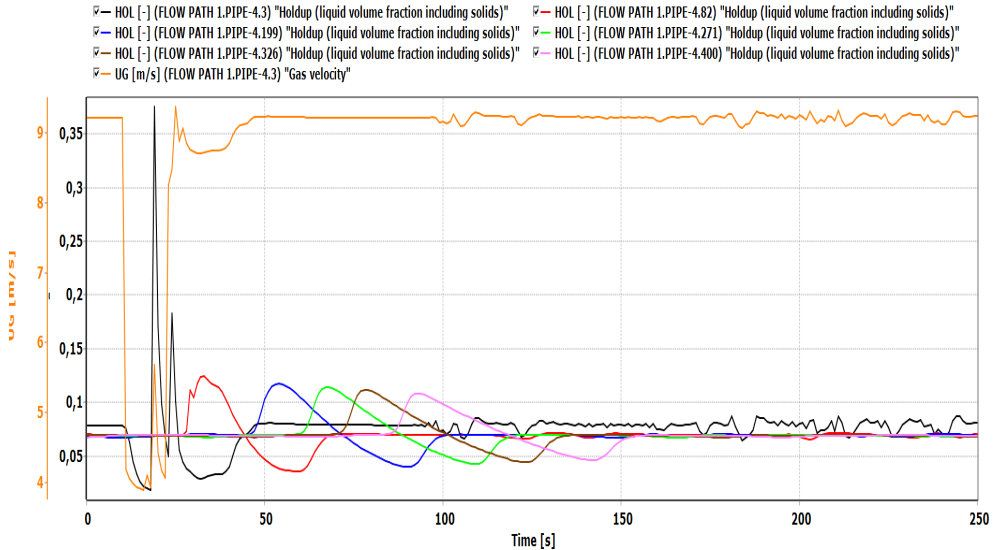
Time [s]	Air Flow Rate [kg/s]	Water Flow rate [kg/s]
0	0.037	0.075
10	0.037	0.075
11	0.013	0.075
22	0.013	0.075
23	0.037	0.075

**Table 5.12:** Additional Input Case 6

Integration time	120 seconds
Mesh	1D

**C.7 Case 7 [ $U_{SG} = 8.5 \text{ m/s}$   $U_{SL} = 0.0264 \text{ m/s}$ ]**

OLGA



File: Case7\_Steinar\_sintef\_RD.tpl

**Figure 5.37:** OLGA 2019.1 hold up plot for Case 7

**Table 5.13:** Flow rate input used to initiate waves for Case 7

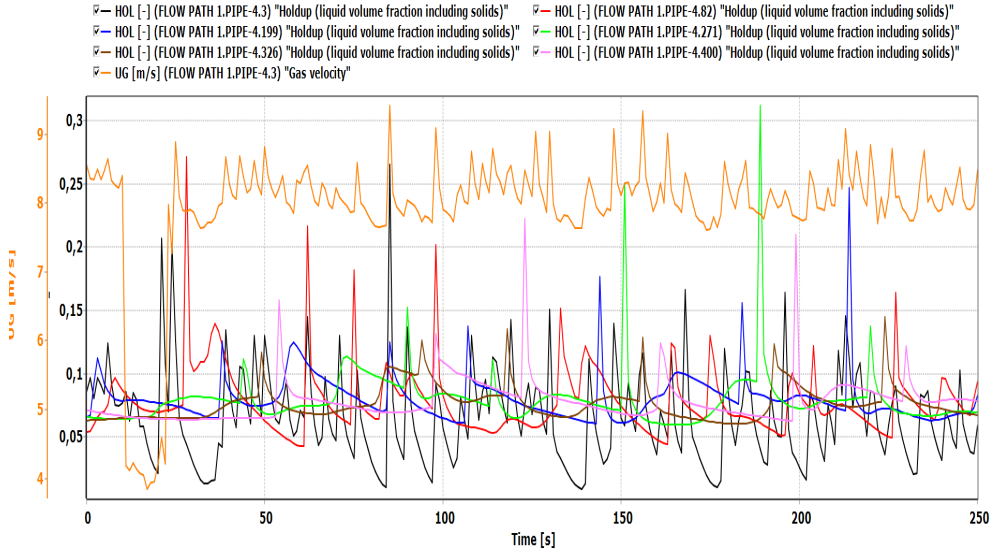
Time [s]	Air source Flow Rate [kg/s]	Water source Flow rate [kg/s]
0	0.029	0.075
10	0.029	0.075
11	0.013	0.075
22	0.013	0.075
23	0.029	0.075

**Table 5.14:** Additional Input Case 7

Integration time	250 seconds
Mesh	2D

**C.8 Case 8 [ $U_{SG} = 7.6 \text{ m/s}$   $U_{SL} = 0.0264 \text{ m/s}$ ]**

OLGA



File: Case8\_Steinar\_sintef\_RD.tpl

**Figure 5.38:** OLGA 2019.1 hold up plot for Case 8

**Table 5.15:** Flow rate input used to initiate waves for Case 8

Time [s]	Air source Flow Rate [kg/s]	Water source Flow rate [kg/s]
0	0.026	0.075
10	0.026	0.075
11	0.013	0.075
22	0.013	0.075
23	0.026	0.075

**Table 5.16:** Additional Input Case 8

Integration time	250 seconds
Mesh	2D

## D Simulation: Three-Phase Surge Wave Simulation

The initial superficial air velocity  $U_{sg} = 7,4$  m/s, which is the lowest  $U_{sg}$  applied. The superficial water velocity was kept constant at  $U_{SL} = 0,0144$  m/s. The large air valve was choked from 22 – 12%. Figures A 57 shows the raw holdup plot from the lab observation. **Table 5.17** shows the flow rates applied to initiate the wave in the simulations.

**Table 5.17:** Flow rate input used to initiate waves for Case 1 [ $U_{SG} = 8.95$  m/s  $U_{SL} = 0.0144$  m/s]

Time [s]	Air Flow Rate [kg/s]	Water Flow rate [kg/s]
0	0.030	0.036
10	0.030	0.036
11	0.012	0.036
22	0.012	0.036
23	0.030	0.036

### D.1 Case 1 - Initial Case

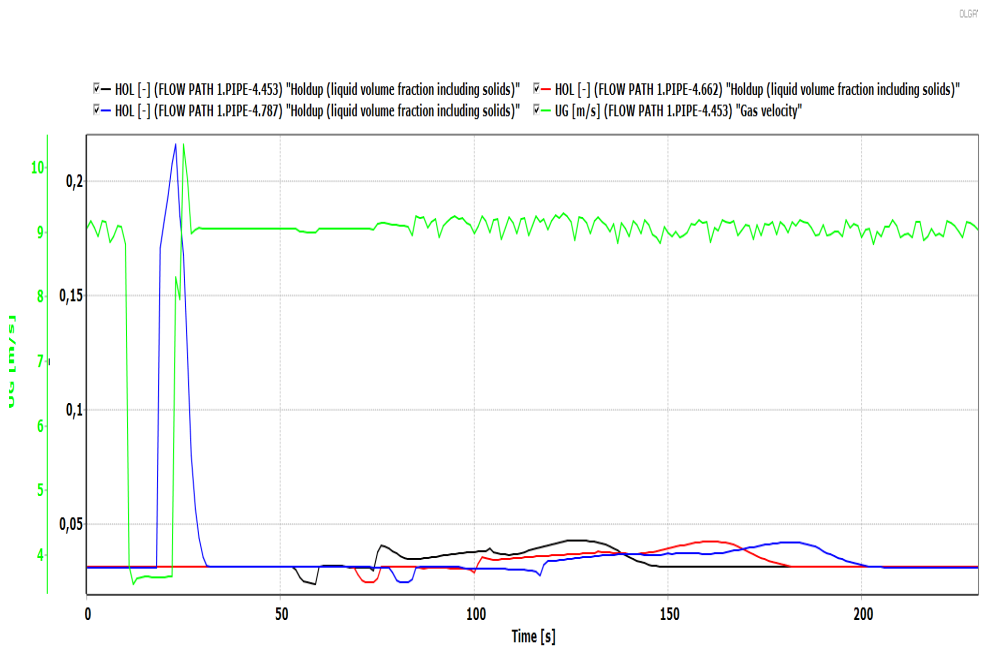


**Figure 5.39:** OLGA 2019.1 hold up plot for Case 1 - 37% Water Cut

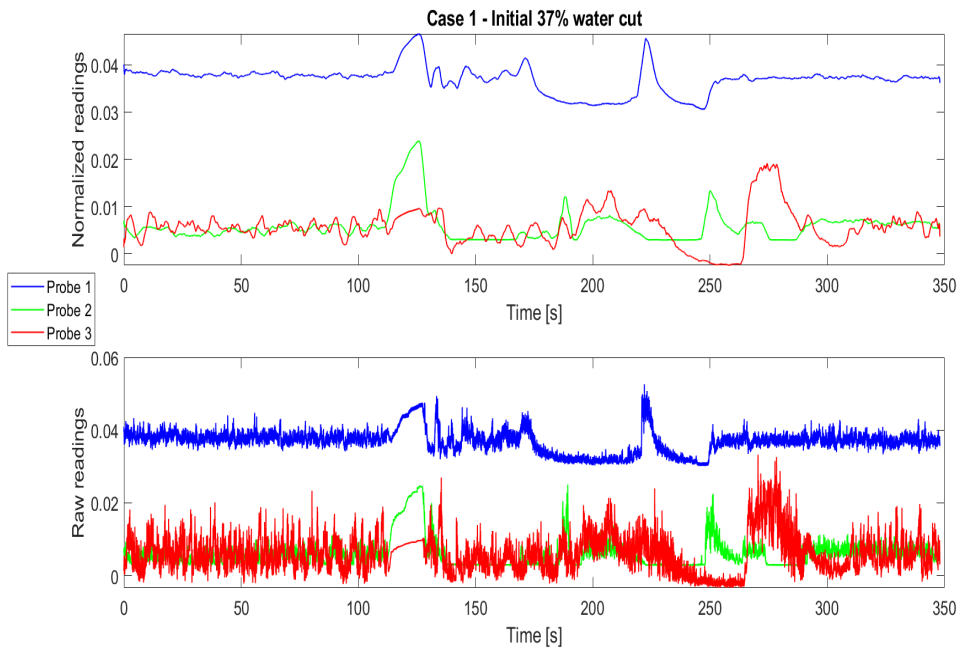


Figure 5.40: Plot showing experimental data for Case 1 with 37% water cut

## D.2 Case 1 - 0% Water Cut

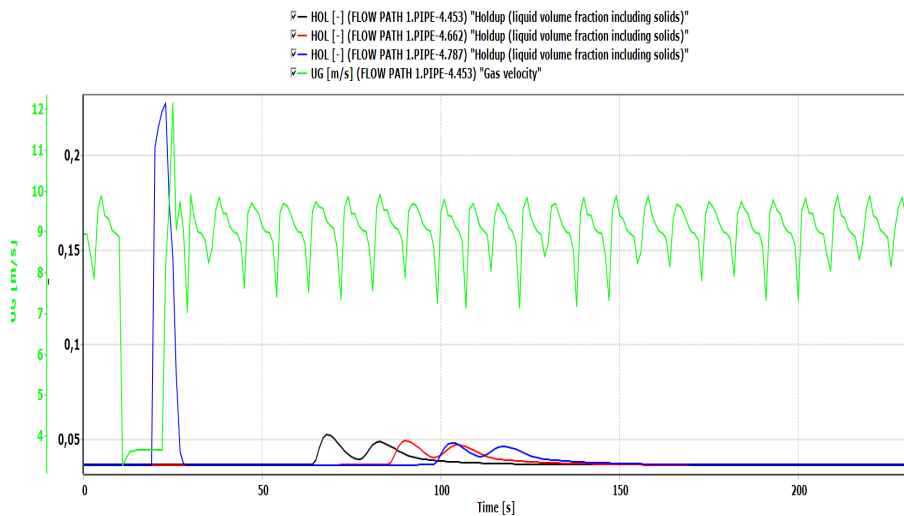
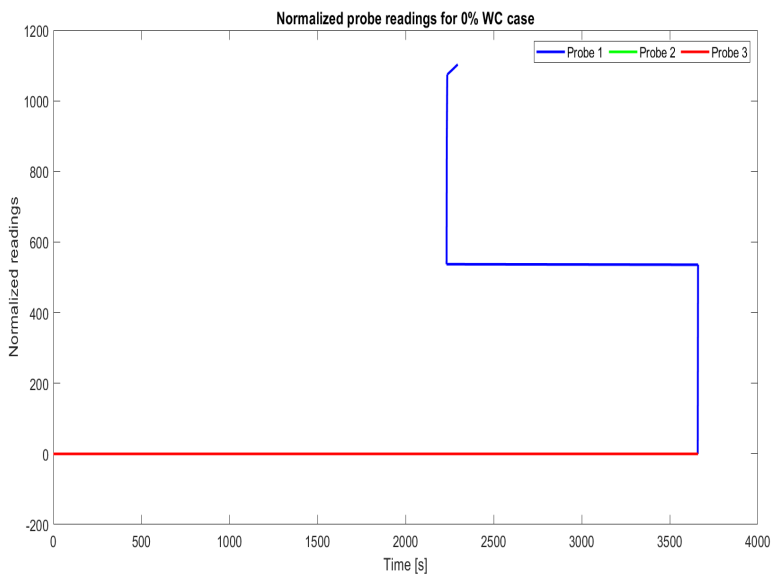
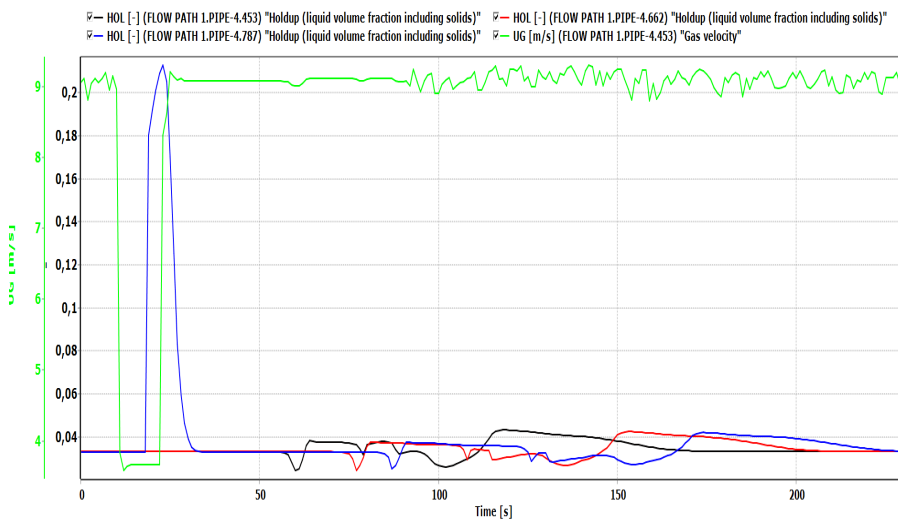


Figure 5.41: OLGA 2019.1 hold up plot for Case 1 - 0% Water Cut



**Figure 5.42:** Plot showing experimental data for Case 1 with 0% water cut

### D.3 Case 1 - 50% Water Cut



**Figure 5.43:** OLGA 2019.1 hold up plot for Case 1 - 50% Water Cut



Figure 5.44: Plot showing experimental data for Case 1 with 50% water cut

#### D.4 Case 1 - 100% Water Cut

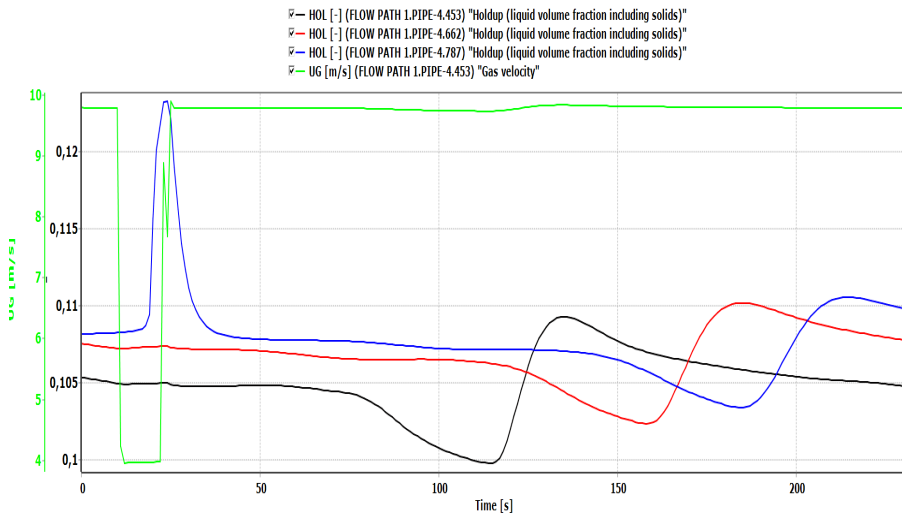
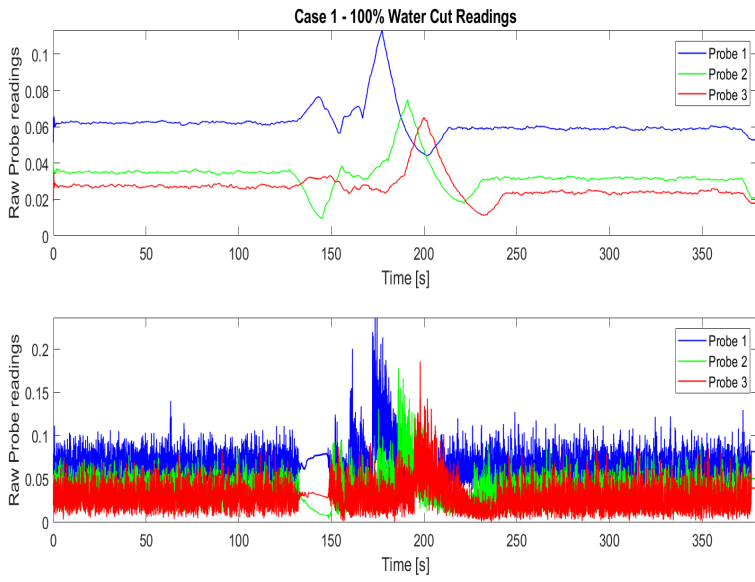


Figure 5.45: OLGA 2019.1 hold up plot for Case 1 - 100% Water Cut



**Figure 5.46:** Plot showing experimental data for Case 1 with 100% water cut



---

---

---

## E Risk Assessment Report



# Risk Assessment Report

## Multiphase Flow - Horizontal Loop

Prosjektnavn	Multiphase Flow - Horizontal Loop
Apparatur	Multiphase Flow - Horizontal Loop
Enhet	NTNU-EPT
Apparaturansvarlig	Ole Jørgen Nydal
Prosjektleder	Ole Jørgen Nydal
HMS-koordinator	Morten Grønli
HMS-ansvarlig (linjeleder)	Terese Løvås
Plassering	FlerfaseLaben
Romnummer	C164
Risikovurdering utført av	Erik Langørgen, Seid Ehsan Marashi, Mariana Diaz, Morten Grønli

### *Approval:*

Apparatur kort (UNIT CARD) valid for:	12 months
Forsøk pågår kort (EXPERIMENT IN PROGRESS) valid for:	12 months

Rolle	Navn	Dato	Signatur
Prosjektleder	Ole Jørgen Nydal		
HMS koordinator	Morten Grønli		
HMS ansvarlig (linjeleder)	Terese Løvås		

## TABLE OF CONTENTS

1	INTRODUCTION .....	1
2	ORGANISATION .....	1
3	RISK MANAGEMENT IN THE PROJECT .....	1
4	DESCRIPTIONS OF EXPERIMENTAL SETUP.....	1
5	EVACUATION FROM THE EXPERIMENTAL AREA .....	1
6	WARNING .....	2
6.1	Before experiments.....	2
6.2	Non-conformance .....	2
7	ASSESSMENT OF TECHNICAL SAFETY .....	3
7.1	HAZOP.....	3
7.2	Flammable, reactive and pressurized substances and gas .....	3
7.3	Pressurized equipment.....	3
7.4	Effects on the environment (emissions, noise, temperature, vibration, smell) .....	3
7.5	Radiation .....	4
7.6	Chemicals.....	4
7.7	Electricity safety (deviations from the norms/standards) .....	4
8	ASSESSMENT OF OPERATIONAL SAFETY .....	4
8.1	Procedure HAZOP .....	4
8.2	Operation procedure and emergency shutdown procedure.....	4
8.3	Training of operators.....	5
8.4	Technical modifications.....	5
8.5	Personal protective equipment.....	5
8.6	General Safety .....	5
8.7	Safety equipment .....	5
8.8	Special predations .....	5
9	QUANTIFYING OF RISK - RISK MATRIX.....	6
10	REGULATIONS AND GUIDELINES .....	7
11	DOCUMENTATION.....	7

## 1 INTRODUCTION

This experiment involves the horizontal flow loop in the multiphase flow laboratory at the energy and process engineering department. The loop will be fed with air, water and oil to create different multiphase flow regimes.

## 2 ORGANISATION

Rolle	
Prosjektleder	Ole Jørgen Nydal
Apparaturansvarlig	Ole Jørgen Nydal
Romansvarlig	Martin Bustadmo
HMS koordinator	Morten Grønli
HMS ansvarlig (linjeleder):	Terese Løvås

## 3 RISK MANAGEMENT IN THE PROJECT

Hovedaktiviteter risikostyring	Nødvendige tiltak, dokumentasjon	DATE
Prosjekt initiering	Prosjekt initiering mal	20.09.2012
Veiledningsmøte Guidance Meeting	Skjema for Veiledningsmøte med pre-risikovurdering	20.09.2012
Innledende risikovurdering Initial Assessment	Fareidentifikasjon – HAZID Skjema grovanalyse	21.10.2012
Vurdering av teknisk sikkerhet Evaluation of technical security	Prosess-HAZOP Tekniske dokumentasjoner	21.10.2012
Vurdering av operasjonell sikkerhet Evaluation of operational safety	Prosedyre-HAZOP Opplæringsplan for operatører	21.10.2012
Sluttvurdering, kvalitetssikring Final assessment, quality assurance	Uavhengig kontroll Utstedelse av apparaturkort Utstedelse av forsøk pågår kort	

## 4 DESCRIPTIONS OF EXPERIMENTAL SETUP

*See Attachments*

## 5 EVACUATION FROM THE EXPERIMENTAL AREA

Evacuate at signal from the alarm system or local gas alarms with its own local alert with sound and light outside the room in question, see 6.2

Evacuation from the rigg area takes place through the marked emergency exits to the assembly point, (corner of Old Chemistry Kjelhuset or parking 1a-b.)

### Action on rig before evacuation:

The pumps should be turned off by emergency button and valve 10001 should be closed manually

## 6 WARNING

### 6.1 Before experiments

Send an e-mail with information about the planned experiment to:

[iept-experiments@ivt.ntnu.no](mailto:iept-experiments@ivt.ntnu.no)

**The e-mail must include the following information:**

- Name of responsible person:
- Experimental setup/rig:
- Start Experiments: (date and time)
- Stop Experiments: (date and time)

You must get the approval back from the laboratory management before start up. All running experiments are notified in the activity calendar for the lab to be sure they are coordinated with other activity.

### 6.2 Non-conformance

#### **FIRE**

If you are NOT able to extinguish the fire, activate the nearest fire alarm and evacuate area. Be then available for fire brigade and building caretaker to detect fire place.

If possible, notify:

NTNU	SINTEF
Morten Grønli, Mob: 918 97 515	Linda Helander, Mob: +4740648621
Terese Løvås: Mob: 918 97 209	
NTNU – SINTEF Beredskapstelefon	800 80 388

#### **GAS ALARM**

If a gas alarm occurs, close gas bottles immediately and ventilate the area. If the level of the gas concentration does not decrease within a reasonable time, activate the fire alarm and evacuate the lab. Designated personnel or fire department checks the leak to determine whether it is possible to seal the leak and ventilate the area in a responsible manner.

#### **PERSONAL INJURY**

- First aid kit in the fire / first aid stations
- Shout for help
- Start life-saving first aid
- **CALL 113** if there is any doubt whether there is a serious injury

#### **OTHER NON-CONFORMANCE (AVVIK)**

##### **NTNU:**

You will find the reporting form for non-conformance on:

<https://innsida.ntnu.no/wiki/-/wiki/Norsk/Melde+avvik>

##### **SINTEF:**

Synergi

## 7 ASSESSMENT OF TECHNICAL SAFETY

### 7.1 HAZOP

Node 1	Water and Oil Loop
Node 2	Air Loop
Node 3	Acrylic pipe

**Attachments: skjema: Hazop\_mal**

**Conclusion:** Working with the facility is simple and does not cause any serious problem. Other problems can be prevented by the emergency shut down.

### 7.2 Flammable, reactive and pressurized substances and gas

Are any flammable, reactive and pressurized substances and gases in use?

YES	Exxsol D 80 has a flash point > 77°C Marcol 52 has a flash point > 148°C NEXBASE 3080 has a flash point > 220°C
-----	---

**Attachments:** Data sheet of Marcol 52, Exxsol D 80, and NEXBASE 3080

**Conclusion:** Exxsol is classified as hazardous. Both will produce flammable vapors and should be treated as flammable.

### 7.3 Pressurized equipment

Is any pressurized equipment in use?

YES	
-----	--

**Attachments:**

**Conclusion:** The steel pipe has been tested by 5bara and it is documented in the attachment. The polycarbonate tube between the multiphase mixer and the STC-Valve has a working pressure of 3 bara, and this tube and the STC-Valve itself is also tested to 5 bara, or 1,5 x maximum pumping pressure of 3,0 bara. The acrylic tube downstream of the STC-Valve is free of flow restrictions. Safety valves are installed in the mixing point of air, oil, and water and on the buffer tank which prevent pressure to exceed 3 bar. The test will be safe, as all parts of the test loop will stand the maximum pump pressure. An option in the Lab view program which increases the air flow gradually will be utilized.

### 7.4 Effects on the environment (emissions, noise, temperature, vibration, smell)

Will the experiments generate emission of smoke, gas, odour or unusual waste?

Is there a need for a discharge permit, extraordinary measures?

YES	Flow leakage from the set-up will make the ground slippery.
-----	---

**Conclusion:** The set-up checked for any leakages and there is not any problem. Be careful not to dispose any oil containing fluid in to the drains. They should be stored in the available barrels.

### 7.5 Radiation

NO	
----	--

**Attachments:**

**Conclusion:**

### 7.6 Chemicals

YES	Marcol 52 Exxsol D80 NEXBASE 3080
-----	---

**Attachments:** Data sheet of Marcol 52, Exxsol D 80, and NEXBASE 3080

**Conclusion:** Marcol 52 contains highly refined base oil and is not considered to present any hazard during normal use. Repeated exposure to Exxsol may cause skin dryness or cracking. If swallowed, may be aspirated and cause lung damage, may be irritating to the eyes, nose, throat, and lungs. Exxsol is classified as hazardous according to health .If Exxsol contact skin, wash contact areas with soap and water. Remove contaminated clothing. Launder contaminated clothing before reuse. If it contacts with eyes, flush thoroughly with water. If irritation occurs, get medical assistance. Exxsol can release vapors that readily form flammable gases. Avoid heat, sparks, open flames and other ignition sources. Health studies have shown that chemical exposure may cause potential human health risks which may vary from person to person.

### 7.7 Electricity safety (deviations from the norms/standards)

NO	
----	--

**Attachments:**

**Conclusion:**

## 8 ASSESSMENT OF OPERATIONAL SAFETY

Ensure that the procedures cover all identified risk factors that must be taken care of. Ensure that the operators and technical performance have sufficient expertise.

### 8.1 Procedure HAZOP

**Attachments:** HAZOP\_MAL\_ Procedure

**Conclusion:** Simplified procedure. Misunderstandings will not lead to unacceptable hazardous situations

### 8.2 Operation procedure and emergency shutdown procedure

Be careful to operate the valves slowly. It is vital that the step-wise start up and shut down procedure included in "HAZOP\_MAL\_ Procedure" is followed by the operators to avoid any severe damage to equipment and injury to the people.

**Attachments:** Procedure for running experiments

**Emergency shutdown procedure:** The pumps should be turned off by emergency bottom and valve 10001 should be closed manually.

### 8.3 Training of operators

The operators are responsible for running the tests in the multiphase loop. They should have knowledge about procedures for the experiments, emergency shutdown, nearest fire and first aid station, and chemical in the loop.

**Attachments:** Training of operators

### 8.4 Technical modifications

The operators only allowed replacing broken parts with new parts similar to the old one. Modifications involving major changes to pressure characteristics of the system should only be done by lab technicians

### 8.5 Personal protective equipment

- Use of eye protection in the rig zone is mandatory.
- Use of gloves when there is contact with Exxsol is mandatory

### 8.6 General Safety

- The area around the rig should be cleaned. Buckets of oil/water should not be left by the rig.
- Gantry crane and truck driving should not take place close to the experiment and they should be turned off during the experiments.
- Operators cannot leave the Lab during experiments.

### 8.7 Safety equipment

Equipment for cleaning and removing of oil and water spill.

### 8.8 Special predations

Web camera should be added to monitor the fluid flow close to the mixing point to reduce the need for operators to be exposed to pressurized acrylic pipe.



## 9 QUANTIFYING OF RISK - RISK MATRIX

The risk matrix will provide visualization and an overview of activity risks so that management and users get the most complete picture of risk factors.

IDnr	Dangerous situation	Probability	Consequences	Combination
1	Oil-water spill: <i>Slippery floor.</i> <i>Oil/water kept in open containers</i>	3	B	B3
2	<i>Eye damage</i>	2	D	D2
3	<i>Long way with stair to emergency shut down for air. (Hurry and unsafe way)</i>	3	C	C3
4	<i>Loose cables and components around the rig. (Stumbling)</i>	3	B	B3

**Conclusion:** Probability of eye damage is small but consequences are dangerous, so, the use of eye protection glasses is mandatory. The ground around the rig should be dry and clean always. Routines for removal of oil spillage have to be established.

Air supply shut down valve is preferred connected to the emergency button.

<b>CONSEQUENCES</b>	Svært alvorlig	E1	E2	E3	E4	E5
	Alvorlig	D1	D2	D3	D4	D5
	Moderat	C1	C2	C3	C4	C5
	Liten	B1	B2	B3	B4	B5
	Svært liten	A1	A2	A3	A4	A5
		Svært liten	Liten	Middels	Stor	Svært Stor
		<b>PROBABILITY</b>				

The principle of the acceptance criterion. Explanation of the colors used in the matrix

Colour	Description
Red	Unacceptable risk Action has to be taken to reduce risk
Yellow	Assessment area. Actions has to be considered
Green	Acceptable risk. Action can be taken based on other criteria

## 10 REGULATIONS AND GUIDELINES

Se <http://www.arbeidstilsynet.no/regelverk/index.html>

- Lov om tilsyn med elektriske anlegg og elektrisk utstyr (1929)
- Arbeidsmiljøloven
- Forskrift om systematisk helse-, miljø- og sikkerhetsarbeid (HMS Internkontrollforskrift)
- Forskrift om sikkerhet ved arbeid og drift av elektriske anlegg (FSE 2006)
- Forskrift om elektriske forsyningsanlegg (FEF 2006)
- Forskrift om utstyr og sikkerhetssystem til bruk i eksplosjonsfarlig område NEK 420
- Forskrift om håndtering av brannfarlig, reaksjonsfarlig og trykksatt stoff samt utstyr og anlegg som benyttes ved håndteringen
- Forskrift om Håndtering av eksplosjonsfarlig stoff
- Forskrift om bruk av arbeidsutstyr.
- Forskrift om Arbeidsplasser og arbeidslokaler
- Forskrift om Bruk av personlig verneutstyr på arbeidsplassen
- Forskrift om Helse og sikkerhet i eksplosjonsfarlige atmosfærer
- Forskrift om Høytrykksspyling
- Forskrift om Maskiner
- Forskrift om Sikkerhetsskiltning og signalgivning på arbeidsplassen
- Forskrift om Stillaser, stiger og arbeid på tak m.m.
- Forskrift om Sveising, termisk skjæring, termisk sprøyting, kullbuemeisling, lodding og sliping (varmt arbeid)
- Forskrift om Tekniske innretninger
- Forskrift om Tungt og ensformig arbeid
- Forskrift om Vern mot eksponering for kjemikalier på arbeidsplassen (Kjemikalieforskriften)
- Forskrift om Vern mot kunstig optisk stråling på arbeidsplassen
- Forskrift om Vern mot mekaniske vibrasjoner
- Forskrift om Vern mot støy på arbeidsplassen

Veiledninger fra arbeidstilsynet

se: <http://www.arbeidstilsynet.no/regelverk/veiledninger.html>

## 11 DOCUMENTATION

- Tegninger, foto, beskrivelser av forsøksoppsetningen
- Hazop\_mal
- Sertifikat for trykkpåkjent utstyr
- Håndtering avfall i NTNU
- Sikker bruk av LASERE, retningslinje
- HAZOP\_MAL\_Procedyre
- Forsøksprosedyre
- Opplæringsplan for operatører
- Skjema for sikker jobb analyse, (SJA)
- Apparatkortet
- Forsøk pågår kort

# Attachment to Risk Assessment report

## Multiphase Flow - Horizontal Loop

<b>Prosjektnavn</b>	Multiphase Flow - Horizontal Loop
<b>Apparatur</b>	Multiphase Flow - Horizontal Loop
<b>Enhet</b>	NTNU-EPT
<b>Apparaturansvarlig</b>	Ole Jørgen Nydal
<b>Prosjektleder</b>	Ole Jørgen Nydal
<b>HMS-koordinator</b>	Morten Grønli
<b>HMS-ansvarlig (linjeleder)</b>	Terese Løvås
<b>Plassering</b>	FlerfaseLaben
<b>Romnummer</b>	C164
<b>Risikovurdering utført av</b>	Erik Langørgen, Seid Ehsan Marashi, Mariana Diaz, Morten Grønli

### TABLE OF CONTENTS

ATTACHMENT A: PROCESS AND INSTRUMENTATION DIAGRAM .....	1
ATTACHMENT C: TEST CERTIFICATE FOR LOCAL PRESSURE TESTING .....	10
ATTACHMENT D: HAZOP PROCEDURE (TEMPLATE).....	11
ATTACHMENT E: PROCEDURE FOR RUNNING EXPERIMENTS.....	12
ATTACHMENT F: TRAINING OF OPERATORS.....	14
APPARATURKORT / UNITCARD.....	15
FORSØK PÅGÅR / EXPERIMENT IN PROGRESS .....	16

**ATTACHMENT B: HAZOP TEMPLATE**

Project: Multiphase flow loop- Horizontal-Loop Experiments Node: 1 Oil and Water Loop						Page	
Ref	Guideword	Causes	Consequences	Safeguards	Recommendations	Action	Date/Sign
1.1	No flow	Pump not working. Operating at low pump frequency. Closed flow line valves. Damaged tubing	None	Physical inspection of pumps and valves. Ensure that the controls are functioning.	Stop pump. Safeguards in procedure.	Check for any pump damage. Check if all the valves are opened. Check tank level.	
1.2	Reverse flow	NA					
1.3	More flow	High pump frequency	Minor vibration of flow lines.	Operate with frequency boundary of 25-40 Hz	Frequency limits in procedure	Check for any frequency converter issue.	
1.4	Less flow	Partial opening of the valves. Low pump frequency	Overloading of the pumps due to partial opening	Operate with frequency boundary of 25-40 Hz		Check for tank level and any frequency converter issue.	
1.5	More level	No air, fill the loop with water	None				
1.6	Less level	Inlet to pump closed or damaged	Pump running dry	Physical inspection of pumps inlet valves			
1.7	More pressure	Damaged tubing, valve not fully open	Safety valve releases the overpressure	Safety valve			
1.8	Less pressure	See 1.1					
1.9	More temperature	NA					
1.10	Less temperature	NA					

Project: Multiphase flow loop- Horizontal-Loop Experiments Node: 1 Oil and Water Loop						Page	
Ref	Guideword	Causes	Consequences	Safeguards	Recommendations	Action	Date/Sign
1.11	More viscosity	NA					
1.12	Less viscosity	NA					
1.13	Composition Change	NA					
1.14	Contamination	NA					
1.15	Relief	High air pressure from air central system	Discharge to the atmosphere	Safety valves and pressure gauge			
1.16	Instrumentation	Dirt, damage to sensors, wrong signal	No control of the system	Ensure the sensors are functioning		System will always also be visually monitored	
1.17	Sampling	NA					
1.18	Corrosion/erosion	NA					
1.19	Service failure	NA					
1.20	Abnormal Operation	NA					
1.21	Maintenance	NA					
1.22	Ignition	NA					
1.23	Spare equipment	NA					
1.24	Safety	Water/oil spill air discharge	Slippy floor Noise from discharging air	Physical inspection			

Project: Multiphase flow loop- Horizontal-Loop Experiments Node: 2 Air Loop						Page	
Ref#	Guideword	Causes	Consequences	Safeguards	Recommendations	Action	Date/Sign
2.1	No flow	Closed flow line valves. No air supply.	Ref: Node 1:1	Ensure that all the flow line valves are open.	Stop pump.	Check if all the valves are opened. If the control valves do not work, close valve 1001 and 10001.	
2.2	Reverse flow	Air in oil/water loop	No hazardous consequences				
2.3	More flow	Ref : Node 2:7					
2.4	Less flow	Partial opening of the valves.	Reverse flow of water/oil. Filling the tubing up to control valve.	Ensure that all the flow line valves are open Operational safety.	Stop pump.	Check if all the valves are opened.	
2.5	More level	NA					
2.6	Less level	NA					
2.7	More pressure	Open the air valve suddenly. Pressure regulator defect or modified	Safety valve opens at 1.5 bar	Pressure regulator check before running experiments	Add to procedure: Pressure regulator check before running experiments	Close the air valve.	
2.8	Less pressure	Ref 4					
2.9	More temperature	NA					
2.10	Less temperature	NA					
2.11	More viscosity	NA					
2.12	Less viscosity	NA					
2.13	Composition	NA					

Project: Multiphase flow loop- Horizontal-Loop Experiments Node: 2 Air Loop						Page	
Ref#	Guideword	Causes	Consequences	Safeguards	Recommendations	Action	Date/Sign
	Change						
2.14	Contamination	NA					
2.15	Relief	High air pressure from air central system	Discharge to the atmosphere. Loudly noise	Safety valves and pressure gauge Ear protection available at operator's residence.			
2.16	Instrumentation	NA					
2.17	Sampling	NA					
2.18	Corrosion/erosion	NA					
2.19	Service failure	NA					
2.20	Abnormal operation	NA					
2.21	Maintenance	NA					
2.22	Ignition	NA					
2.23	Spare equipment	NA					
2.24	Safety	Increasing the air pressure.	Noise from discharging air. Breaking the Acrylic pipe.	Ear protection available at operator's residence.	Physical inspection		

Project: Multiphase flow loop- Horizontal-Loop Experiments						Page	
Node: 3 Acrylic pipe, horizontal loop							
Ref#	Guideword	Causes	Consequences	Safeguards	Recommendations	Action	Date/Sign
3.1	No flow	Ref node 1.1 and 1.2	None	.			
3.2	Reverse flow	Ref node 1.1 and 1.2	No hazardous consequences				
3.3	More flow	High flow in oil/water loop and air loop	Vibrations in polycarbonate /acrylic tubing	Operational safety	Frequently and closer inspections of acrylic components must be added to the procedure		
3.4	Less flow	Ref node 1.1 and 1.2					
3.5	More level	Ref node 3.3					
3.6	Less level	NA					
3.7	More pressure	Open the air valve suddenly. Pressure regulator defect or modified	Safety valve opens at 1.5 bar Breaking the Acrylic pipe.	Open the air control valve gradually. Safety valve will open at 1.5 bar.			
3.8	Less pressure	Ref node 1.1 and 1.2					
3.9	More temperature	NA					
3.10	Less temperature	NA					
3.11	More viscosity	NA					
3.12	Less viscosity	NA					
3.13	Composition Change	NA					
3.14	Contamination	NA					
3.15	Relief	Leaks from the piping	Oily and slippery floor	Ref 3			
3.16	Instrumentation	NA					



Project: Multiphase flow loop- Horizontal-Loop Experiments						Page	
Node: 3 Acrylic pipe, horizontal loop							
Ref#	Guideword	Causes	Consequences	Safeguards	Recommendations	Action	Date/Sign
3.17	Sampling	NA					
3.18	Corrosion/erosion	NA					
3.19	Service failure	Experiments with Cracked pipe components	Leaks or blow out of acrylic parts	Frequently (2. Times a year) re testing of the loop.			
3.20	Abnormal operation	NA					
3.21	Maintenance	Ref 19					
3.22	Ignition	NA					
3.23	Spare equipment	NA					
3.24	Safety						

**ATTACHMENT D: HAZOP PROCEDURE (TEMPLATE)**

Project: Node: 1							Page
Ref#	Guideword	Causes	Consequences	Safeguards	Recommendations	Action	Date/Sign
	Not clear procedure	Procedure is too ambitious, or confusingly					
	Step in the wrong place	The procedure can lead to actions done in the wrong pattern or sequence					
	Wrong actions	Procedure improperly specified					
	Incorrect information	Information provided in advance of the specified action is wrong					
	Step missing	Missing step, or step requires too much of operator					
	Step unsuccessful	Step has a high probability of failure					
	Influence and effects from other	Procedure's performance can be affected by other sources					

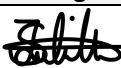
**ATTACHMENT E: PROCEDURE FOR RUNNING EXPERIMENTS**

<b>Prosjekt</b> Multiphase Flow Horizontal-Loop	<b>Dato</b>	<b>Signatur</b>
<b>Apparatur</b> Multiphase Flow Horizontal-Loop		
<b>Prosjektleder</b> Ole Jørgen Nydal	7/18/20	<i>Ole Jørgen Nydal</i>

<b>Conditions for the experiment:</b>	<b>Completed</b>
Experiments should be run in normal working hours, 08:00-16:00 during winter time and 08.00-15.00 during summer time. Experiments outside normal working hours shall be approved.	
One person must always be present while running experiments, and should be approved as an experimental leader.	
An early warning is given according to the lab rules, and accepted by authorized personnel.	
Be sure that everyone taking part of the experiment is wearing the necessary protecting equipment and is aware of the shut down procedure and escape routes.	
<b>Preparations</b>	<b>Carried out</b>
Post the "Experiment in progress" sign.	
Clear the area around the loop. There should be no open containers with oil/water or oil/water on the floor.	
Check pressure regulator for air system -35	
See that there is free access to the air valve, HV 1001 from air tank in basement. Emergency shutdown valve for the system	
First start the air loop by slowly opening HV1001. HV4003 and HV10012 shall be kept open. Other valves (HV10006, HV10007, HV10008, HV10009, HV10010 have to be opened according to the procedure for small or large air flow) Control valves can be opened slowly using labview. The other valves are used of small flowrates are desired. At the end of the S-riser there is a control valve, but this has been disconnected and is always open to avoid pressure buildup.	
Then start the water loop by opening HV2003. Next you open the valve in front and behind the pump you choose. Make sure HV2002, HV3014, HV11001, HV11003 and HV11012 are always closed during operation. HV11002, HV11011 shall be open.	
Then switch the pump on and control its point of operation by adjusting its frequency and adjusting the control valves. If the frequency is too low ( less than 10 Hz) you may not get any flow.	
<b>During the experiment</b>	
<i>Control of leakage in the set-up</i>	
Control air pressure, and that's enough for not filling tank V-35 with water	
<b>End of experiment</b>	
Turn off the liquid pumps and close the control valves.	
Purge the loop with air.	

	Then slowly close of the air control valve.	
	Valves should be back at the initial position or as needed for the next experiment. The final valves positions have to be in accordance with the use of the loop: <ul style="list-style-type: none"> <li>• Centrifugal pumpes or positive displacement pumps.</li> <li>• Riser or horizontal rig.</li> </ul>	
	Remove all obstructions/barriers/signs around the experiment.	
	Tidy up and return all tools and equipment.	

**Operator(s):**

Navn	Dato	Signatur
Susan Dorothy Lyimo		

## ATTACHMENT F: TRAINING OF OPERATORS

<b>Prosjekt</b> Multiphase Flow – Horizontal-Loop	<b>Dato</b>	<b>Signatur</b>
<b>Apparatur</b> Multiphase Flow – Horizontal-Loop		
<b>Prosjektleder</b> Ole Jørgen Nydal		

	<b>Knowledge to EPT LAB in general</b>	
	Lab <ul style="list-style-type: none"> <li>• Access</li> <li>• routines and rules</li> <li>• working hours</li> </ul>	
	Knowledge about the evacuation procedures.	
	Activity calendar for the Lab	
	Early warning, <a href="mailto:iept-experiments@ivt.ntnu.no">iept-experiments@ivt.ntnu.no</a>	
	<b>Knowledge to the experiments</b>	
	Procedures for the experiments	
	Emergency shutdown.	
	Nearest fire and first aid station.	
	Knowledge about the fluid in the loop <ul style="list-style-type: none"> <li>• Marcol 52</li> <li>• Exxsol D80</li> <li>• NEXBASE 3080</li> </ul>	
	Practical training to run the experiment	

I hereby declare that I have read and understood the regulatory requirements has received appropriate training to run this experiment and are aware of my personal responsibility by working in EPT laboratories.

### Operator(s):

Navn	Dato	Signatur
Susan Dorothy Lyimo		